

# **HPLC and Mass Spectrometry Analysis of the Free Radical Degradation of Chondroitin Sulfate and its Implications in Osteoarthritis**

*Ashley Matthey (BSc)*

Submitted in accordance with the requirements for the degree of  
Master of science (By research)



The candidate confirms that the work submitted is his own and that appropriate credit has been given where reference has been made to the work of others. This copy has been supplied on the understanding that it is copyright material and that no quotation from the thesis may be published without proper acknowledgement

## Contents page

### Contents

Abbreviations.....	9
HPLC and ESI-MS analysis of free radical degradation of Chondroitin sulfate .....	11
1. Abstract.....	11
2 INTRODUCTION.....	12
2.1 Chondroitin sulfate.....	12
2.2 Dermatan sulfate .....	13
2.3 Production.....	14
2.4 Physiological role .....	14
2.5 Generating CS disaccharide .....	15
2.6 HPLC and mass spectrometry analysis of CS.....	15
2.7 Extraction .....	16
2.8 ESI analysis of CS.....	17
2.9 Disaccharide analysis .....	17
2.10 Oxygen Free radicals.....	18
2.11 Age and ROS.....	18
2.12 Arthritis and oxidative stress .....	18
2.13 Alkaptonuria.....	19
2.14 AKU and arthritis.....	21
2.15 Homogentisic acid.....	21
2.16 Oxidation of tyrosine .....	22
2.17 Interactions of HGA with CS.....	23
2.18 Superoxide dismutase preventing oxidative stress .....	24
3. Aims and objectives .....	25
4. Material.....	25
5 Methods.....	25
5.1 Enzyme depolymerisation of intact CS .....	25
5.2 Free radical depolymerisation of intact CS.....	26
5.3 Free radical depolymerisation of digested CS .....	26
5.4 HPLC analysis of free radical and enzyme depolymerised CS and DS.....	26
5.5 MS sample prep and parameters.....	26
5.6 MS sample prep for HGA .....	27

5.7 HPLC analysis of HGA interaction with intact CS .....	27
5.8 HPLC analysis of HGA interaction with enzyme .....	27
5.9 Mass spectrometry Anlysis of SOD incubation with CS and Fenton reaction.....	27
6 Results .....	28
6.1 Enzymatic depolymerisation of intact CS .....	28
6.1.1 HPLC analysis of Digest .....	28
6.1.2 MS digest CS.....	30
6.2 HPLC of intact CS.....	32
6.3 HPLC profiles of depolymerised CS .....	34
6.4 MS intact CS .....	36
6.5 MS depolymerised CS .....	37
6.6 Relative intensity results .....	41
6.7 Summary of proposed Structures generated following ESI-MS analysis of free radical depolymerised CS .....	43
6.8 MS analysis of HGA .....	46
6.9 MS analysis of HGA and CUSO <sub>4</sub> .....	49
6.10 MS <sup>2</sup> data from HGA and CUSO <sub>4</sub> .....	49
6.11 HGA and Iron citrate .....	50
6.12 HPLC analysis of HGA interaction with CS disaccharide .....	52
6.13 MS HGA and intact CS .....	53
6.14 MS HGA and enzyme depolymerised CS.....	56
6.15 Mass spec analysis of SOD reaction .....	57
7 Discussion.....	62
7.1 HPLC analysis of enzymatically digested CS.....	62
7.2 HPLC of free radical depolymerised CS.....	62
7.3 MS of Enzyme depolymerisation .....	63
7.4 MS of free radical depolymerisation.....	66
7.4.1 Shark .....	66
7.4.2 m/z 240.8 .....	67
7.4.3 m/z 214.8 .....	69
7.4.4 m/z 184.8 and 154.8 .....	71
7.4.5 Bovine .....	71
7.4.6 m/z154.8 .....	71
7.4.7 m/z Porcine .....	71

7.5 Proposed mechanism of free radical depolymerisation of CS.....	72
7.6 Conversion of homogentisic acid into homogentisate .....	74
7.7 Semiquinones and generation of ROS .....	74
7.8 Oxidation and coupling of phenol.....	75
7.9 Phenoxy reactions.....	77
7.10 Oxidation of hydroquinone by copper .....	77
7.11 Benzoquinone dimerization.....	77
7.12 HGA dimerization.....	78
7.13 HGA and the generation of ROS.....	80
7.14 HGA interaction with CS.....	82
7.15 Addition of SOD preventing free radical depolymerisation of CS.....	83
8. Conclusions .....	85
9. References .....	87

## Figures

Figure 1: Chondroitin sulfate polymer consisting of alternate GlcA and GalNAc residues with a tertrasaccharide linkage region. ....	12
Figure 2: Disaccharide unit of CS-A: $\beta$ -glucuronic acid-( $\alpha$ 1-3)-N-acetyl- $\beta$ -galactosamine-4-sulfate. CS-B: (Dermatan sulphate) $\beta$ -iduronic acid-( $\alpha$ 1-3)-N-acetyl- $\beta$ -galactosamine-4-sulfate. CS-C: $\beta$ -glucuronic acid-( $\alpha$ 1-3)-N-acetyl- $\beta$ -galactosamine-6-sulfate. ....	14
Figure 3: Structure of an unsaturated 4/6monosulfated disaccharide .....	15
Figure 4: Tyrosine degradation pathway.. ..	20
Figure 5 A-Homogentisic acid (2,5-dihydroxyphenylacetic acid), B- Homogentisic acid semiquinone phenoxyl radical, C- Homogentisate ion.....	<b>Error! Bookmark not defined.</b>
Figure 6: Proposed mechanism of L-Tyrosine oxidation to a tryosyl radical via a cation intermediate and various isoforms of the tyrosyl radical.....	23
Figure 7: A. Chromatogram (refractive index) of intact porcine CS subjected to ABC lyase digestion B. size exclusion chromatogram of intact Porcine CS.....	28
Figure 8: Chromatogram (refractive index) of intact porcine CS (dissolved in water) subjected to chondroitin ABC lyase digestion and left for 24hrs.. ..	29
Figure 9: A. MS spectra of intact porcine CS subjected to enzyme depolymerisation by chondroitin ABC lyase.....	30
Figure 10: MS spectra of intact shark CS subjected to enzyme depolymerisation by chondroitin ABC lyase .....	31
Figure 11: MS2 analysis of m/z 457.9 from the negative ion spectra of intact porcine CS subjected to enzyme depolymerisation.....	31
Figure 12: Size exclusion chromatogram 200ul 10mg/ml of intact bovine CS at an elution rate of 0.4ml/min.....	32
Figure 13: Chromatogram (refractive index) of intact porcine CS .....	32
Figure 14: Chromatogram (refractive index) of intact shark CS .....	33
Figure 15 Size exclusion chromatogram of intact shark CS subjected to free radical depolymerisation via Fenton type reaction .....	34
Figure 16: MS spectra of A. intact shark CS B. intact bovine CS C. intact porcine CS .....	36
Figure 17: MS spectra of intact Shark CS that has been subjected to free radical depolymerisation..	37
Figure 18: Proposed structure of m/z 297.9 and 315.9 obtained from the free radical depolymerisation of intact CS.....	38
Figure 19: MS2 spectra of 240.8 fragment selected form the negative ion spectra of intact shark CS subjected to free radical depolymerisation.....	38
Figure 20: Negative ion spectra of intact bovine CS that has been subjected to free radical depolymerisations. ....	39
Figure 21: Negative ion spectra of intact porcine CS subjected to free radical depolymerisation .....	39
Figure 22: MS2 analysis of selected ions from the negative ion spectra obtained from free radical depolymerised shark and bovine.....	40
Figure 23: Negative ion spectra of 0.1M HGA .....	46
Figure 24: MS2 analysis of m/z 166.8 from the negative ion spectra of HGA and the proposed structure of m/z 122.8 ion .....	47

Figure 25: MS2 fragmentation spectra obtained from the negative ion spectra of 0.1M HGA at increased fragmentation energy of 1.5A. ....	48
Figure 26: Standard curve of increasing HGA concentration when analysed via ESI-MS. ....	48
Figure 27: Negative ion spectra of 0.1M HGA mixed with 10mg/mlCuSO4 and left for 24hrs. ....	49
Figure 28: MS2 analysis of m/z 194.7 obtained from the negative ion spectra of HGA and CUSO4. ..	50
Figure 29: Negative ion spectra of 0.1M HGA mixed with 10mg/ml FeC6H5O7 and left for 24hrs. ....	50
Figure 30: Proposed fragmentation pathway of HGA when analysed by ESI-MS in the negative ion mode with a fragmentation energy of 0.7V. ....	51
Figure 31: Left, size exclusion chromatogram of digested shark CS with the addition of HGA and CUSO4. Right, size exclusion chromatogram of intact shark CS subjected to free radical depolymerisation via fenton. ....	52
Figure 32: Negative ion spectra of intact Porcine CS with the addition of HGA and CuSO4. ....	53
Figure 33: Proposed structures of m/z 473.9 following free radical depolymerisation and its MS2 fragment m/z 393.9. ....	55
Figure 34: MS2 spectrum obtained from the fragmentation of m/z 395.9. ....	56
Figure 35: Negative ion spectra of Porcine CS digest with the addition of HGA and CuSO4. ....	56
Figure 36: Negative ion spectra of Shark CS digest with the addition of HGA and CuSO4. ....	57
Figure 37: Negative ion spectra of intact bovine CS with the addition of SOD before subjecting the mixture to fenton-like reaction and leaving for 24hrs. ....	58
Figure 38: Negative ion spectra of A.HGA and B.HGA and SOD what have both been left at room temp for 24hrs. ....	59
Figure 39: Negative ion spectra of A. HGA and CuSO4 left for 24hrs, B. SOD in the tube before the addition of HGA and CuSO4 then left for 24hrs. ....	60
Figure 40: Negative ion spectra of A. enzyme depolymerised porcine CS which was then added to HGA and CuSO4. B. Enzyme depolymerised porcine CS which was then added to SOD and then to HGA and CuSO4. ....	61
Figure 41: proposed fragmentation pathway of unsaturated monosulfated disaccharide. ....	65
Figure 42: Proposed monosaccharide structures as a result of intact CS being subjected to free radical depolymerisation. ....	66
Figure 43: Possible fragmentation pathway of m/z 240.8 of intact shark CS. ....	68
Figure 44: Main proposed fragmentation pathway of m/z 240.8. ....	69
Figure 45: 2 possible MS2 fragmentation pathways of m/z 214.8. ....	70
Figure 46: Proposed structure of m/z 475.9. ....	72
Figure 47: Proposed mechanism of the free radical degradation of chondroitin sulfate. ....	73
Figure 48: Mechanism of HGA oxidation to HGA benzoquinone (homogentisate) via a cation intermediate. ....	74
Figure 49: Unusual HGA Reaction. ....	75
Figure 50: Proposed square mechanism of the oxidation of phenol. ....	76
Figure 51: structure of hippoduric acid (orange pigment). ....	78
Figure 52: Proposed structures of HGA dimers based on the coupling of phenoxyl radicals. ....	79
Figure 53: Proposed mechanism of HGAs oxidation to a semiquinone and its unusual reaction with molecular oxygen to produce. ....	80
Figure 54: Proposed structure of HGA polymer after the generation of the HGA benzoquinone. ....	81

## Tables

Table 1: Mean relative abundance of fragments obtained from the negative ion spectra of intact CS subjected to enzyme depolymerisation.....	32
Table 2: Relative abundance of specific ions detected following free radical depolymerisation .....	41
Table 3: relative abundance of specific ions detected in figure 13 .....	42
Table 4: Relative abundance of specific ions detected in figure 15 .....	42
Table 5: Proposed structures of m/z 315.9, 299.9 and 297.9.....	43
Table 6: Proposed structures of m/z 214.8 and 184.8 .....	44
Table 7: Proposed structures of m/z 154.8.....	45



## **Acknowledgements**

**I would like to thank Dr Bob Lauder for his support in the research and writing of this thesis. I would also like to thank Dr Adam Taylor for his expertise in AKU and homogentisic acid. Finally I would like to thank my friends and family for their continued support throughout.**

## **Abbreviations**

AKU: Alkaptonuria

CAD: Collision activated dissociation

CS Chondroitin sulfate

DESI: desorption electrospray ionisation

DS: Dermatan Sulfate

ESI: Electrospray ionisation

GAG: Glycosaminoglycan

GalNAc: N-acetyl galactosamine

GlcA: Glucuronic acid

GlcNAc: N-acetyl glucosamine

HGA: Homogentisic acid

HPLC: High Performance liquid chromatography

IdoA: Iduronic acid

LC-MS: Liquid chromatography mass spectrometry

MALDI: matrix-assisted laser ionisation

OA: Osteoarthritis

PG: Proteoglycans

RNS: Reactive nitrogen species

ROS: Reactive oxygen species

SEC: Size exclusion chromatography

SOD: Superoxide dismutase

SPLET: sequential proton-loss electron transfer

# HPLC and ESI-MS analysis of free radical degradation of Chondroitin sulfate

## 1. Abstract

Chondroitin sulfate (CS) is vital component of bone and cartilage; it is widely used as a daily supplement in the management of arthritis. Reactive oxygen species (ROS) are involved in vast array of biological processes ranging from regulatory functions to damaging effects in disease pathogenesis. Mass spectrometry is a major tool in deciphering unknown chemical structures, particularly tandem MS. In this study mass spectrometry coupled with High performance liquid chromatography (HPLC) gives some insight into the potential mechanisms involved when ROS are made to attack CS. HPLC and coupled mass spectrometry showed that the free radical depolymerisation of CS yielded an *N*-acetylgalactosamine (GalNAc) and a uronic acid with varied sulfation. This led us to investigate the possibility of other means of free radical generation with the potential to degrade CS.

Alkaptonuria an ultra-rare (1:100000-1:250000) in born error of metabolism resulting in the accumulation of homogentisic acid (HGA) due to a deficiency in homogentisate1,2-dioxygenase. Polymerised HGA is excreted in the urine and deposited as an ochronotic pigment in cartilage. The mechanism of HGAs polymerisation is yet to be concluded due to the complexity of its reactions. This study aims to breakdown individual steps in HGAs biochemistry using mass spectrometry. This will provide further insight into the potential reactions HGA can undergo in the body and propose some mechanisms on how it may polymerise. Using mass spectrometry it became apparent that HGA polymerised when in the presence of copper and whilst HGA in water also yielded a dimer, the structure of which was proposed computationally.

Little is known on the mechanisms that underpin the displayed symptoms of AKU, it is known however that the polymerisation of HGA does play a role and is responsible for the ochronotic pigmentation in AKU patients. HPLC and ESI-MS was used to investigate the potential interactions between HGA and CS and propose that HGA is able to degrade CS disaccharides when in the presence of a copper catalyst. And that this interaction will play a role in the early onset of arthritis in AKU patients.

## 2 INTRODUCTION

### 2.1 Chondroitin sulfate

Chondroitin sulfate (CS) is a linear heteropolysaccharide first isolated from cartilage in 1884 and described in 1925. It consists of a repeating disaccharide motif composing of glucuronic acid (GlcA) and a C4/C6 sulfated *N*-acetyl galactosamine (GalNAc) joined by  $\beta(1\rightarrow4)$  or  $\beta(1\rightarrow3)$  linkages (Lauder 2009). It is found in many tissue types and a varied sulfation profile that varies on the source organism, tissue type and age (Clegg et al 2006); for example bovine tracheal CS is predominantly 4 sulfated whereas articular is mostly 6 sulfated (Bayliss et al 1995) (Table1).

It is a member of the important glycan class of glycosaminoglycans (GAGs) that includes: Keratan sulfate (KS), heparan sulfate (HS), heparin and dermatan sulfate (DS) and hyaluronan (HA). These GAGs, with the exception of HA, are covalently bound to a protein core forming the proteoglycans such as NeuraCan (CS), prelecan (HS) and fibromodulin (KS). More specifically, CS is bound to the protein component via a tetrasaccharide linkage region that is O-linked to a serine on the core (Figure 1). Other classes of glycans can be attached to protein via an asparagine residue and are known as *N*-glycans.

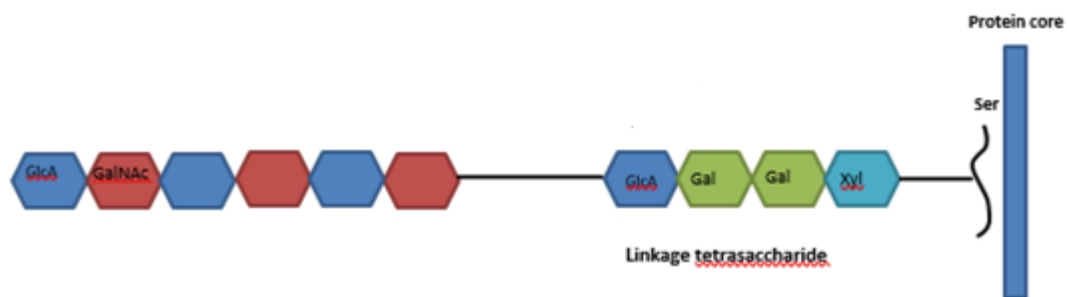


Figure 1: Chondroitin sulfate polymer consisting of alternate GlcA and GalNAc residues with a tetrasaccharide linkage region O-linked to serine residue on the protein core. This tetrasaccharide linkage region is also shared with DS polymers.

Chondroitin sulfate can be present in a number of forms, the most common of which is chondroitin-4-sulfate (CS-A), there are many types of Chondroitin sulfate (CS-O,A,B,C,D,E,F,K) that all vary based on their disaccharide linkage or sulfation (e.g. CS-B is also referred to as Dermatan sulfate, the major difference being that DS is composed of iduronic acid rather than uronic acid). In this study only chondroitin-6-sulfate (CS-C) dermatan sulfate (CS-B) and CS-A will be reviewed. It is possible that different CS chains may contain a mixture disaccharides with varied sulfation and may be of varying length depending on where they are most abundant in the body (Volpi 2009). Chain length can also vary with age exercise and joint injury (Brown et al 2007).

## **2.2 Dermatan sulfate**

Dermatan sulfate is a naturally occurring GAG found mostly in connective tissue and skin in humans. DS can also be found across species such as in Ascidians that possess 2-sulfated iduronic acids (Pavão et al 1998). It is synthesized by changing the stereochemistry of C5 of GlcA into an iduronic acid (idoA) which is an epimer of GlcA; this allows for the difference in function compared to CS (Figure 2). As a result of the position of the carboxygroup in IdoA, DS has a more flexible polysaccharide chain (Thelin et al 2013). In both CS and DS the tetrasaccharide linkage region (attached to a serine on the core protein) is almost identical because of the 4-O sulfation arising from the epimerization.

A major difference between CS and DS is that DS is known as a copolymer in that it can be composed of 2 types of disaccharide repeating unit- GalNAc and GlcA or GalNAc and IdoA (Silbert and Sugumaran 2002). CS on the other hand is believed to be composed only of the GalNAc-GlcA disaccharide (Thelin et al 2013). DSPGs can influence structure and function of the ECM as well as cellular behaviour (Seidler and Dreier 2008).

CS can exist with varied length dependant on the source or on the degree of cartilage degeneration. This means that the molecular weight of CS can vary from 20 to 100kDa which is important when determining the method of separation from complex mixtures. The chain length is dependent on the core protein, tissue location and disease contexts. So CS is a complex polysaccharide with a varied molecular weight which contributes to its chemical properties (Tat et al 2010).

Variation in CS structure can also occur due to the degree of sulfation which can occur on any of the free OH groups (4/6SGalNAc or 2/3SGlcA) which can generate a possible 16 isomers. These isomers may behave and respond differently to reactions such as hydrolysis or polymerisation (Hardingham and Fosang 1992).

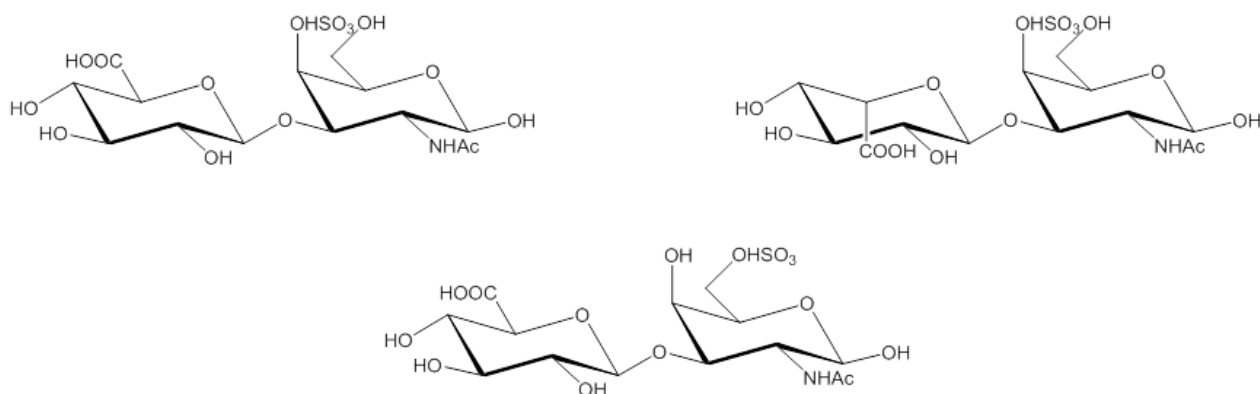


**Figure 2:** Disaccharide unit of CS-A:  $\beta$ -glucuronic acid-( $\alpha$ 1-3)-N-acetyl- $\beta$ -galactosamine-4-sulfate. CS-B: (Dermatan sulphate)  $\beta$ -iduronic acid-( $\alpha$ 1-3)-N-acetyl- $\beta$ -galactosamine-4-sulfate. CS-C:  $\beta$ -glucuronic acid-( $\alpha$ 1-3)-N-acetyl- $\beta$ -galactosamine-6-sulfate.

## 2.3 Production

For analytical studies (Also in this study) CS is commercially available in a powder form which is extracted from animal cartilage and purified (Tat et al 2007). The extraction process in commercial CS results in degradation and reduction in molecular weight to 10-40kDa which needs to be considered when devising a protocol for purification and analysis. It should also be noted that highly alkaline conditions and high temperatures should be avoided to prevent chemical and structural modifications (Martel-Pelletier et al 2015). In addition to this, acidic conditions may lead to the deacetylation of the GalNAc monomer. Purification techniques used commercially are vital to minimize the effect of contaminants which may be other GAGs, proteins or solvents (Calamia et al 2012, Lauder 2009). In these series of experiments commercially available CS was studied which stopped the need for extraction processes.

## 2.4 Physiological role

Chondroitin sulfate derived proteoglycans are vital throughout many tissue types and are involved in cellular processes such as cell adhesion and receptor binding whilst also maintaining ECM integrity (Rhodes and Fawcett, 2004). CS chains are an important molecule in water retention in cartilage due to its negative charge and are taken as a daily supplement to maintain joint health and also play a major role in cartilage growth and function. The CS domains of aggrecan (A large aggregating PG) provide a viscous gel that absorbs compressive force. CS also stimulates synovial cells to produce hyaluronan which maintains synovial fluid viscosity (David-Raoudi et al 2009).

## 2.5 Generating CS disaccharide

Enzymes that degrade intact CS are known as chondroitin lyases/ Chondroitinases (E.C No.232-777-9), these can be classified as ABC, AC, B and C based on what substrates they act upon. The lyase can act based upon linkage or sulfation (or both) e.g. chondroitin lyase AC will degrade Chondroitin A and C which are 4 and 6 sulfated respectively. Chondroitinase ABC can be divided ABCI and ABCII which differ in their kinetic parameters and modes of action (Chen et al 2015). Chondroitinase ABC degrades polysaccharides that contain 1,4-beta-D-hexosamiyl and 1,3-beta-D-glucuronosyl linkages. This means the enzyme will primarily act on Chondroitin4/6sulfate and dermatan sulfate to generate an unsaturated disaccharide represented above. Enzyme or chemical depolymerisation of the chains allows for a more effective MS analysis and a number of bacterial lyases are commercially available.

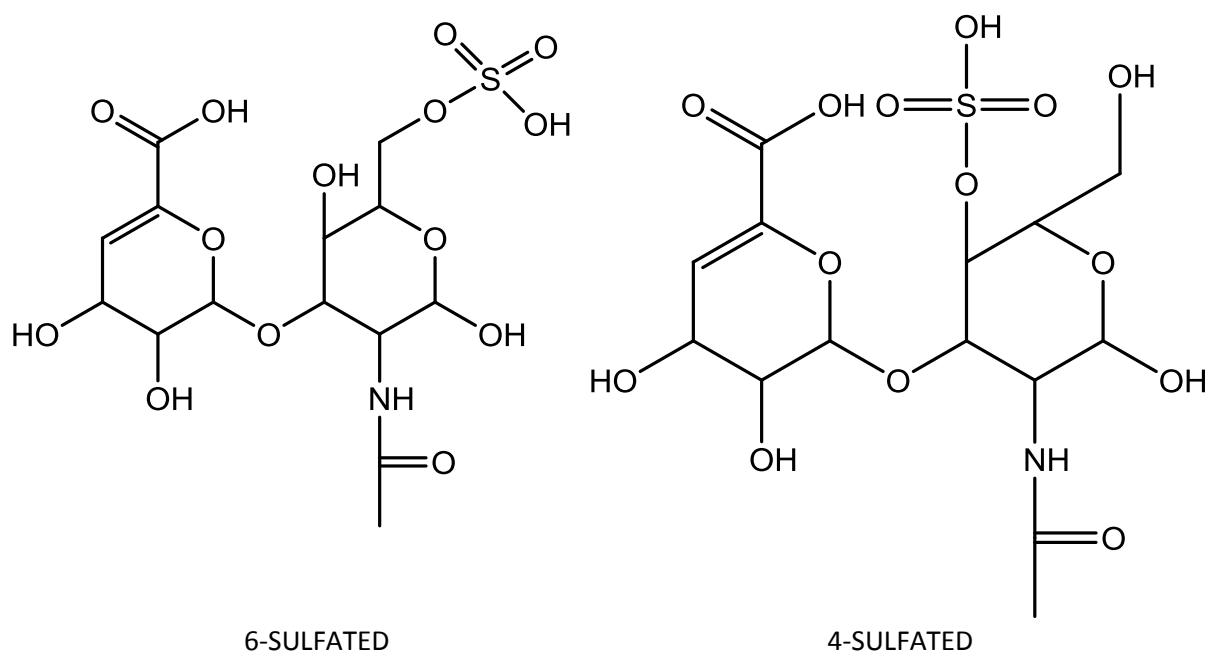


Figure 3: Structure of an unsaturated 4/6monosulfated disaccharide consisting of unsaturated GlcA and a 4/6S GalNAc that is the repeating unit of CS polymer and the product of the chondroitinase treated CS.

## 2.6 HPLC and mass spectrometry analysis of CS

Size exclusion chromatography (SEC) is a universal separation mechanism and can be utilised when studying CS due to its free solubility in aqueous solvents (Staples and Zaia 2011). A disadvantage of SEC is the limited ability for it to be scaled down i.e. from preparative to analytical scale as you quickly lose resolution in the chromatogram; however it is still possible to generate data for 10ug quantities of CS. HPLC analysis of chondroitin sulfate is difficult due to its hydrophilicity and is weakly retained on reverse phase adsorbents (Kosman et al 2017). In general HPLC analysis can be particularly challenging and often requires an additional UV active tag to achieve baseline

separation. In fact, the generation of an unsaturated disaccharide via enzymatic degradation would allow for HPLC analysis with a UV detector. Pulsed amperometric detection (PAD) may also be used, however this technique is very destructive and you may only use a small amount of material.

Mass spectrometry is a powerful technique enabling the elucidation of organic and inorganic structures. It allows illustration of fragmentation pathways and provides evidence of a molecule's elemental and isotopic formula. The chosen ionisation method will lead to varied fragmentation. The ionisation sources most frequently are electrospray ionisation (ESI), matrix-assisted laser ionisation (MALDI) and desorption electrospray ionisation (DESI). The principle of each technique is the same; a molecular ion is ionised then accelerated by an electric field. The fragment is separated by their mass:charge via an electromagnetic field. MALDI can be used to study carbohydrates up to  $10^6$  Da and requires a matrix for molecule ionization. This technique usually utilizes a nitrogen laser, the analyte is embedded in the matrix and absorbs energy emitted from the laser. A fraction of that analyte is then ionized.

There have been many protocols showing that GAG quantification is possible via MS/MS e.g. sulfated GAGs in cell lines (Kiselova et al 2014). The major advantage of ESI-MS over MALDI is the ability to couple an LC system which then allows quantification of GAGs. Analysis via MALDI would need prior purification and is much more difficult to achieve absolute quantification. Overall these MS/MS techniques contribute greatly to analysing the primary and secondary metabolites of GAGs.

## **2.7 Extraction**

It is essential that CS can be extracted from small quantities of tissue to allow analysis which will reveal the spatial and temporal regulation that is of interest to us. Usually CS and other GAGs are cleaved from the core via non-specific proteases, the sugar component is then extracted using guanidine hydrochloride (Ledin et al 2004). The bond between the xyl of the linkage region and Ser of the protein backbone is cleaved under reducing conditions using alkaline-Beta-elimination. After this the GAGs are usually subjected to anion exchange chromatography or solvent precipitation, this acts to enrich the released GAGs (Conrad 2001). It was found that the use of papain digestion, alkaline borohydride release, solid phase extraction and ethanol precipitation in CS extraction eliminated contaminants that usually generated high levels of noise (Hitchcock et al 2008).



## 2.8 ESI analysis of CS

ESI-MS is a technique used to ionize molecules in solution (up to 15kDa), this technique often ionises analytes into ions with a varied charge state which allows the analysis of high mass ions with a low m/z limit (Ho et al 2003). CS samples were analysed using ESI due to its soft ionization processes which enables the use of negative polarity without adding ion pairs to stabilize the sulfate groups (Staples and Zaia 2011). This is preferred over MALDI due to in-source dissociation (in MALDI) which generated weak signals and an abundant loss of SO<sub>3</sub> (Sisu et al 2011). In ESI-MS of CS each sulfate will render a charge of one, if there is no sulfation the carboxyl group will carry the charge. With ESI being the softest ionization, it allows the use of tandem MS through collision induced dissociation. The soft ionization of ESI-MS allows ion transfer from liquid to the gas phase via an eluent from a liquid chromatography system which have been investigated in previous studies

Tandem MS (MS/MS) can be used in GAG analysis to determine number of acetates or sulfates per monosaccharide and allows isobaric molecules to be distinguished based on their fragmentation. When analysing CS it may be used to produce information on the position of sulfates and uronic acid epimers (Bayliss et al 1999). This is important as mentioned earlier that CS sulfation can be at the 4O or 6O of GalNAc or the 2O of GlcA (Hitchcock et al 2006). The different CS types will produce distinct MS ions, the abundances of these specific ions will correlate to epimerisation and the sulfation pattern (Miller et al 2006).

Tandem MS analysis of CS and other GAGs is quite complex due the high charge states of their precursor ions. This results in MS ions with more than one charge state. There is a gap in GAG research that could be filled with sequencing toolkits that would increase the output of GAG MS2 analysis. There is no similar toolkit for CS there is one similar toolkit for heparin oligosaccharides. This is an algorithm that cross checks all possible sequences for a GAG composition with disaccharide analysis, tandem MS data and digestion enzyme activities (Ceroni et al 2008).

## 2.9 Disaccharide analysis

Previous studies have used ESI-MS to quantify GAG disaccharides whilst collision activated dissociation (CAD) has been used to differentiate isomers (Saad et al 2005). Small quantities of CS extracted from neural tissue have also been analysed by Nano-ESI interference. A reserve phase LC/MS system may also be used to quantify aminated GAG disaccharides. This technique quantifies disaccharides by using a stable isotope variant of the reductive amination tag (Lawrence et al 2008).

## **2.10 Oxygen Free radicals**

In order to understand the free radical degradation of macromolecules, the fundamentals of ROS must first be understood. As a consequence of cellular respiration, free radicals (a highly reactive uncharged molecule with an unpaired electron) are generated during redox reactions such as when ATP is produced in the mitochondria. The majority of radical by products are reactive oxygen species (ROS) or reactive nitrogen species (RNS)(Pham-Huy et al 2008). At low concentrations they function in a variety of cellular processes such as regulation of cellular signalling (Ray et al 2012), at high concentrations they adversely modify cell components such as lipids carbohydrates and proteins as a consequence of oxidative stress (Birben et al 2012). Oxidative damage of extracellular components (e.g. PGs) has been implicated in a number of diseases such as arthritis and cardiovascular disease (Alfadda and Sallam 2012).

## **2.11 Age and ROS**

Reactive oxygen species are a natural by-product of normal cellular metabolism, the negative effects of ROS generated in this way can be managed by the bodies antioxidant pathways. This system can be overrun by ROS generated from exposure to certain lifestyle choices. With an increase in age comes an increase in exposure to factors such as UV, cigarette smoking and alcohol consumption. These factors have the potential to generate ROS, UVB for example is known to stimulate the production of ROS in keratinocytes. Further to this, the elderly are more susceptible to infection, the inflammatory response to these infections will further generate ROS (Bhattacharyya et al 2014).

## **2.12 Arthritis and oxidative stress**

Rheumatoid Arthritis is a chronic and debilitating autoimmune disease caused by the long term inflammation of joints and its surrounding tissues. This is due to the infiltration of T-cells and macrophages (Walston et al 2006). Disease pathogenesis occurs due to ROS and RNS being generated during the inflammation process. Previous studies have revealed that isoprostanes and prostaglandins levels in serum increase as a result of oxidative damage-thus proving the resulting disease pathogenesis (Mahajan and Tandon 2004). Arthritis is mostly an age related disease, with the elderly suffering the most. Exceptions to this rule are patients of diseases such as AKU that suffer from early onset arthritis due to ochronotic pigmentation in cartilage.

A number of factors contribute to the development of arthritis- It is believed that alterations in the subchondral bone may occur early in the arthritis process and may be part of the initiation process. A number of morphological transformations occur that result in an increased production of osteoclasts. This occurs due to an excess in favourable biochemical conditions generated from osteoblasts (Cantley et al 2013). This same study showed that CS treatment suppressed osteoclast

activity as well as bone resorption. A study on shark CS also found that oversulfation significantly reduced osteoclast differentiation (Miyazaki et al 2010). This provides evidence to the suggestion that CS may be beneficially used in the treatment of arthritis.

The potential benefits of CS as a treatment for arthritis have been explored by somewhat low quality clinical trials with relatively small patient numbers tested (Uebelhart 2008) . These trials revealed that CS treatment (alone or combined with glucosamine) improved pain relief in patients in short term studies. Chondroitin treatment also had a lower risk of serious side effects when compared to controls. It was concluded that more high quality studies are needed to truly test the effectiveness of CS treatment. The popularity of CS as a daily supplement may be down to the efficacy and low risk associated with CS (Singh et al 2015).

GAGs such as CS and glucosamine are controversially considered to be slow acting drugs for arthritis, Some are even suggested to demonstrate a potential for disease modification (Henrotin et al 2014). The actual effectiveness of CS as an over the counter supplement is still disputed. Several guidelines such as NICE 2013 and OARSI 2014 do not recommend the administration of CS as a treatment for CS, whereas EULAR does (Henrotin et al 2014). Further study is required to determine CS functions in relation to cartilage before it can be considered a beneficial supplement.

A variety of meta-analyses have shown that CS has a positive effect on arthritis pain and symptoms (Hochberg et al 2008, Richey et al 2003). However several studies have also shown little effect of CS which may be due to the inclusion of studies using non-pharmaceutical grade CS (Martel-Pelletier et al 2015). A clinical trial of the use of CS as a treatment to arthritis also generated conflicting results when trying to illustrate the beneficial effects of CS in arthritis treatment (Rainsford 2009) .

### **2.13 Alkaptonuria**

Alkaptonuria(AKU) or black urine disease is an incurable rare autosomal recessive condition and the first in born error of metabolism as described by Garrod (1908). With a low incidence of 1 in 250000 to 1 in 1000000 live births (Tharini et al., 2011). The first noticeable symptom is the black urine, as the disease progresses the individual will suffer from Ochronosis (Black pigmentation of connective tissue) and by the age of 30, ochronotic arthropathy. It is caused by a mutation in the *HGO* gene coding for the enzyme homogentisate-1,2-dioxygenase, deficiency in this enzyme results in the blockage of the tyrosine metabolic pathway (Figure 4) and the accumulation of homogentisic acid (HGA) in mmol/L concentrations (Phornphutkul et al., 2002, O'brien, La Du and Bunim, 1963). It is thought that the presence of polymerised HGA in cartilage plays a role in the development of early onset arthritis.

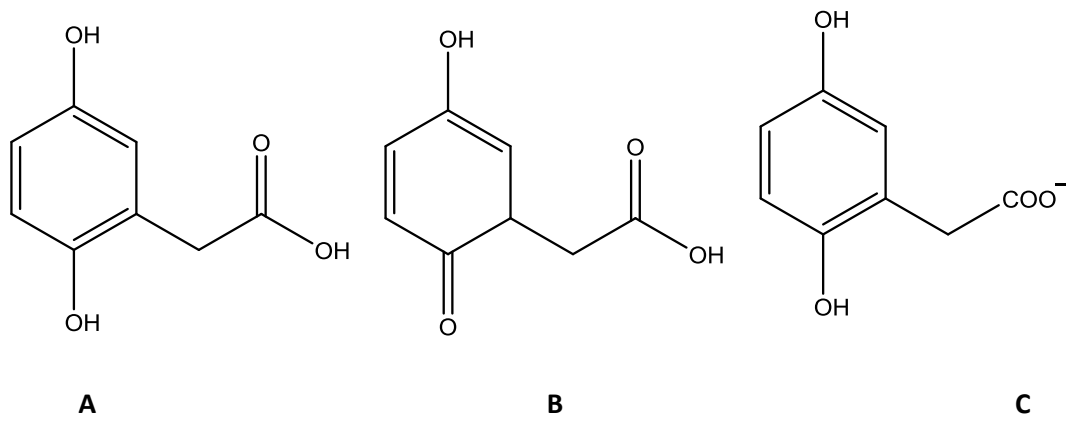


Figure 4 A-Homogentisic acid (2,5-dihydroxyphenylacetic acid), B- Homogentisic acid semiquinone phenoxyl radical, C- Homogentisate ion

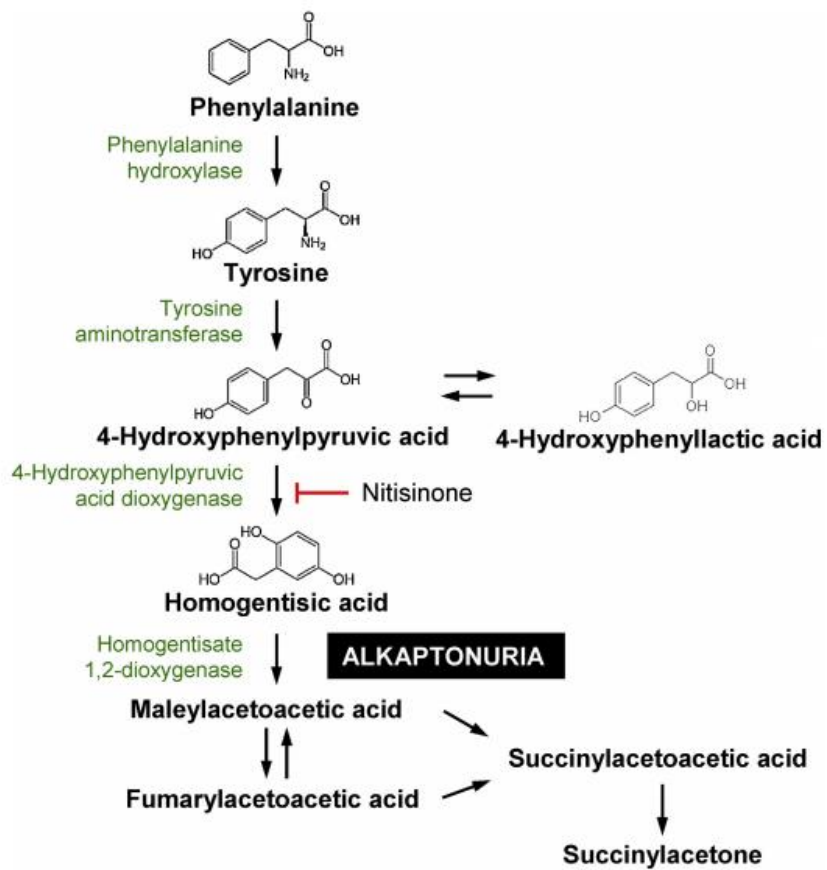


Figure 5 : Tyrosine degradation pathway. AKU develops due to the deficiency in homogentisate-1,2-dioxygenase resulting in an accumulation of homogentisic acid and the development of AKU (Hughes et al., 2014).

### **2.14 AKU and arthritis**

The most debilitating symptom of AKU is the early onset of arthritis caused by the ochronotic pigmentation in cartilage. Murine and invitro models of AKU have been developed and have allowed for better understanding in the progression of ochronosis and osteoarthropathy. Previous AKU studies have found that HGA is present in healthy cartilage, however it only becomes susceptible to degradation after biochemical change in HGA (Taylor et al 2011). There have been several overlaps in the pathogenesis between AKU and arthritis. These have arose from better understanding of the importance of subchondral bone and determining factors that affect cartilage integrity (Hayami et al 2004). Some of these factors include chondrocyte function and biochemical stresses which both affected in AKU athropathy (Karsdal et al 2008).

### **2.15 Homogentisic acid**

Homogentisic acid (2,5-dihydroxyphenylacetic acid) is a phenolic acid (Figure 5) that accumulates as a result of AKU and it part of the tyrosine degradation pathway. It can oxidize to its corresponding benzoquinone (and polymerises) with the generation of reactive oxygen species (ROS) which can then go on to degrade cellular components which may include macromolecules such as CS. These ROS can also go on to impact on several cascades and processes. HGA binds to connective tissue, in particular articular cartilage and it is though that ionic interactions play a role in this binding. The location of the pigmentation brings it close to cartilage macrocolecules such a s CS and means interactions are possible (i.e. the degradation of CS by HGA) It is known that the accumulation of polymerised HGA is the cause of the ochronotic pigmentation found in AKU patients. When left in water, the mixture will turn purple and it is presumed that this purple pigment is polymerised HGA, the mechanism of which is still disputed. There are a number of studies that investigate the potential polymerisation of HGA as well as its dimerization (Hegedus and Nayak 1994). Ochronosis leads to bone degradation and eventual joint replacement as a consequence of early onset arthritis. Other symptoms may include: aortic stenosis, increase in prostate and kidney stones (Phornphutkul et al., 2002). It has also been implicated in DNA damage through the generation of oxygen free radicals (Hiraku, Yamasaki and Kawanishi, 1998).

The generation of ROS by the polymerisation of HGA can have implications on a number of cascades such as the inflammatory response. Oxidative stress is a major contributor to the pathogenesis of a number of processes leading to conditions such as arthritis, alzheimers and inflammatory conditions. It is becoming more apparent that oxidative stress results from the accumulation of reactive oxygen species (ROS) or a compromised antioxidant defence (Suhr et al 1998) that can arise from a number of diseases such as cancer. In this study we will investigate the potential interactions between HGA and CS via the proposed generation of ROS by HGA. Reactive oxygen species are commonly

generated in biological systems by enzymatic and metal-catalysed oxidation . This is relevant in the study of HGAs biochemistry because it is believed that the metal catalysed oxidation/ polymerisation of HGA also generates ROS. The mechanism of which is believed to be similar to that of the Fenton reaction used to depolymerise intact CS.

### **2.16 Oxidation of tyrosine**

The oxidation of HGA is a vital early step in its polymerisation and is essential for the reaction to go ahead. Unfortunately there is very little literature on the mechanism of HGA oxidation; however there have been previous studies on the oxidation of tyrosine which is the parent molecule of HGA. In order to propose a mechanism for HGAs oxidation and polymerisation we must also understand the behaviour of its parent molecules in redox systems.

Tyrosine is one of the most oxidatively sensitive amino acid residues and so HGA is believed to have similar properties. Oxidation involves a one-step electron oxidation to form tyrosyl radicals (Figure 6) and may also undergo dimerization in a reaction similar to HGAs (Ali et al 2004). Tyrosyl radicals are vital components in many cellular processes such as enzyme maturation (Birben et al 2012, Pham-Huy et al 2008), for example the formation of a tyrosine radical is one of the PTMs in the generation of mature galactose oxidase. The first step in tyrosine oxidation is the addition of OH and the slow elimination of OH<sup>-</sup> (figure 6) It can then undergo reactions with other oxidants due to the deprotonation of the radical cation (Bergès et al 2011). A number of products can be generated via this reaction, these include: DOPA, dopamine and its quinone as well as dityrosine (Eickhoff et al 2001). Similarity in tyrosines and HGAs oxidation can be highlighted by figure 6 where several tyrosyl radical isoforms have very similar structures to the homogentisate ion.

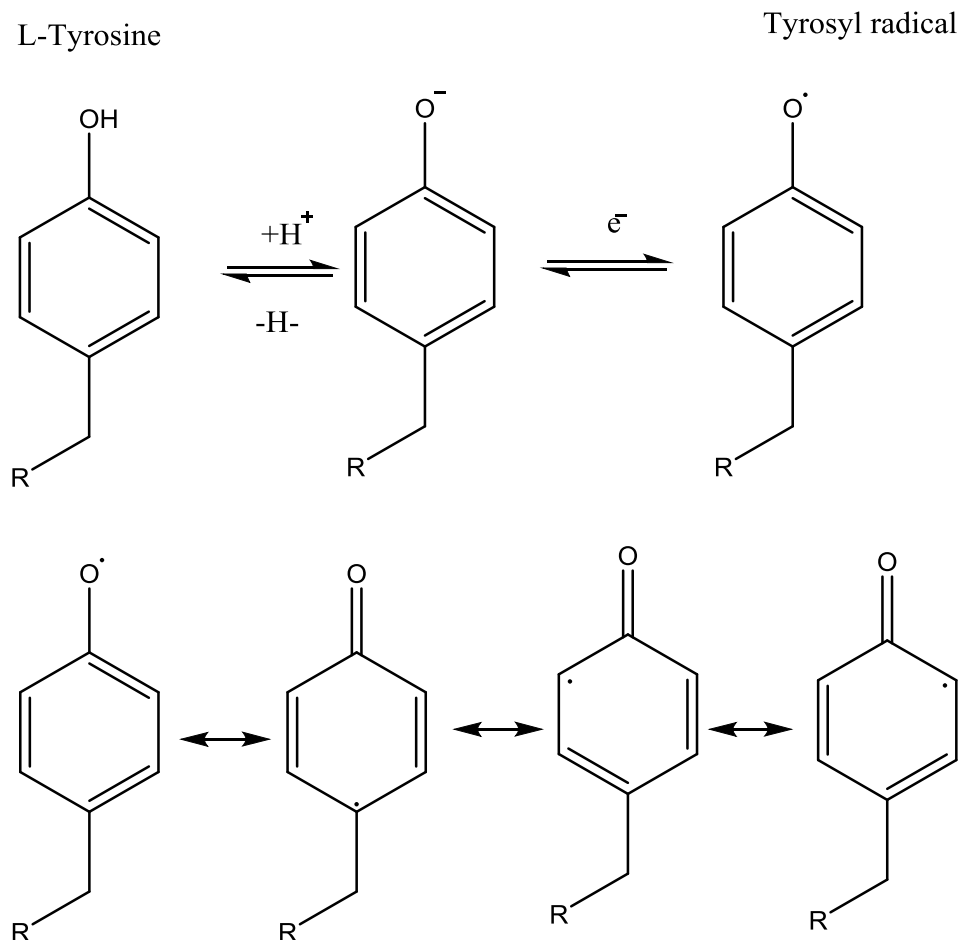


**Figure 6: Proposed mechanism of L-Tyrosine oxidation to a tyrosyl radical via a cation intermediate and various isoforms of the tyrosyl radical.**

The parallels between Tyr and HGA oxidation continues with the reaction being catalysed by Cu. As with HGA, the exact mechanism of this catalysis is still not well understood due to the formation of multiple oxidation products and the role of co-factors (Fang and Miller 2012). For the purpose of this study we will assume that Cu catalyses the oxidation of HGA in the same manner to tyrosine. This assumption is based on HGA and tyrosine undergoing similar mechanisms in reactions.

### 2.17 Interactions of HGA with CS

It is well documented in literature that HGA plays a role in the early onset of arthritis in AKU patients, however little is known about the mechanisms underlying the symptoms displayed by AKU patients. It was previously shown that HGA can potentially generate ROS via an unusual reaction with molecular oxygen and it has also been shown that CS is damaged by ROS. 3.2.2 HGA and Chondroptosis

The metal catalysed degradation of CS by HGA is a contributing factor explaining why AKU patients prematurely suffer from arthritis. The interactions between HGA and bone have previously been investigated but none have suggested this theory. AKU cartilage is known to consist of apoptotic

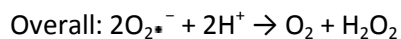
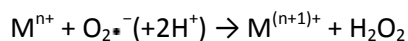
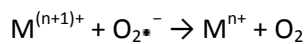
features of chondrocytes such as prominent Golgi and autophagic destruction (Millucci et al 2015). This increase in autophagic destruction will result in the culmination of oxidative stress being generated in the cell microenvironment (Braconi et al 2015). This can then go on to interact and degrade other biomolecules such as chondroitin sulfate.

### **2.18 Superoxide dismutase preventing oxidative stress**

SOD is a natural endogenous enzyme that acts as the cells first line of defence against oxidative stress. It eliminates superoxides ( $O_2^{\bullet -}$ ) by catalysing their dismutation into  $O_2$  and  $H_2O_2$  (Batinić-Haberle et al 2010). Dismutation or disproportionation is a specific redox reaction producing an oxidation and reduction product. The antioxidant properties of SOD can be mimicked through synthetic antioxidant compounds such as Mn porphyrin (Tovmasyan et al 2014). SOD mimics can be utilised to scavenge other radicals such as: peroxy nitrates, peroxy radicals and alkoxy radicals (Hidalgo and Donoso 2008) and are therefore not specific to scavenging superoxides.

SODs can be classified into 4 groups based on their metal cofactor- Iron-SOD, manganese-SOD, copper-zinc-SOD and nickel-SOD (Abreu and Cabelli 2010). CuZn-SOD is the most abundant SOD and is found in the cytosol and extracellular matrix. It has also been found that Mn can also act as a backup for CuZn-SOD independent of its role as an Mn-SOD cofactor (Reddi et al 2009).

The mechanism by which SOD functions is known as a 'ping-pong' mechanism. This involves a step by step oxidation and reduction of the metal centre with the accompanying oxidation and reduction of superoxide radicals (Reddi et al 2009). This occurs at diffusion controlled rates in neutral pH range. The metal catalysed dismutation has 2 major differences to an oxy radical spontaneous disproportionation. One is that there is no observable reaction of  $O_2^{\bullet -}$  with itself which leads to pH dependent disproportionation. Two is that the radical half-life becomes slower as oxy radical concentrations decrease.





### 3. Aims and objectives

The aim of the study was to propose some of the structures generated from the free radical degradation of intact and CS disaccharide. Structures were proposed using the fragments generated in ESI-MS. The connection between the polymerisation of HGA and CS will then be studied using the same methods of HPLC and ESI-MS. HGA polymerisation was proposed using CuSO<sub>4</sub> as the catalyst.

The aim of this study is to find a link between the generation of ROS via HGA polymerisation by mass spectrometry. Firstly the proposed dimer structure was proposed following MS<sub>2</sub> analysis of HGA. The copper catalysed polymerisation of HGA will then be investigated, and finally we will compare and contrast the mechanism of fenton-mediated ROS production to that of the HGA mediated mechanism. The proposal is that the polymerisation of HGA leads to the generation of oxygen free radicals that can then go on to breakdown CS disaccharides. The ability to halt the free radical degradation of CS was then studied using superoxide dismutase which was also confirmed using ESI-MS.

### 4. Material

Shark, porcine and bovine chondroitin sulfate were purchased from Sigma Aldrich. Chondroitin ABC lyase from *Proteus vulgaris* (E.C 232-777-9) , 30% H<sub>2</sub>O<sub>2</sub> (Cat No.95321) and Cu(II)SO<sub>4</sub> (E.C 231-847-6) purchased from Sigma Aldrich. SES column was a TOYOPEARL® HW-40S Bulk Media (Cat No. 807451) purchased from Sigma Aldrich, analysis of HPLC chromatograms were performed using Unicorn software and Microsoft excel. MS analysis was performed using Microsoft excel. Homogentisic acid was purchased from sigma Aldrich (E.C2 07-192-7) . Superoxide dismutase purchased from Sigma Aldrich (E.C 232-943-0). HPLC was performed on an AKTA purifier with HW40S column and Ammonium citrate mobile phase. MS experiments were performed on A bruker daltonics ESI-MS.

## 5 Methods

### 5.1 Enzyme depolymerisation of intact CS

20mg/ml (water) Chondroitin sulfate from shark cartilage, porcine trachea and bovine trachea samples were prepared in 1.5ml eppendorfs. 100ul of solubilised CS was digested with 0.008U chondroitin ABC lyase and incubated for 24hrs at 37°C. The reaction was stopped via the addition of

methanol to precipitate the protein component and the sugar component (in the aqueous layer) was analysed via ESI-MS and HPLC.

## 5.2 Free radical depolymerisation of intact CS

50ul aliquots of 20mg/ml CS porcine, bovine and shark were depolymerised by a Fenton type reaction using (see below) 175ul 30% v/v H<sub>2</sub>O<sub>2</sub> and 20ul of 10mg/ml CuSO<sub>4</sub> and left at 37°C for 24h. The crude reaction mixture was analysed via ESI-MS and HPLC. The same procedure with bovine, porcine and shark CS was then followed apart from the use of 10ul 20mg/ml Fe<sup>(III)</sup> Citrate instead of CuSO<sub>4</sub>.

The effect of H<sub>2</sub>O<sub>2</sub> volume and CuSO<sub>4</sub> concentration on the degree of CS degradation was investigated respectively. The volumes of H<sub>2</sub>O<sub>2</sub> used were as follows: 10ul, 17.5ul, 175ul and 1.75ml, concentrations and volumes of CS and CuSO<sub>4</sub> remained constant to the values noted earlier. The concentrations of CuSO<sub>4</sub> were as follows: 5mg/ml, 10mg/ml, 20mg/ml and 40mg/ml.



## 5.3 Free radical depolymerisation of digested CS

100ul of solubilised CS was digested with 0.008U chondroitin ABC lyase and incubated for 24hrs at 37°C. 100ul aliquots of enzyme digested porcine, shark and bovine CS were then treated with 175ul 30% v/v H<sub>2</sub>O<sub>2</sub> and 20ul 10mg/ml CuSO<sub>4</sub> and left for a further 24hrs at 37°C. Changing the volume of H<sub>2</sub>O<sub>2</sub> had no significant effect on the depolymerisation of enzymatically digested CS.

## 5.4 HPLC analysis of free radical and enzyme depolymerised CS and DS.

1ml of solubilised CS was digested with 0.008U chondroitin ABC lyase and incubated for 24hrs at 37°C. 200ul of digested CS were subjected to size exclusion chromatography using a Toyopearl HW40-S column at a flow rate of 300ul/min at room temp and using 0.1M ammonium acetate as the running buffer. Absorbance at 232nm was monitored and samples were collected manually. V<sub>0</sub> and V<sub>1</sub> were determined using 0.1M bovine serum albumin. 200ul of depolymerised CS was also subjected to the same method.

## 5.5 MS sample prep and parameters

Samples were prepared using 45% MS-grade H<sub>2</sub>O, 50% MS grade acetonitrile and 5% of sample. Samples infused via a syringe into a HCT ultra Bruker Daltonics MS at a rate of 200ul/min. Analysis in the negative ion mode. Data was acquired using Bruker Daltonics Esquire software (2 mins per sample) and analysed by Bruker Daltonics software.

Mass range 50-1000 m/z, smart target 20000, capillary voltage +3600, end plate offset -500V, skimmer -32V, capillary exit -100V, trap driver 44V, Octopole 1 DC = -9.67V, Octopole 2 DC = -1.6V, Lens 1 = 9.5V, Lens 2 = 85V, Temp = 280°C, Dry gas flow = 4l/min. MS/MS fragmentation was performed using the same parameters using fragmentation energy of 0.7V and a range of +/- 2Da.

### **5.6 MS sample prep for HGA**

MS samples were initially prepared as followed: 50% MS grade ACN 5%Sample and 45% MS grade water . To study the effect of solvents on HGA oxidation , 5ul 0.1M HGA was added to either: 95ul Acetonitrile, 95ul MS-grade water or 50ul acetonitrile and 45ul MS-grade water.To investigate metal catalysed HGA polymerisation, 10ul 0.1M HGA was prepared in water and then added to 10ul 10mg/ml CuSO<sub>4</sub> and left for 24hrs at room temp. The crude reaction mixture was then subjected to ESI-MS using the same instrument as stated in 1.6.5.

### **5.7 HPLC analysis of HGA interaction with intact CS**

20mg/ml (water) Chondroitin sulfate from shark cartilage, porcine trachea and bovine trachea samples were prepared in 1.5ml eppendorfs. 200ul of solubilised CS was digested with 0.008U chondroitin ABC lyase and incubated for 24hrs at 37°C. 20ul 0.01M HGA (in water) and 20ul 10mg/ml CuSO<sub>4</sub> was then added to the digest and left to incubate for a further 24hrs at room temp.

### **5.8 HPLC analysis of HGA interaction with enzyme depolymerised CS**

200ul of digested CS with HGA was then subjected to size exclusion chromatography using a Toyopearl HW40-S column at a flow rate of 300ul/min at room temp and using 0.1M ammonium acetate as the running buffer. Absorbance at 232nm was monitored and samples were collected manually.

### **5.9 Mass spectrometry Anlysis of SOD incubation with CS and Fenton reaction**

20ul SOD (5000U) was added to 20ul 20mg/ml CS, 10ul of 20mg/ml CuSO<sub>4</sub> and 10ul H<sub>2</sub>O<sub>2</sub> were then added to the mixture and left at room temperature for 24hrs. Controls were also ran alongside this experiment (1. Without SOD, 2. Without H<sub>2</sub>O<sub>2</sub> and CuSO<sub>4</sub>). The same experiment was then set up but with iron citrate instead of CuSO<sub>4</sub> as a means of forming superoxide radicals. A mixture was then set up containing 5% sample, 45% HPLC grade water and 50% ACN and for mass spec analysis.

Investigation into the free radical damage of intact CS was set up according to the methods in chapter one. 20ul SOD was added to this mixture and sample mixture was prepared for mass spec analysis in the same way as above.

## 6 Results

### 6.1 Enzymatic depolymerisation of intact CS

#### 6.1.1 HPLC analysis of Digest

When running BSA standards through the column to determine  $V_0$  it became apparent that around 12ml was the void volume. Size exclusion chromatography analysis of CS from 3 different species all showed very similar profiles. They all composed of a defined peak around 12.4ml eluent volume which corresponds to intact CS. A large trough was also seen at 22.5ml elution volume which corresponded to the water in the sample. It seems that intact porcine and bovine had a more defined peak at 12.4ml elution volume when compared to intact shark.

Intact CS from shark, bovine and porcine were subjected to enzymatic depolymerisation via chondroitinase ABC. The resulting product was subjected to HPLC analysis as seen below. 20mg/ml of intact CS was treated with 0.008U of Chondroitinase ABC overnight at 37°C. Separation was achieved using Toyopearl HW40-S resin at a flow rate of 0.3ml/min and a total eluent volume of 25ml.

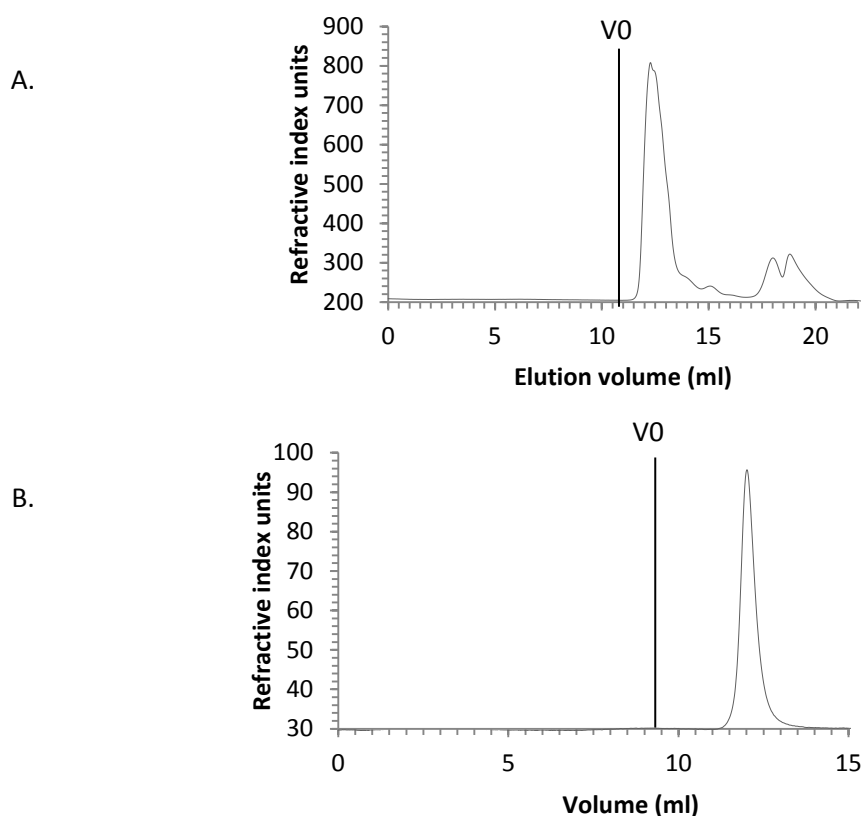
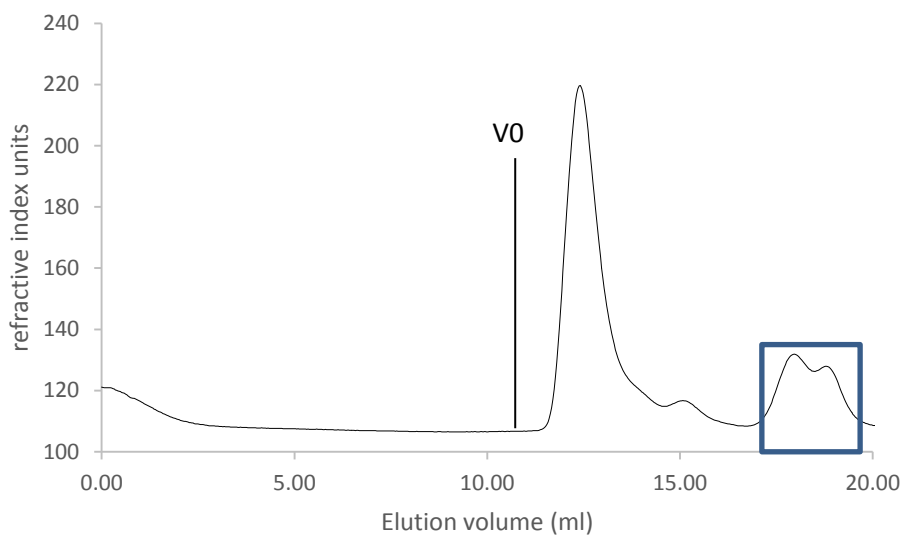


Figure 7: A. Top Chromatogram (refractive index) of intact porcine CS (dissolved in ammonium phosphate) subjected to ABC lyase digestion and left for 24hrs. B. size exclusion chromatogram of intact Porcine CS. Analysis was performed on an AKTA purifier using toyopeal 40S stationary phase.

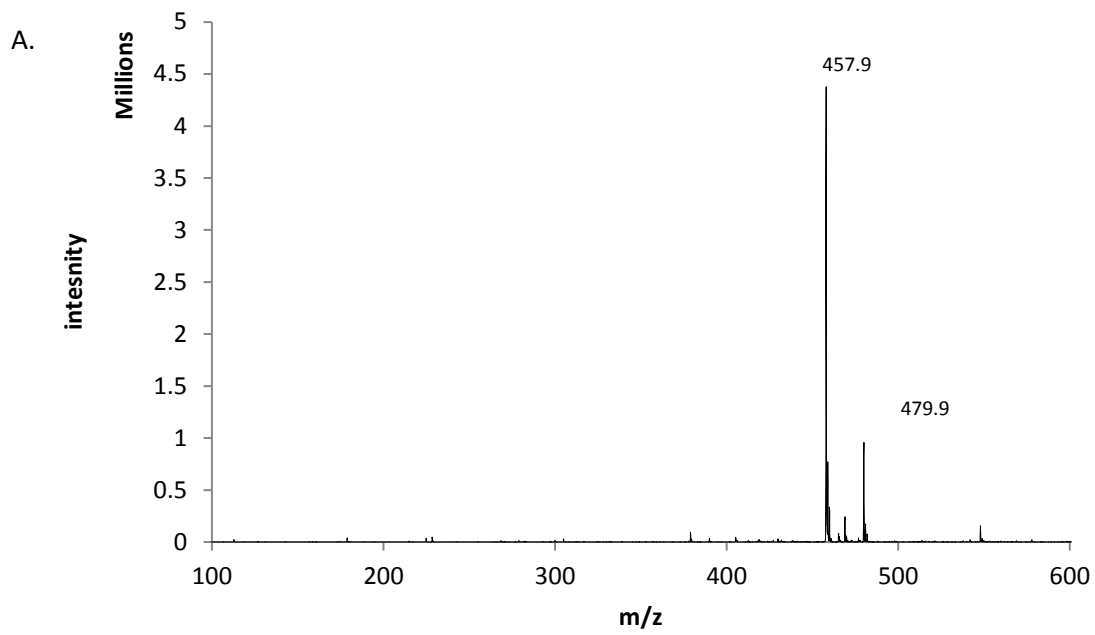
The large peak at 12.4ml eluent volume corresponds to intact CS whilst the split peak at 18-19ml eluent volume corresponds to the CS disaccharide. This was confirmed when subjecting the fractions to ESI-MS (figure 9).



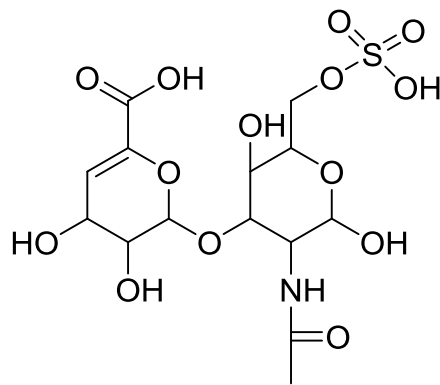
**Figure 7: Chromatogram (refractive index) of intact porcine CS (dissolved in water) subjected to chondroitin ABC lyase digestion and left for 24hrs. The highlighted blue region (Elution volume 18-19ml) consists of the fractions that contain the disaccharide products of the depolymerisation and are investigated further for MS analysis.**

The effect of the diluent (water and ammonium phosphate) in the enzyme digest of intact porcine CS was then investigated. We can see from figure 6 and 7 that this had very little impact on the obtained profile. ESI-MS analysis of fractions within the 18-19ml eluent volume showed an abundance of  $m/z$  457.9 (blue region on figure 9) corresponding to the monosulfated disaccharide.

### 6.1.2 MS digest CS



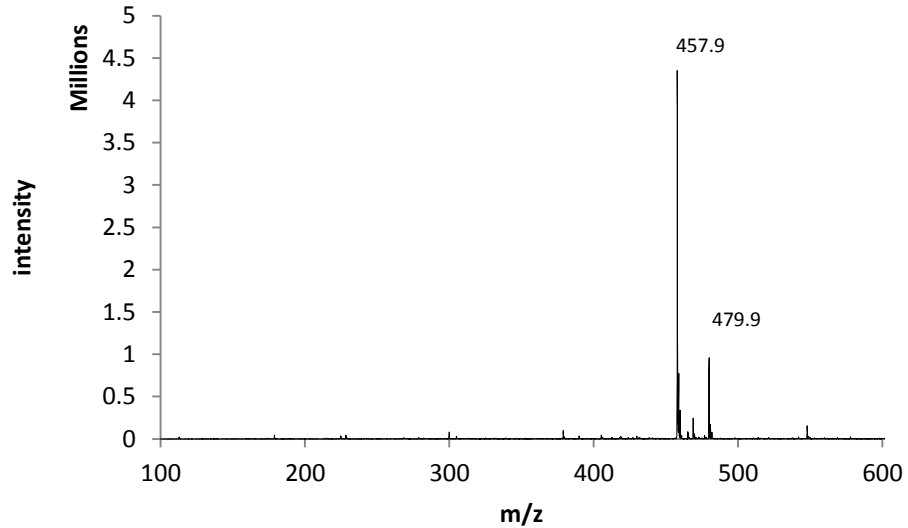
B.



Exact Mass: 459.0683

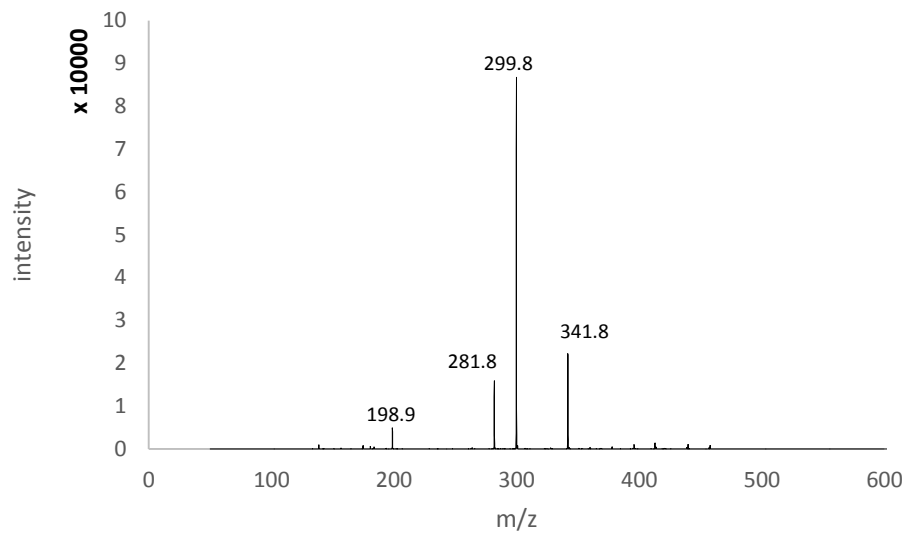
Recorded m/z 457.9

Figure 8: A. ESI-MS spectra of intact porcine CS subjected to enzyme depolymerisation by chondroitin ABC lyase. B. predicted structure of m/z 457.8 ( $479.9 - [M+Na^+]$ ) corresponding to a monounsaturated 6-sulfated disaccharide.



**Figure 9: Negative ion spectra of intact shark CS subjected to enzyme depolymerisation by chondroitin ABC lyase, major peaks of 457.9 and 479.9 corresponds to the monounsaturated 6-sulfated disaccharide**

The mass spectra show the presence of 2 major ions- 457.9 and 479.9. 457.9 was present in the digestion of porcine, bovine and shark CS. m/z 457.9 corresponds to the protonated adduct of the monounsaturated 6S-disaccharide whilst m/z 479.9 corresponds to its sodiated adduct.



**Figure 10: MS2 analysis of m/z 457.9 (Monounsaturated disaccharide) from the negative ion spectra of intact porcine CS subjected to enzyme depolymerisation (Figure 10).**

	457.9	479.9	341.8	299.8	228.8
Porcine	100.00%	18.85%	0.65%	1.98%	0.30%
Shark	100.00%	18.92%	0.50%	1.84%	0.33%
Bovine	100.00%	18.84%	0.52%	1.88%	0.30%

Table 1: Mean relative abundance of fragments obtained from the negative ion spectra of intact CS subjected to enzyme depolymerisation.

## 6.2 HPLC of intact CS

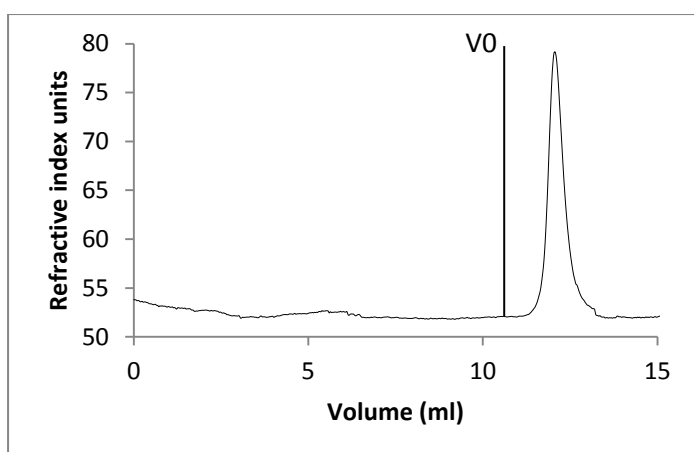


Figure 11: Size exclusion chromatogram of 200ul 10mg/ml of intact bovine CS (water) at an elution rate of 0.4ml/min.

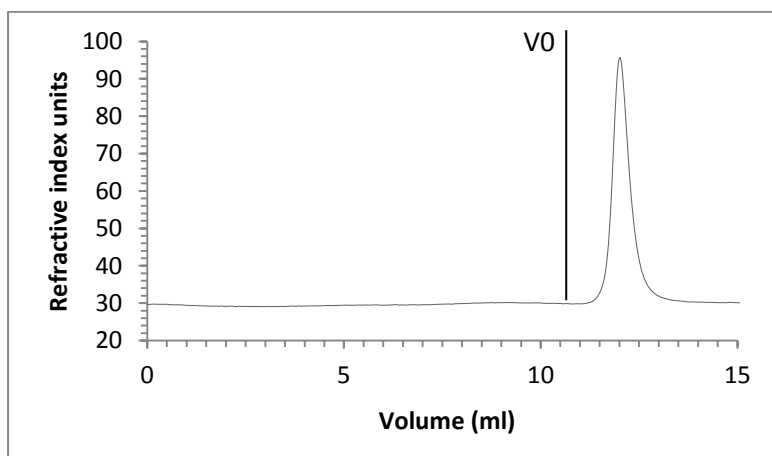
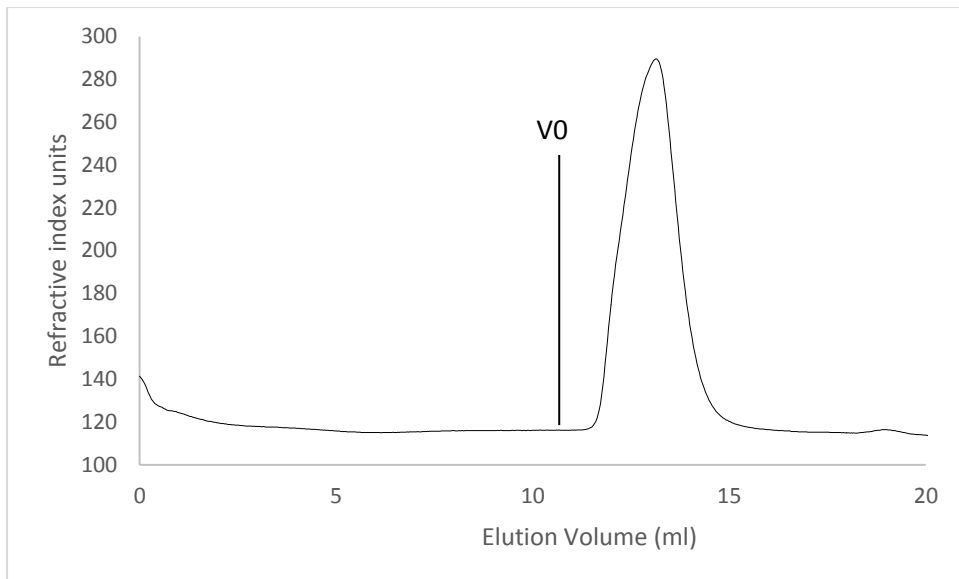


Figure 12: Chromatogram (refractive index) of 200ul of 10mg/ml intact porcine CS (dissolved in water) at an elution rate of 0.4ml/min





**Figure 13: SEC Chromatogram (refractive index) of intact shark CS (dissolved in water) at an elution rate of 0.4ml/min with ammonium acetate mobile phase.**

### 6.3 HPLC profiles of depolymerised CS

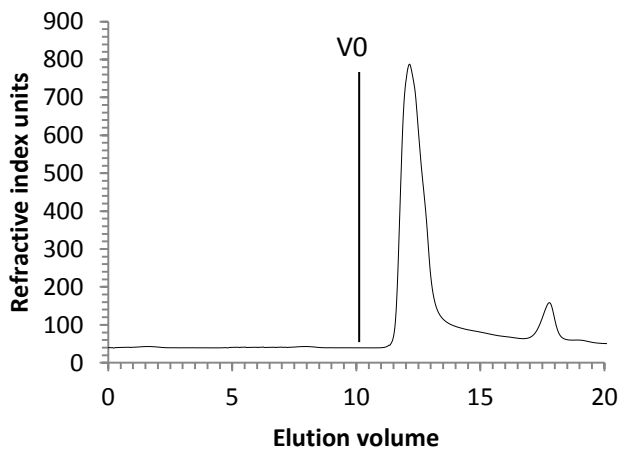


Figure 14 Size exclusion chromatogram of intact shark CS subjected to free radical depolymerisation via Fenton type reaction and left for A. 2hrs B. 24hrs C. 3 days

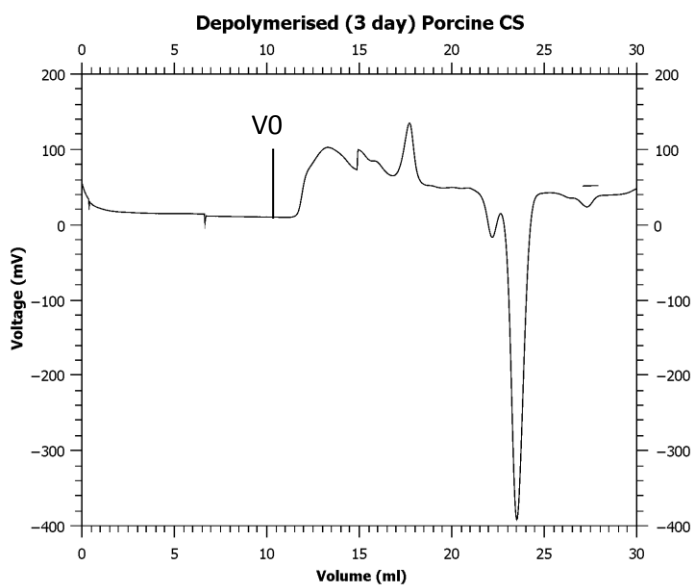
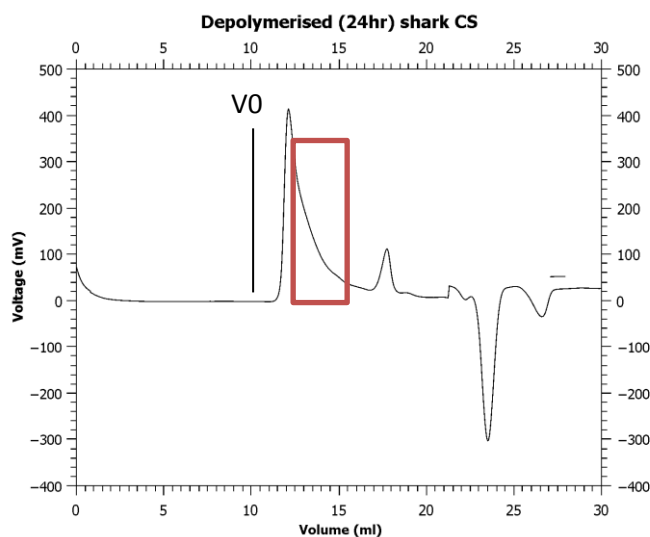
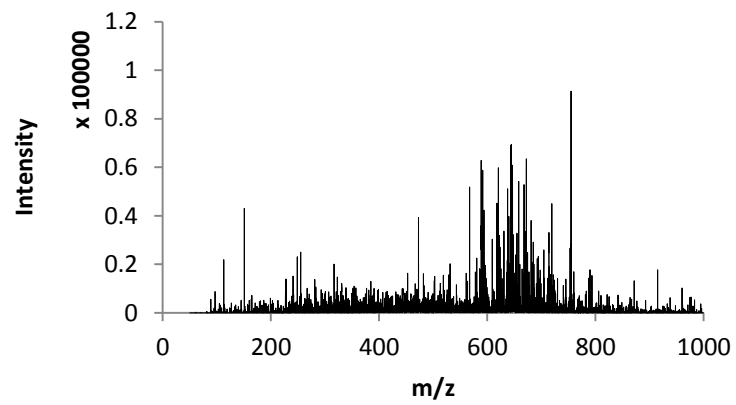


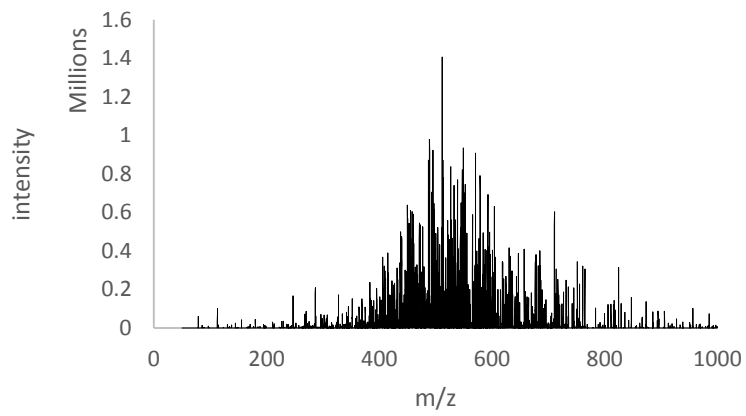
Figure 15 shows the size exclusion chromatograms obtained following free radical depolymerisation of intact CS. As you can see after 2hrs there is a large peak at 12ml elution volume corresponding to the intact CS and a small peak at 17ml corresponding to CuSO<sub>4</sub>. After 24hrs the intact CS peak is still present however this is followed by a steady slope that is believed to contain the free radical depolymerised CS/ After 3 days the sharp peak at 12ml is no longer present and instead replaced with a broader region that stretches to around 17ml elution volume. This is the region that is believed to contain the depolymerisation products.

## 6.4 MS intact CS

A.



B.



C.

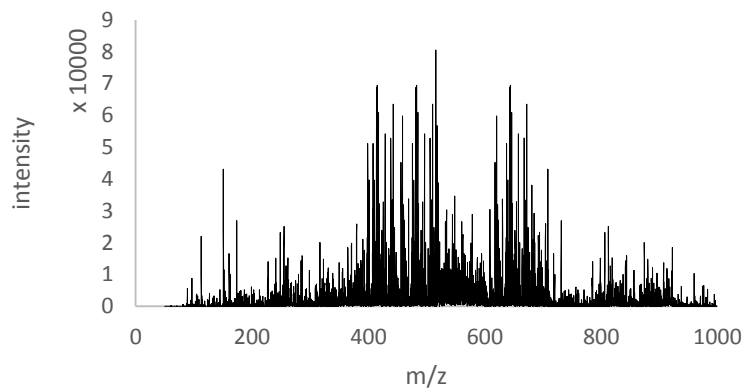
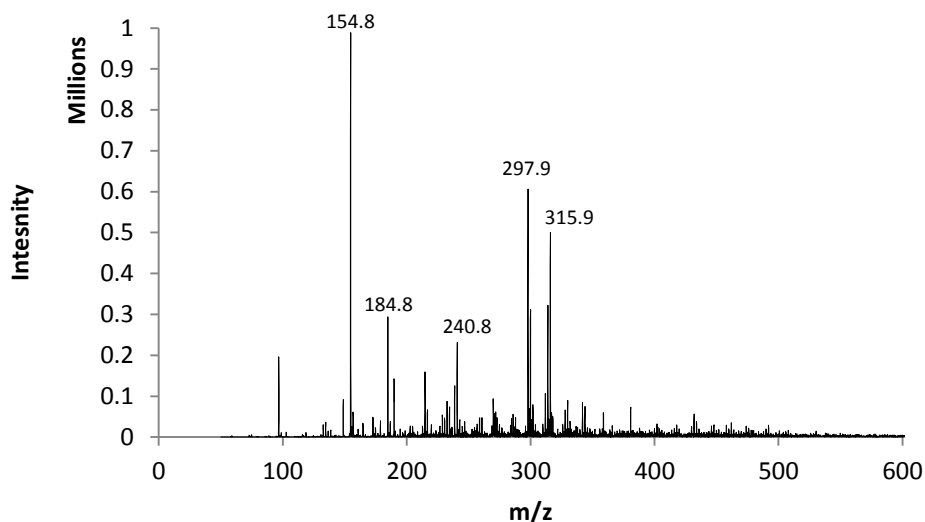


Figure 15: Negative ion spectra of 10ul 1mg/ml of A. intact shark CS B. intact bovine CS C. intact porcine CS

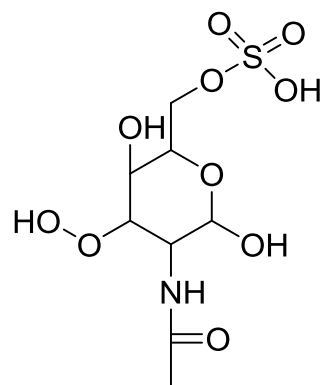
ESI-MS analysis of intact CS shows a spectra with undefined peaks and a large number of signals at various  $m/z$ . In all spectra a large number of signals are seen which makes it very difficult to define individual  $m/z$  values. These undefined peaks corresponds to the various CS chains that are fragmented when passed through the mass spec and each producing their own signal.

## 6.5 MS depolymerised CS



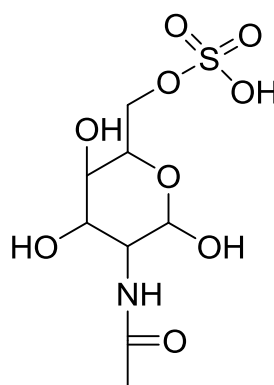
**Figure 16: Negative ion spectra of intact Shark CS that has been subjected to free radical depolymerisation via Fenton type reaction and left for 24hrs.**

Following free radical depolymerisation 5 peaks of interest were generated: 154.8, 184.8, 240.8, 297.9 and 315.9. These peaks were further investigated via MS2 analysis and theoretical construction. Experiments in a previous study showed the identity of 297.9 and 315.9 to be an saturated and saturated 6S-GalNAc respectively (figure17). The other fragments have not yet been characterised. The 154.8 fragment which yielded the greatest intensity was used as the base peak for relative intensity analysis for this spectra. The only notable difference between shark and bovine and porcine spectra is the presence of a peak at an  $m/z$  of 240.8 which isn't initially noticeable in porcine and bovine.



Exact Mass: 317.0417

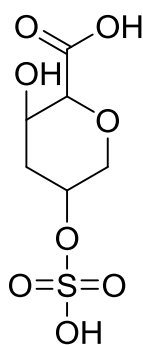
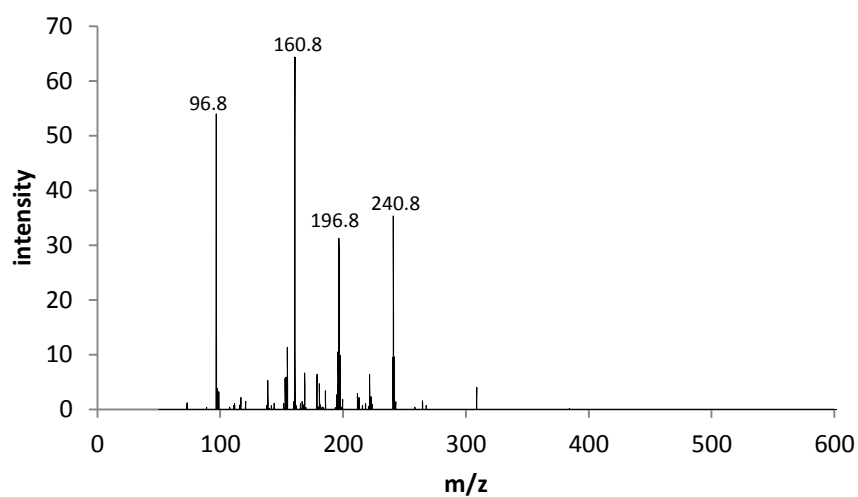
m/z 315.9



Exact Mass: 301.0468

m/z 297.9

Figure 17: Proposed structure of m/z 297.9 and 315.9 obtained from the free radical depolymerisation of intact CS



Exact Mass: 242.0096

Recorded m/z 240.8

Figure 18: MS2 spectra of 240.8 fragment selected from the negative ion spectra of intact shark CS subjected to free radical depolymerisation via Fenton type reaction. B. proposed structure of m/z 240.8 which corresponds to 4S glcA.

Fragmentation of the 240.8 ion yields 4 major peaks of  $m/z$ : 240.8, 296.8, 160.8 and 96.8. Although these intensities are very low, relatively they still produce a signal to warrant further analysis.

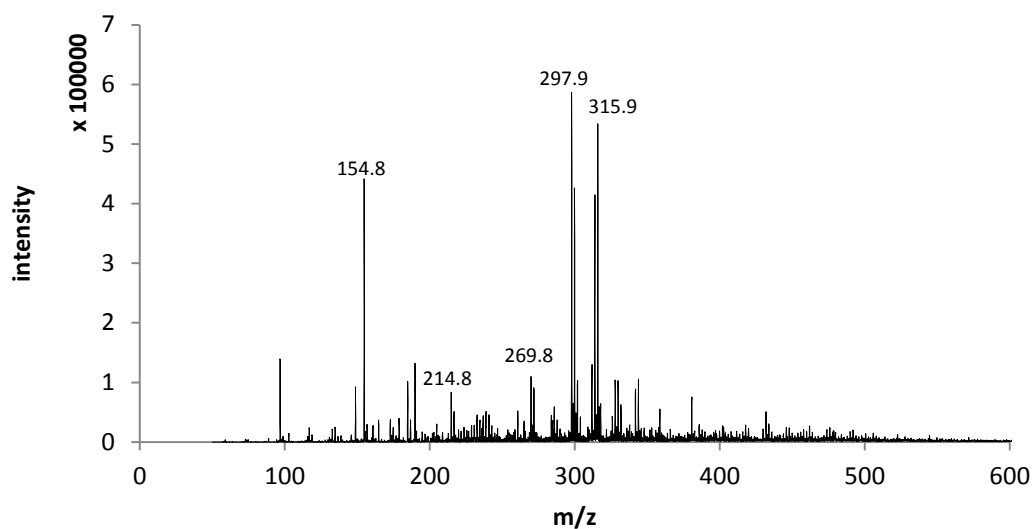


Figure 19: Negative ion spectra of intact bovine CS that has been subjected to free radical depolymerisation via Fenton type reaction and left for 24hrs the base peak of  $m/z$  297.9 corresponds to an unsaturated 4S GalNAc .

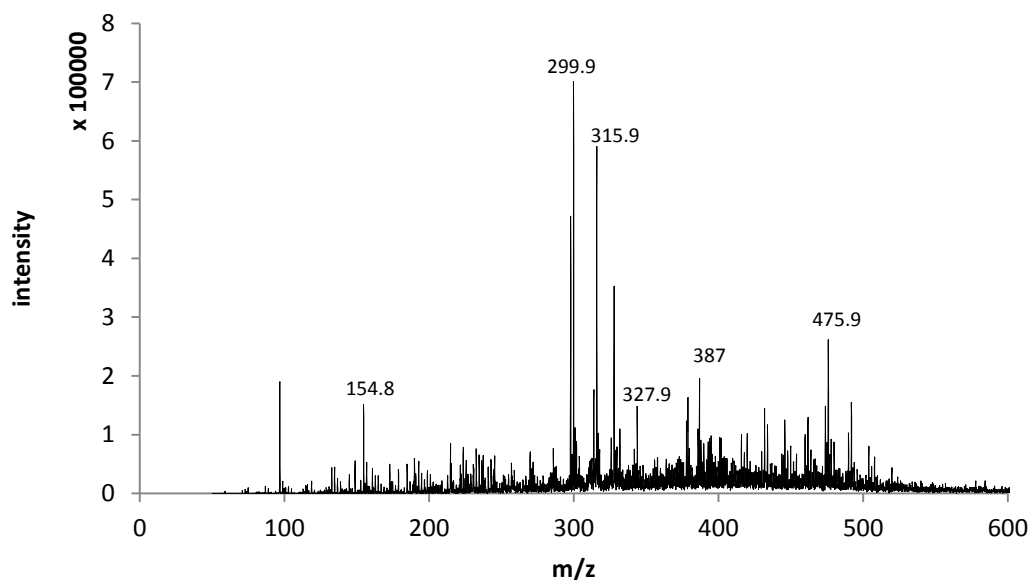


Figure 20: Negative ion spectra of intact porcine CS subjected to free radical depolymerisation via Fenton type reaction and left for 24hrs.

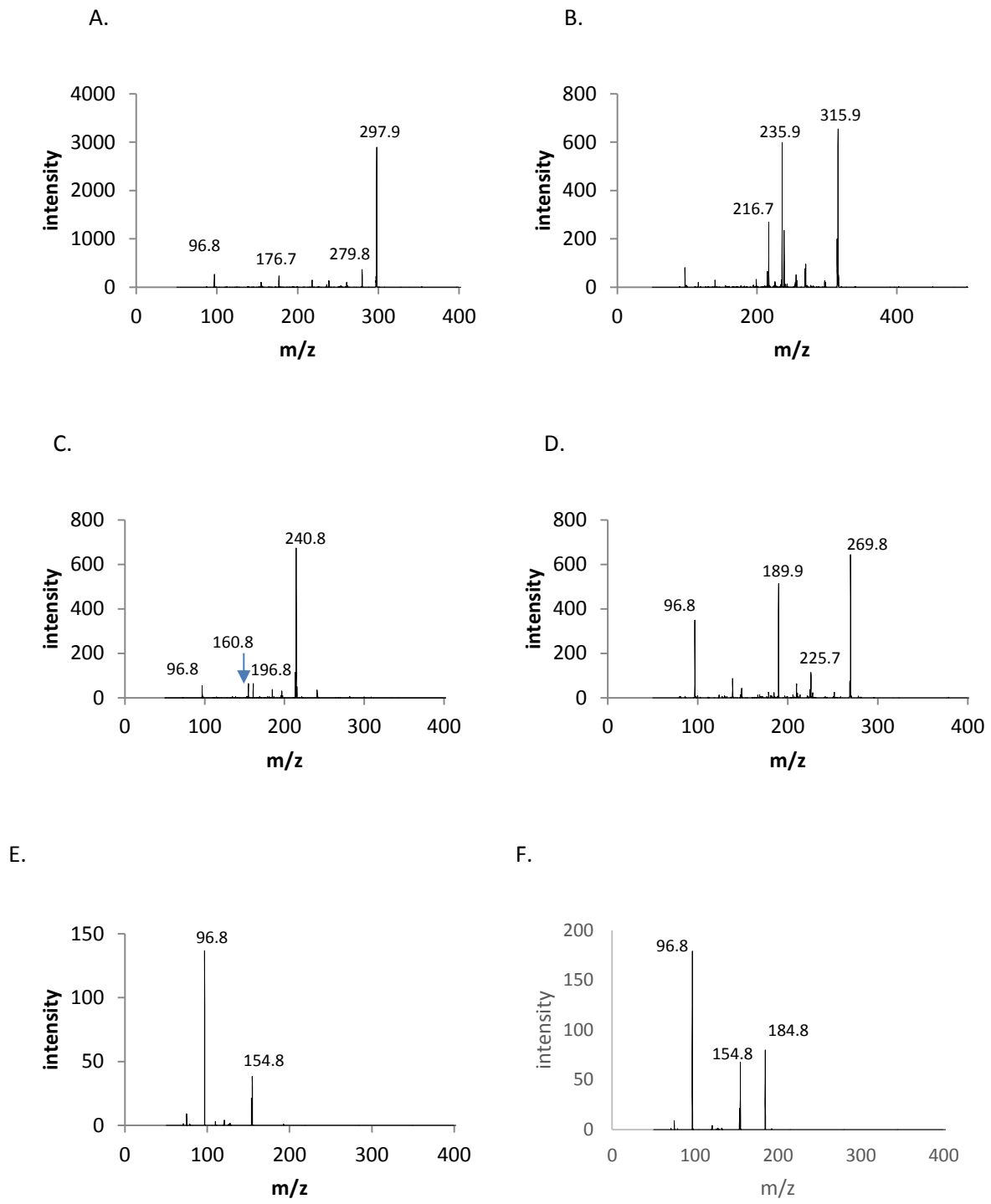


Figure 21: MS2 analysis of selected ions from the negative ion spectra obtained from free radical depolymerised shark and bovine CS. A. 297.9 fragment, B. 315.9 fragment, C. 240.8 fragment, D. 269.8 fragment, E. 154.8 fragment and F. 184.8 fragment.



Further MS2 analysis of the 297.9 fragment shows an MS2 spectra dominated by that m/z with an intensity of 2836.32. on further examination the m/z 297.9 fragmentation also yielded 3 noticeable peaks at m/z: 279.8, 176.7 and 96.8. Other peaks obtained were considered negligible for further analysis.

MS2 analysis of m/z 315.9 fragmentation yielded 3 major peaks of noticeable intensity, m/z: 315.9, 235.9 and 216.7 with 315.9 being the most intense signal. Analysis of m/z 269.8 yielded 4 peaks in MS2 fragmentation: 269.8, 225.7, 189.8 and 96.8. MS2 fragmentation of the 240.8 ions yielded 4 peaks of interest: 240.8, 196.8, 160.8 and 96.8 with 240.8 being the most intense signal. Further analysis of 154.8 fragmentation showed the ion yielded 2 major peaks: 154.8 and 96.8 with 96.8 being the most intense signal (Table 2).

### 6.6 Relative intensity results

m/z	intact CS	CS+CuSO4 24hrs	CS+CuSO4+H2O2 24hrs
<b>154.8</b>	0.000	0.002	0.698
<b>184.8</b>	0.002	0.002	0.120
<b>214.8</b>	0.002	0.002	0.150
<b>240.8</b>	0.002	0.002	0.054
<b>297.9</b>	0.003	0.002	1.000
<b>299.8</b>	0.002	0.002	0.729
<b>315.9</b>	0.001	0.000	0.848

**Table 2** Relative abundance of specific ions detected in figure 16 following 24hr free radical depolymerisation of intact bovine CS.

For each selected m/z the relative intensity was much higher in the mixture containing all reaction components (e.g H2O2, CuSO4 and CS). The intensities recorded in the intact CS and the CuSO4 control (table 3) were no greater than the background intensity. This means we were unable to distinguish any peak that is generated as a result of the CS and CuSO4 being present. The background intensity will be generated. The base peak for CuSO4 differs on individual experiments due to the heterogeneous nature of the fragmented CS generated in the mass spec.

<b>m/z</b>	<b>intact CS</b>	<b>CS+CUSO4 24hrs</b>	<b>CS+CUSO4+H2O2 24hrs</b>
<b>154.8</b>	0.001	0.002	0.201
<b>184.8</b>	0.002	0.002	0.122
<b>214.8</b>	0.002	0.002	0.129
<b>240.8</b>	0.000	0.002	0.058
<b>297.9</b>	0.000	0.000	0.626
<b>299.8</b>	0.000	0.000	1.000
<b>315.9</b>	0.001	0.000	0.850

**Table 3: relative abundance of specific ions detected in figure 13 following 24hr free radical depolymerisation of intact porcine CS.**

As with the MS analysis of bovine CS, intact porcine CS spectra also yielded very low intensities of the m/z listed above. Addition of CUSO4 did not have an impact on the relative intensities of the selected ions and are not statistically different.

<b>m/z</b>	<b>intact CS</b>	<b>CS+CUSO4 24hrs</b>	<b>CS+CUSO4+H2O2 24hrs</b>
<b>154.8</b>	0.000	0.002	1.000
<b>184.8</b>	0.002	0.002	0.240
<b>214.8</b>	0.002	0.002	0.131
<b>240.8</b>	0.002	0.002	0.275
<b>297.9</b>	0.003	0.002	0.627
<b>299.8</b>	0.002	0.002	0.346
<b>315.9</b>	0.001	0.000	0.471

**Table 4: Relative abundance of specific ions detected in figure 15 following 24hr free radical depolymerisation of intact shark CS.**

## 6.7 Summary of proposed Structures generated following ESI-MS analysis of free radical depolymerised CS

The m/z listed below are generated by the free radical degradation of intact CS to its constituent monosaccharides (4/6S-GalNAc and GlcA), the mechanism of which is shown in figure 47.

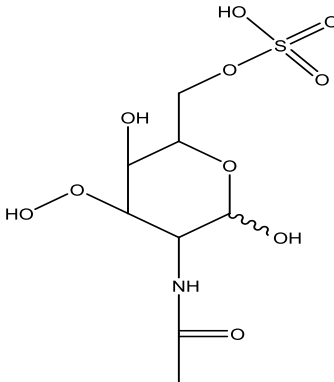
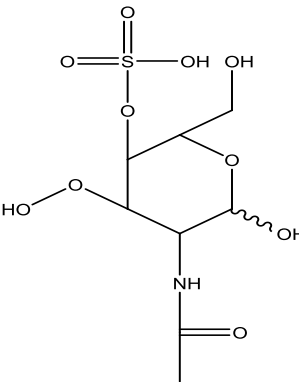
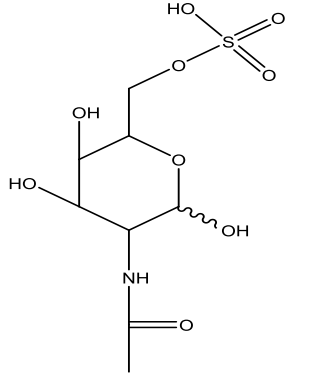
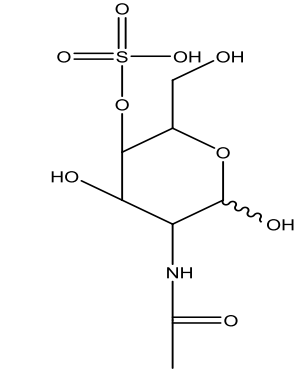
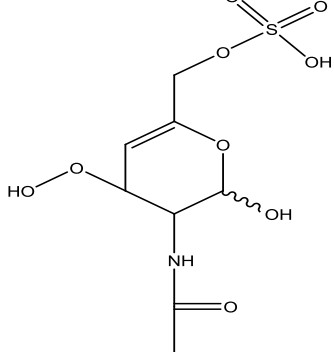
m/z	Structure	
	6-sulfated	4-sulfated
315.9		
299.9		
297.9		

Table 5 Proposed structures of m/z 315.9, 299.9 and 297.9 interest and their corresponding structure analysed via ESI-MS after subjecting intact porcine/bovine CS to free radical degradation via Fenton reaction.

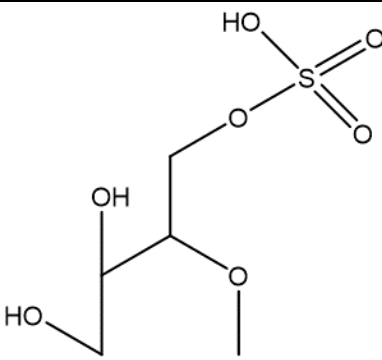
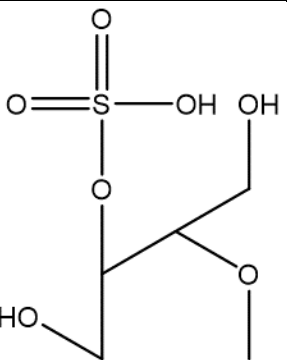
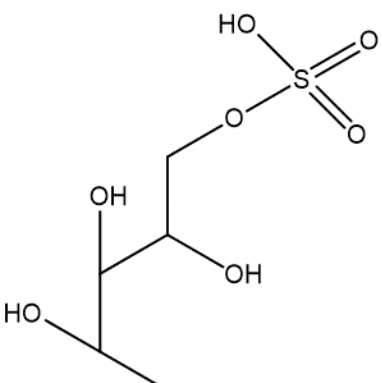
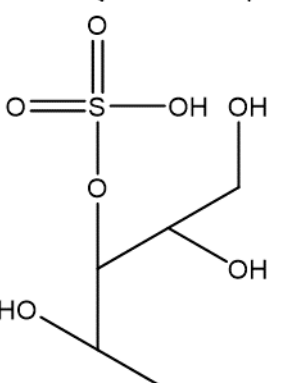
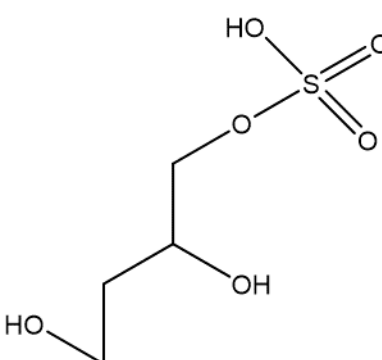
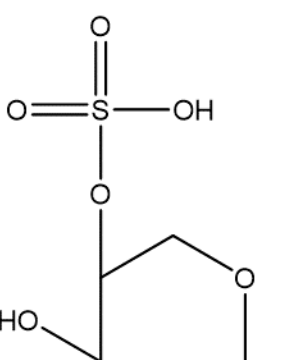
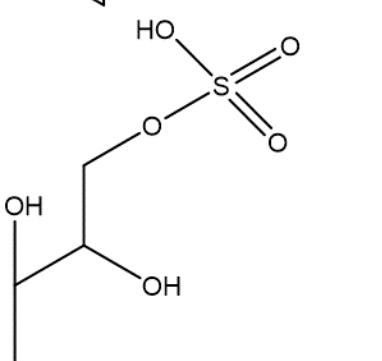
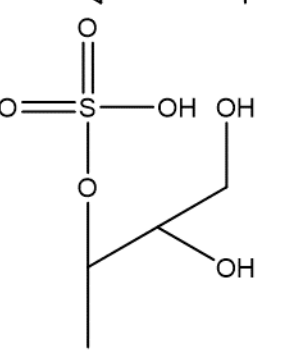
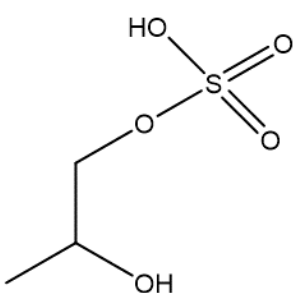
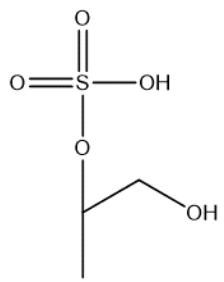
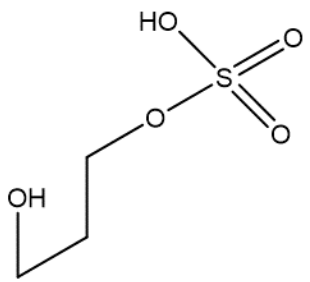
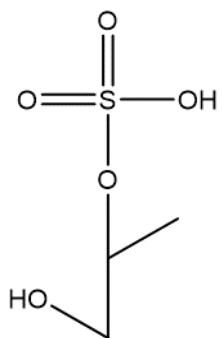
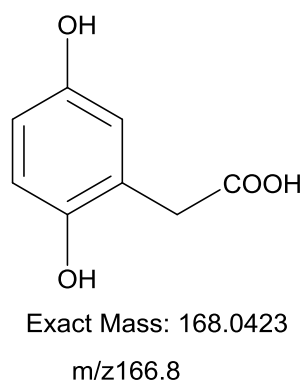
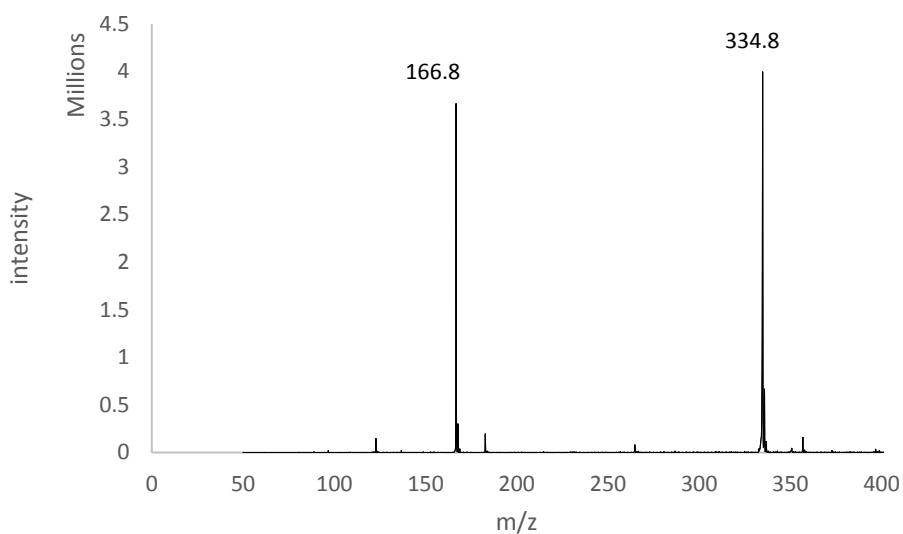
m/z	Structure	
	6-sulfated	4-sulfated
214.8		
		
184.8		
		

Table 6: Proposed structures of m/z 214.8 and 184.8 and their corresponding m/z following MS analysis of free radical degradation of intact bovine, porcine and shark CS via Fenton reaction.

m/z	Structure	
	6-sulfated	4-sulfated
154.8		
		

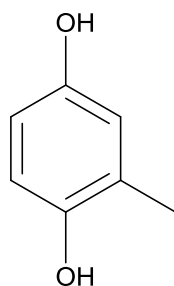
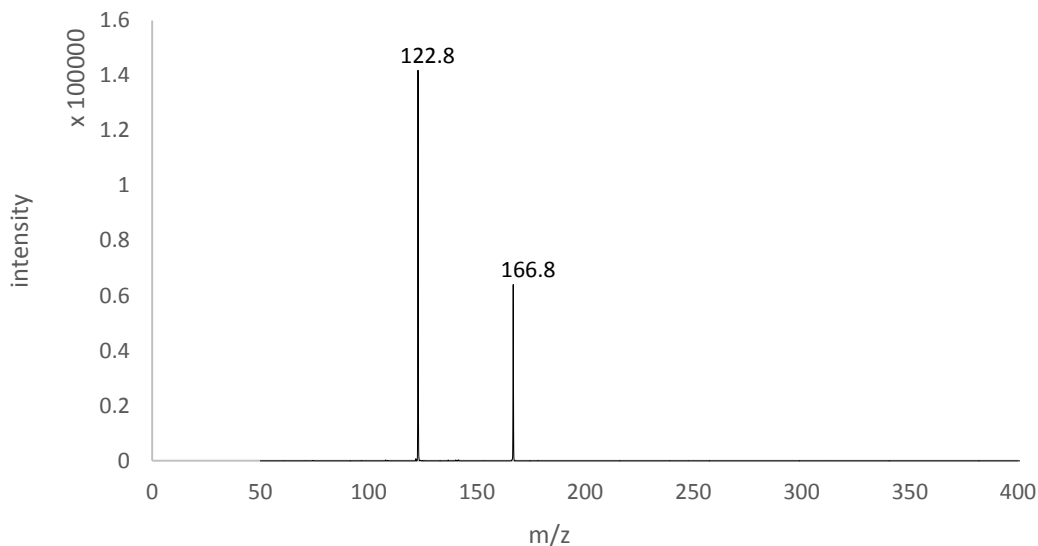
**Table 7: Proposed structures of m/z 154.8 analysed by ESI-MS following the free radical degradation of intact porcine, shark and bovine CS via Fenton reaction.**

## 6.8 MS analysis of HGA



**Figure 22: Negative ion spectra of 0.1M HGA (in water) and then diluted 10fold in ACN and the structure of HGA with the corresponding m/z**

The peak at m/z 166.8 corresponds to HGA whilst evidence suggested the peak at m/z 334.8 to be the dimer of HGA (figure 42) and subsequent MS2 analysis of that peak showed it was mostly composed of 166.8 and 334.8. The experiment was performed in 3 conditions- MS-grade H<sub>2</sub>O only, Acetonitrile only and finally MS-grade H<sub>2</sub>O and Acetonitrile. There was no significant difference in the relative intensity of either 166.8 or 334.8. The 3 conditions were tested because studies have highlighted the effect of solvents on the electrochemical and polymerisation behaviour of HGA (Eslami et al 2014)



Exact Mass: 124.0524

m/z 122.8

**Figure 23: MS2 analysis of m/z 166.8 from the negative ion spectra of HGA and the proposed structure of m/z 122.8 ion**

We propose that m/z 122.8 corresponds to HGA minus its carboxyl group. This also highlights the ease of fragmenting the COOH compared to the 2 OH groups which opens the door for the proposed structure of hippoduric acid which is the proposed structure of a HGA dimer. This acid can be seen to compose of the benzoquinone form of HGA as well as a semiquinone form with COOH lacking.

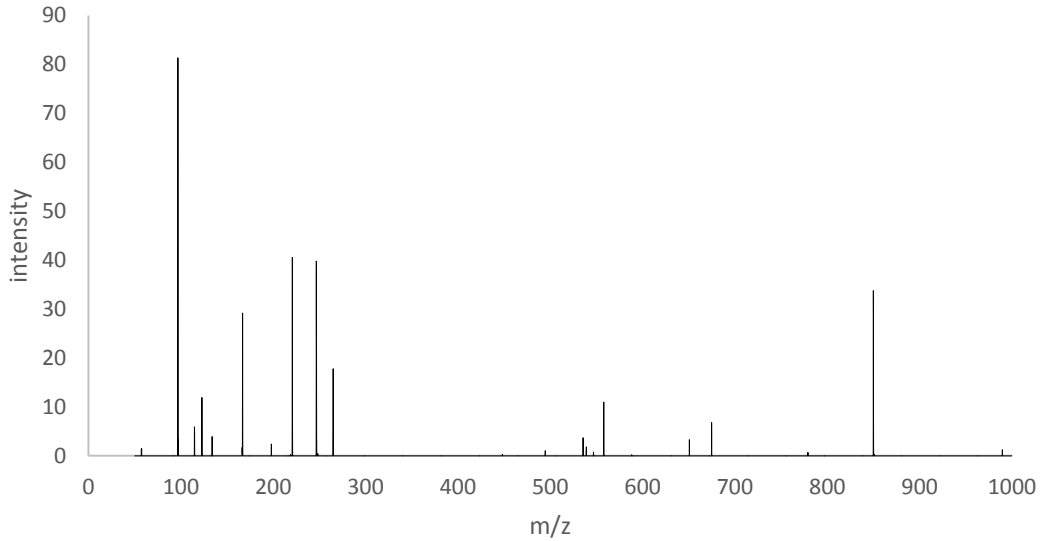


Figure 24: MS2 fragmentation of m/z 166.8 obtained from the negative ion spectra of 0.1M HGA at increased fragmentation energy of 1.5A.

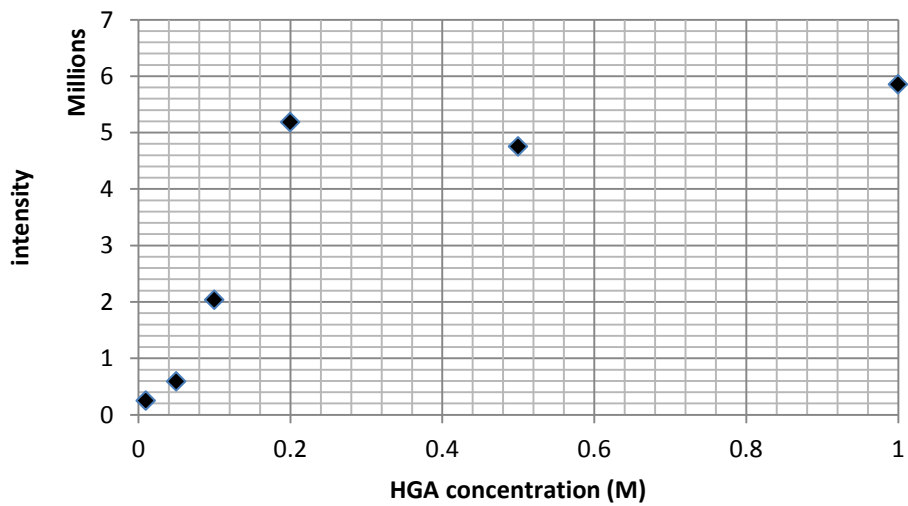


Figure 25: Standard curve of increasing HGA concentration when analysed via ESI-MS in the negative ion mode.

Figure 28 shows that the relationship between relative intensity and HGA concentration seems to follow a logarithmic shape. Mass spec analysis alone is not a quantitative representation of the amount of sample present. However this experiment was used to determine a reasonable concentration of HGA to use in future experiments.



## 6.9 MS analysis of HGA and CUSO4

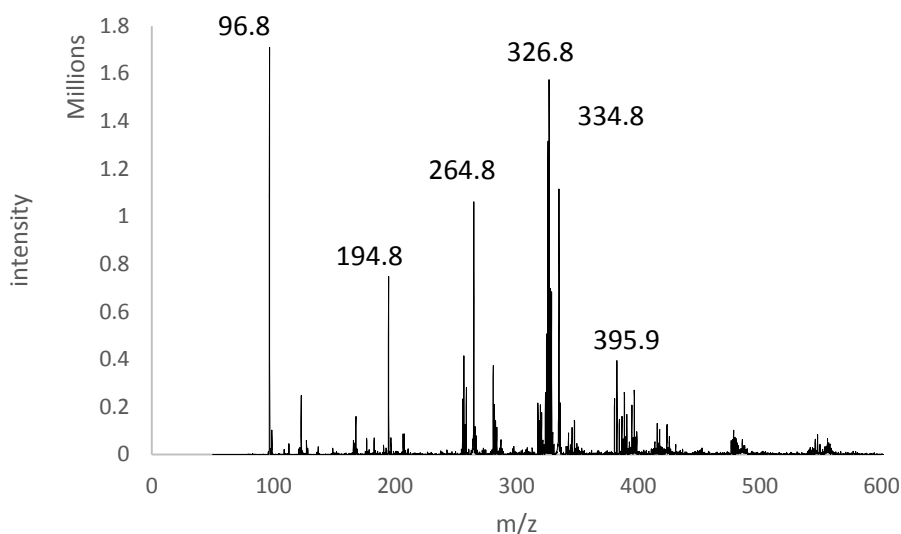


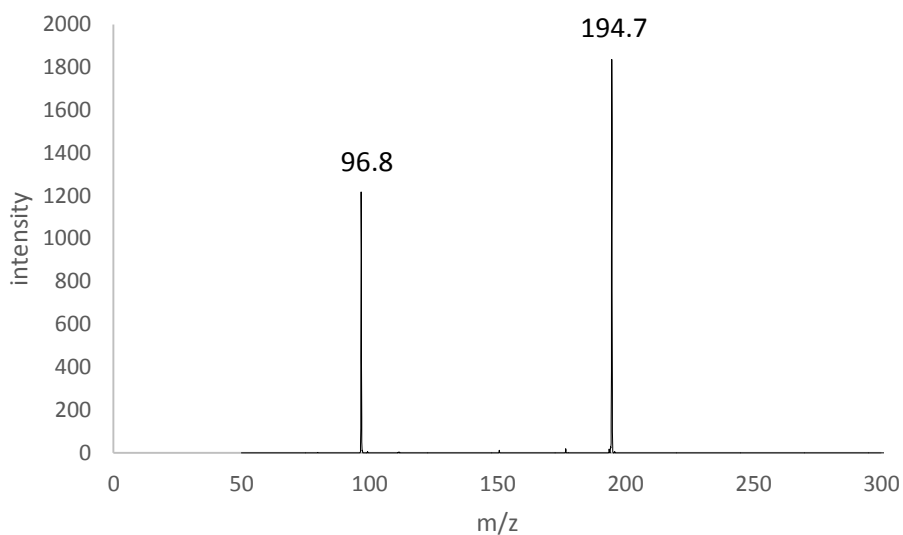
Figure 26: Negative ion spectra of 0.1M HGA mixed with 10mg/ml CuSO<sub>4</sub> and left for 24hrs.

Figure 27 shows a noticeable difference to the HGA only and CuSO<sub>4</sub> only spectra. The intensity of m/z 166.8 (HGA) is considerably reduced in this spectrum and is significantly different. The intensity of m/z 264.8 326.8 and 395.9 ions are all significantly greater in this spectrum. This provides some substance to the theory proposed earlier, that the addition of a metal catalyst such as Cu<sup>2+</sup> will catalyse the oxidation and polymerisation of HGA. Although the structures of these fragments remain elusive.

One m/z of interest would be that of the proposed benzoquinone form of HGA that is generated from its oxidation. The m/z of this ion would correspond to around 164.8 in our mass spec studies. The relative intensity of this ion was found to be 0.33%, from this we deduced in this experiment we were not seeing this ion in the spectra. This could be due to a number of factors, such as this benzoquinone being an unstable intermediate to further polymerisation structures. It may have also been the MS technique used to analyse HGA which in this case was ESI in the negative ion mode.

## 6.10 MS<sup>2</sup> data from HGA and CuSO<sub>4</sub>

From the negative ion spectra of HGA mixed with CuSO<sub>4</sub> we have highlighted some major peaks to further investigate via tandem MS. These m/z are as follows: 194.7, 256.6, 264.8, 280.8, 326.7, 382.5 and 415.7. It is hoped that further analysis of these ions will provide some insight into the potential HGA polymerisation mechanism.



**Figure 27: MS2 analysis of m/z 194.7 obtained from the negative ion spectra of HGA and CUSO4.**

MS2 analysis of m/z 194.7 ion from figure 35 indicates the fragment contains a sulfate group due to the presence of m/z 96.8 ion. The structure of m/z 194.7 remained elusive.

### 6.11 HGA and Iron citrate

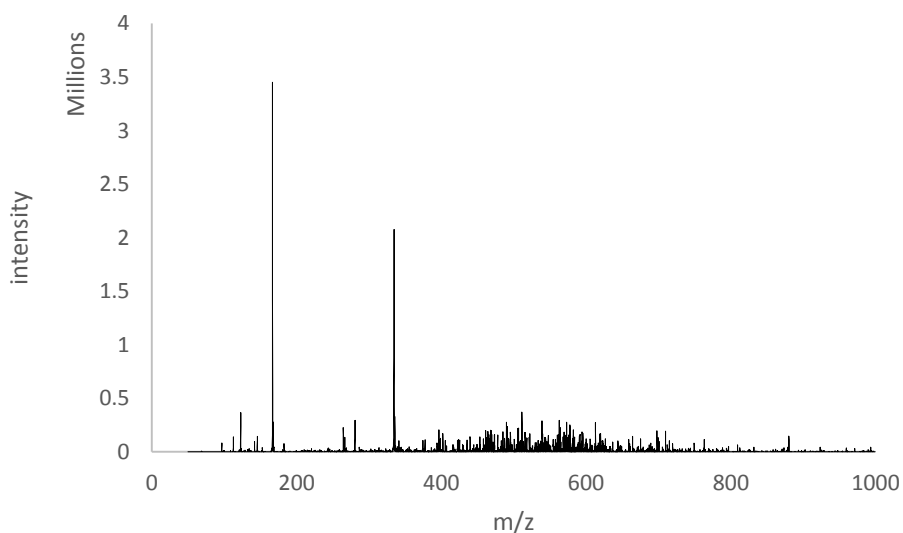


**Figure 28: Negative ion spectra of 0.1M HGA mixed with 10mg/ml FeC6H5O7 and left for 24hrs.**

Comparing figure 35 (page 57) and 37 we can see that there are distinct differences suggesting reactions taking place are different when using Fe instead of Cu as the metal catalyst. The sharp peaks in figure 33 (believed to be the fragments of the polymerising HGA) are instead replaced with less defined peaks in figure 36 (apart from the 166.8 and 334.8 peaks). Firstly the relative intensity of

m/z 166.8 (HGA) is greatly reduced in the Cu spectrum compared to Fe which suggests that the starting material is present in the FE spectra and not the Cu. The relative intensity of 334.8 is quite similar in both spectra. The relative intensities of the m/z's thought to be involved in HGAs polymerisation are greatly reduced in the Fe spectra. This again suggests that there is less generation of HGA polymerisation products due to the much greater intensities of m/z 166.8 and 334.8 ions that correspond to the HGA monomer and dimer respectively.

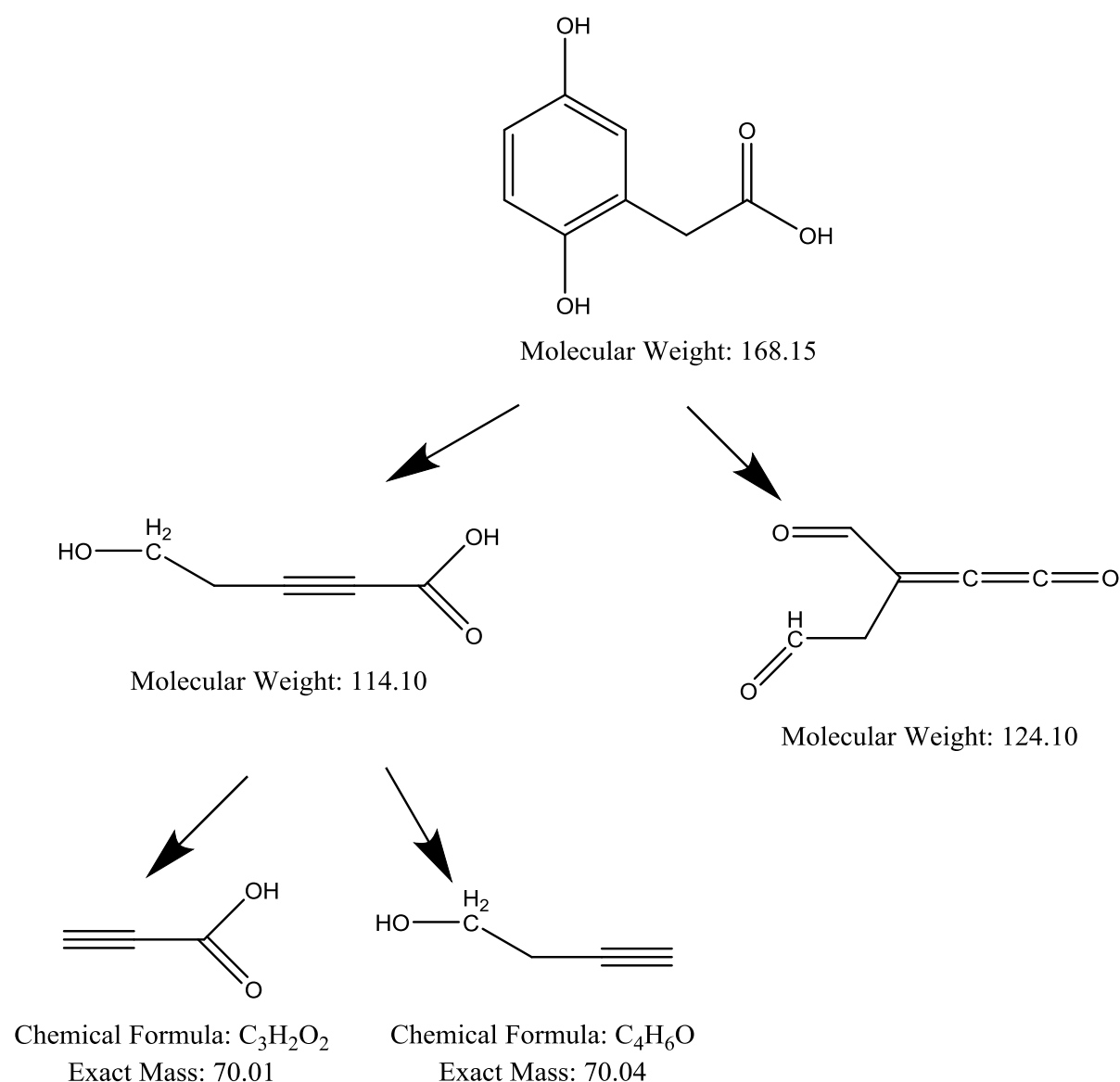


**Figure 29: Proposed fragmentation pathway of HGA when analysed by ESI-MS in the negative ion mode with a fragmentation energy of 0.7V.**

## 6.12 HPLC analysis of HGA interaction with CS disaccharide

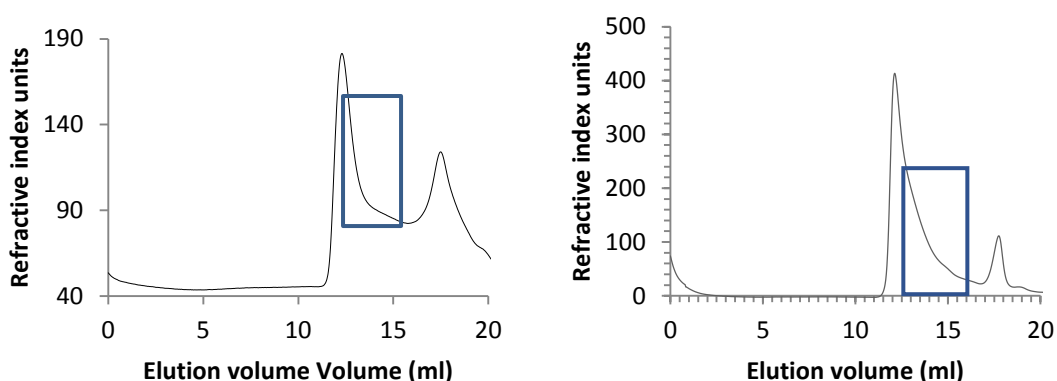


**Figure 30:** Left, size exclusion chromatogram of digested shark CS with the addition of HGA and  $\text{CuSO}_4$ . Right, size exclusion chromatogram of intact shark CS subjected to free radical depolymerisation via fenton. The highlighted blue region refers to the fractions believed to compose of depolymerised CS as a result of HGA mediated degradation.

From all the HPLC profiles obtained in previous shark CS experiments (figure 15), it is the 24hr free radical depolymerisation which is the most similar to the profile generated from HGA induced depolymerisation of CS digest. This reaction is composed of the Cu catalyst (for HGA polymerisation), HGA and intact shark CS. The highlighted region on the chromatograms show the similarity between the profiles. When comparing the profiles obtained from the HGA-CS depolymerisation we can see that both the 2hr and 3 day profiles are quite different.

We can see in both profiles there is a large peak around 12.4ml corresponding to larger CS chains. The peak around 18ml corresponds to the  $\text{CuSO}_4$  eluting as in figure 12. The area of each profile highlighted in blue corresponds to products of free radical depolymerisation. This will include fragments such as the 4/6S-GalNAc. One major difference in the 2 profiles is the large peak in the HGA sample compared to the Fenton sample. As this large peak is present after the trough of  $V_0$  this can be considered artefact.

### 6.13 MS HGA and intact CS

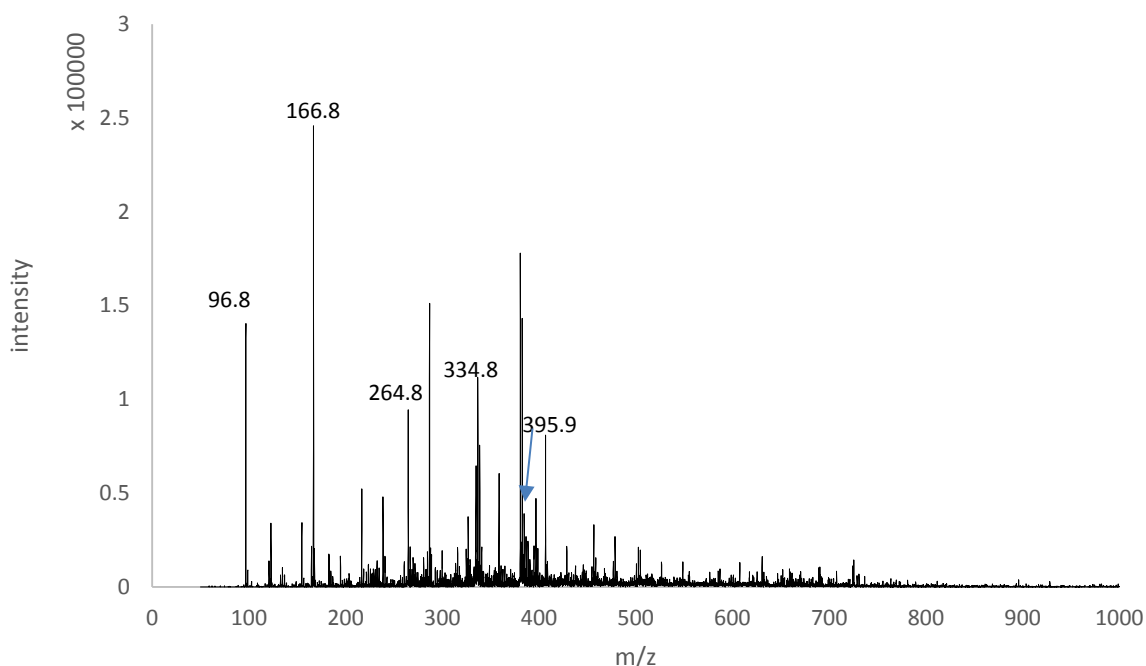


**Figure 31: Negative ion spectra of intact Porcine CS with the addition of HGA and CuSO<sub>4</sub>**

The spectra in the figure 32 shows the peak at 166.8 corresponding to HGA as well m/z 334.8 (corresponding to the HGA dimer) which appears in a spectra of just HGA. The fragment at m/z 264.8 is also present which is thought to be a structure involved in the metal catalysed polymerisation of HGA. At first glance it was thought that the fragment at m/z 395.9 corresponded to an desulfated unsaturated disaccharide which appears in the MS<sub>2</sub> analysis of an unsaturated monosulfated disaccharide (Figure 2). However further MS<sub>2</sub> analysis showed that this was not the case. Further analysis of m/z 393.9 shows a similar fragmentation to 457.9 with the appearance of m/z that correspond to the GlcA and GalNAc.

It was then proposed that this ion may be a GalNAc with a HGA coupled to it via one of the free OH groups. It was believed that the most likely point of bonding would be the OH that is generated when the glycosidic bond is broken by an ROS which is highlighted in a previous chapter (figure 25). This is entirely plausible as we are suggesting that through HGAs metal catalysed oxidation and polymerisation we get the generation of ROS that can easily break the glycosidic bond of the disaccharide. It would then be possible for HGA to couple to this OH group in a similar mechanism to its own polymerisation (figure 43). Indeed we also see a coupling when using H<sub>2</sub>O<sub>2</sub> and CuSO<sub>4</sub> to generate ROS. In this case we see an OH. Coupling to the free oxygen from the broken glycosidic bond. We can see in the mechanism of HGAs oxidation that a HGA. Is generated and will is likely to react with local molecules.

Comparison of the fenton-induced and the HGA-induced depolymerisation of CS yields 2 very different spectra. This should not be surprising considering the complexity of the HGA-induced degradation compared to the fenton-induced. The first thing to consider is that for HGA to be able to depolymerise CS it must first undergo its own oxidation and polymerisation. Even metal catalysis of this process will not yield as many ROS as the quite intense reaction of H<sub>2</sub>O<sub>2</sub> and CuSO<sub>4</sub> in the time frame we are using. It is proposed that HGA is unable to breakdown intact CS in the presence of a metal catalyst in this short time frame. We propose that it is the accumulation of ROS through HGAs polymerisation will lead to the degradation of CS over time. This also should not be surprising when considering that it takes decades for Alkaptonuripatients to develop arthritis as a result of ochronosis.

In the Fenton spectra we can see 2 major peaks at m/z 299.8 and 315.9 which corresponds to 4/6S-GAINAc and a hydroxy-coupled 4/6S-GAINAc. This is not the case when HGA and CuSO<sub>4</sub> is added to intact CS. It seems that the HGA polymerisation structures dominate the spectra and any m/z that were previously observed corresponding to CS fragments are masked by the background noise.

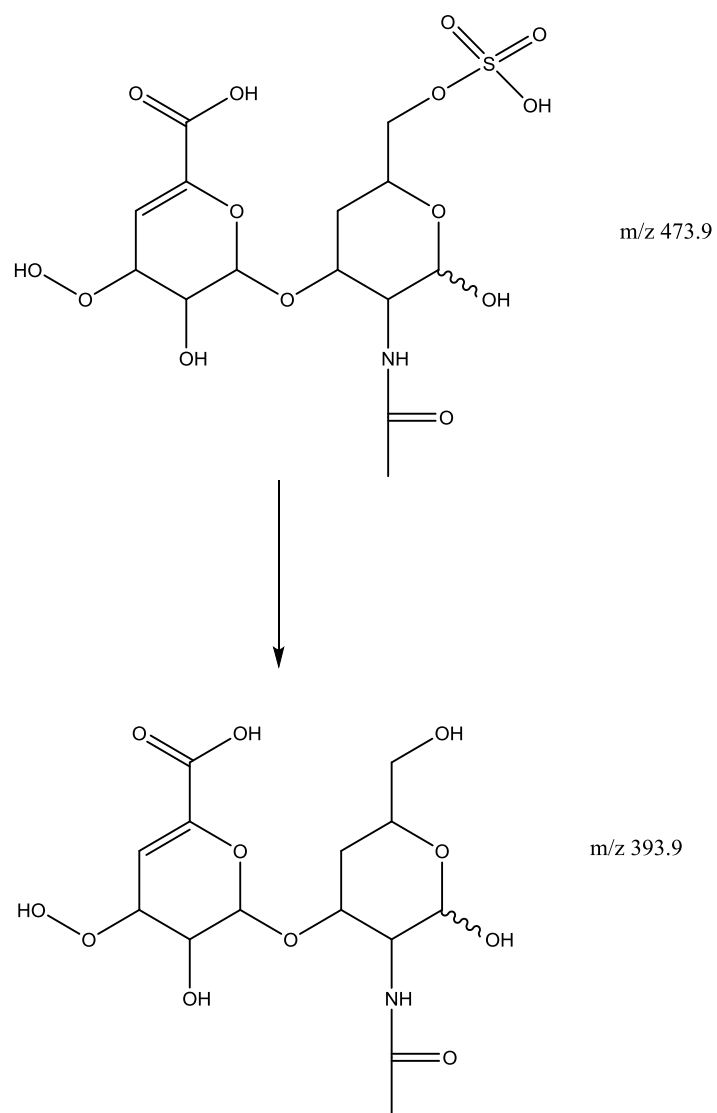


Figure 32: Proposed structures of  $m/z$  473.9 following free radical depolymerisation of intact CS and its MS2 fragment  $m/z$  393.9.

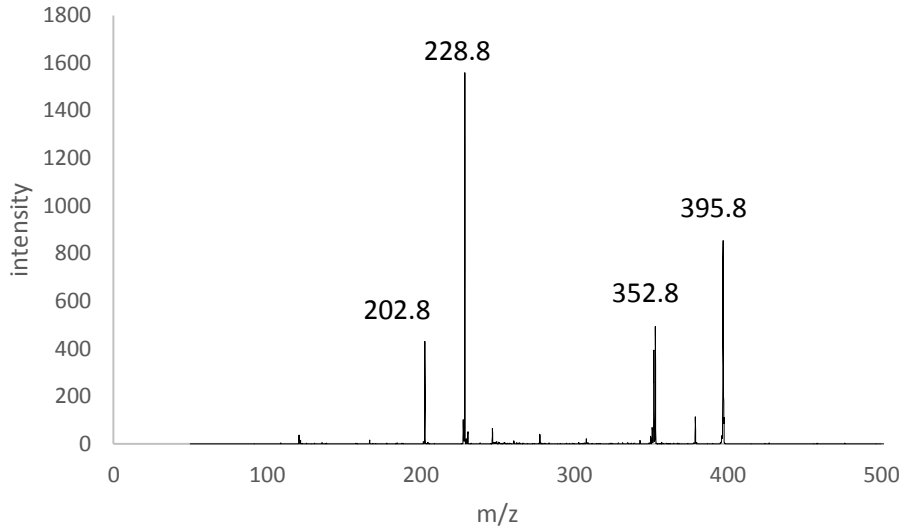


Figure 33: MS2 spectrum obtained from the fragmentation of m/z 395.9 from figure 33.

### 6.14 MS HGA and enzyme depolymerised CS

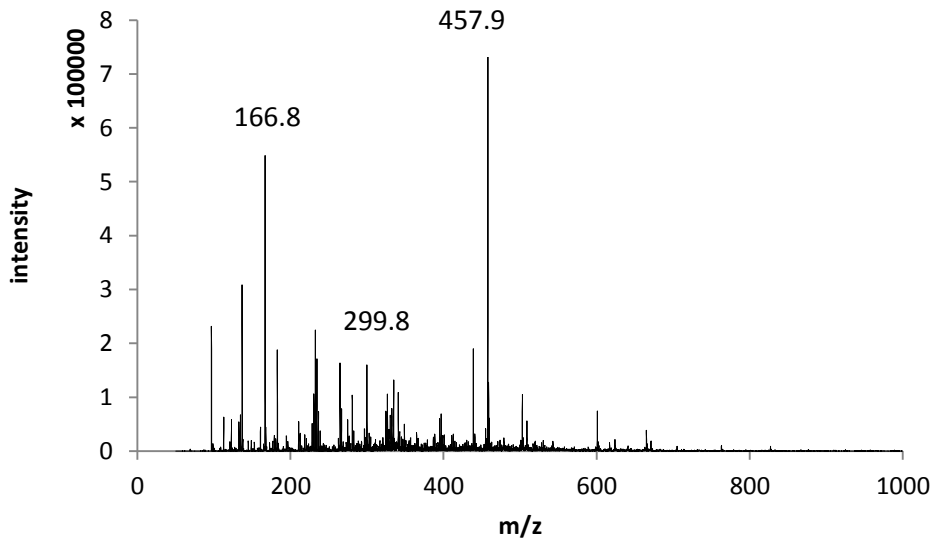
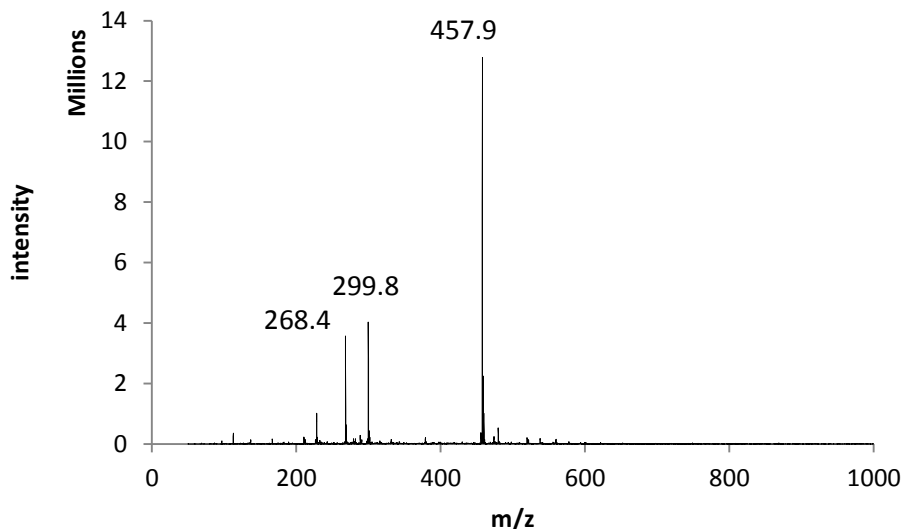


Figure 34: Negative ion spectra of Porcine CS digest with the addition of HGA and CuSO<sub>4</sub>





**Figure 35: Negative ion spectra of Shark CS digest with the addition of HGA and CuSO<sub>4</sub>**

There is a clear difference between the spectra obtained in figure 36 and 37. In Figure 36 there is no observable presence of the 166.8 signal corresponding to HGA. Figure 49 spectra looks much more like the spectra obtained from the reaction of HGA and CuSO<sub>4</sub> with the addition of the 457.9 ion that corresponds to the unsaturated disaccharide.

In figure 49 we observe a spectra that is suggesting HGA polymerisation (in the presence of CuSO<sub>4</sub>) and also the breakdown of the 457.9 ion (unsaturated disaccharide) to 299.8 ion (4/6S GalNAc) which is not observed when using intact CS rather than enzyme depolymerised CS.

### **6.15 Mass spec analysis of SOD reaction**

Figure 51 shows the result of intact porcine CS that has been subjected to free radical depolymerisation. The 2 major ions of interest are m/z 297.9 and 315.9 which correspond to a saturated- monosulfated GAINAc and a hydroxy-coupled monosulfated GAINAc respectively. These structures were confirmed in the previous chapters. Comparing depolymerised with intact CS we can see there is a large number of undefined peaks and a noticeably lower ion intensity in the intact CS. This is because the mass spec cannot differentiate between such large chain lengths so they are fragmented in a random fashion. This yields a 'messy' spectrum with no major ions dominating the spectra.

The mechanism of CS depolymerisation is shown in figure 47. The ROS are generated via fenton-type reaction which generated oxy radicals from H<sub>2</sub>O<sub>2</sub> and Cu(II). The oxy radical cleave the CS at the glycosidic bond which yields GlcA and GalNAc. The hydroxy-coupled product is generated due to the presence of free OH radicals that can bind to the free oxygen from the cleaved glycosidic bond.

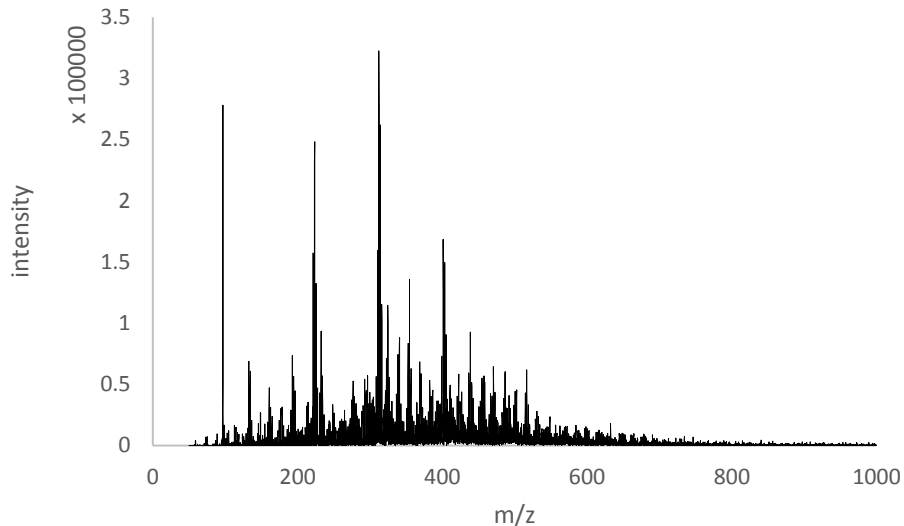


**Figure 36: Negative ion spectra of intact bovine CS with the addition of SOD before subjecting the mixture to fenton-like reaction and leaving for 24hrs.**

Straight away it becomes apparent that m/z 297.9 and 315.9 are no longer the 2 major ions in the spectrum. You can also see the slight reappearance of a number of undefined peaks seen in intact CS. When comparing the 2 spectra statistically it became apparent that the relative intensity of both 297.9 and 315.9 were statistically significant between the intact and depolymerised spectra. If we assume that the presence of m/z 297.9 and 315.9 are strong indicators of free radical depolymerisation we can postulate that the addition of SOD to the mixture before the initiation of Fenton will at least reduce the effect of ROS attack.

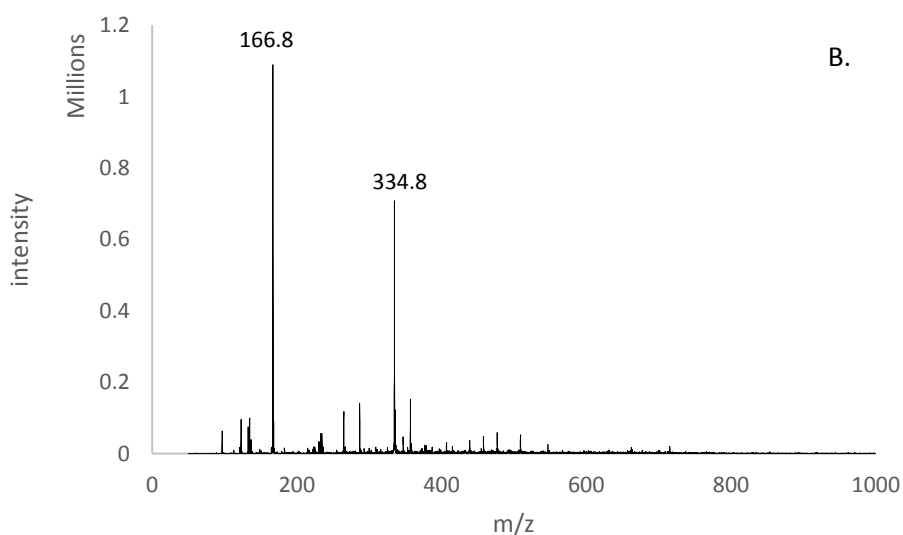
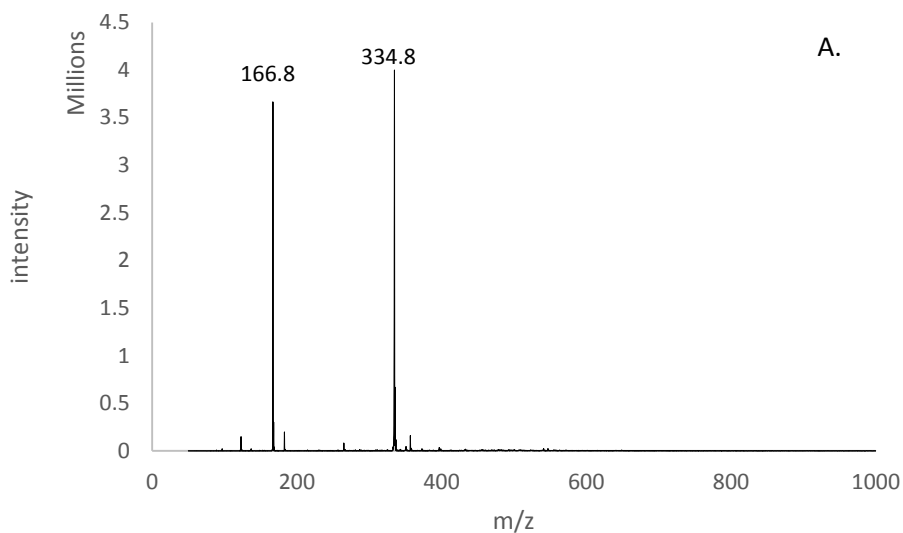


**Figure 37: Negative ion spectra of A.HGA and B.HGA and SOD what have both been left at room temp for 24hrs.**

The addition of SOD to HGA seemed to have little effect on the spectra generated. The 2 major ions of m/z 166.8 and 334.8 (expected because we propose that the addition of a Cu catalyst is required for its polymerisation). The main difference is the reduced relative intensity of m/z 334.8 in the HGA-SOD spectra compared to the HGA spectra. There also seems to be more noticeable ions present on the HGA-SOD spectra however this may be due to the base peak having a lower intensity compared to that of the HGA spectra.

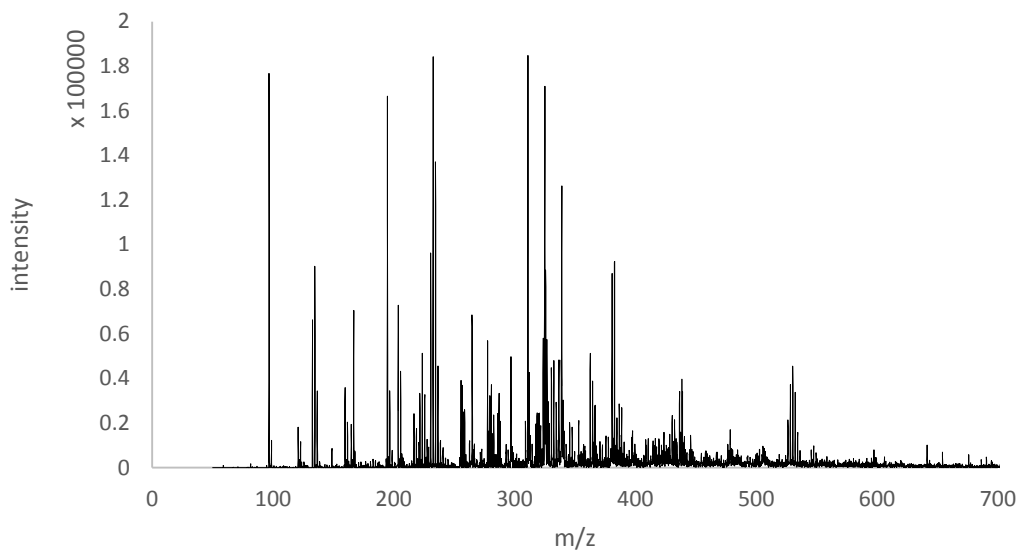
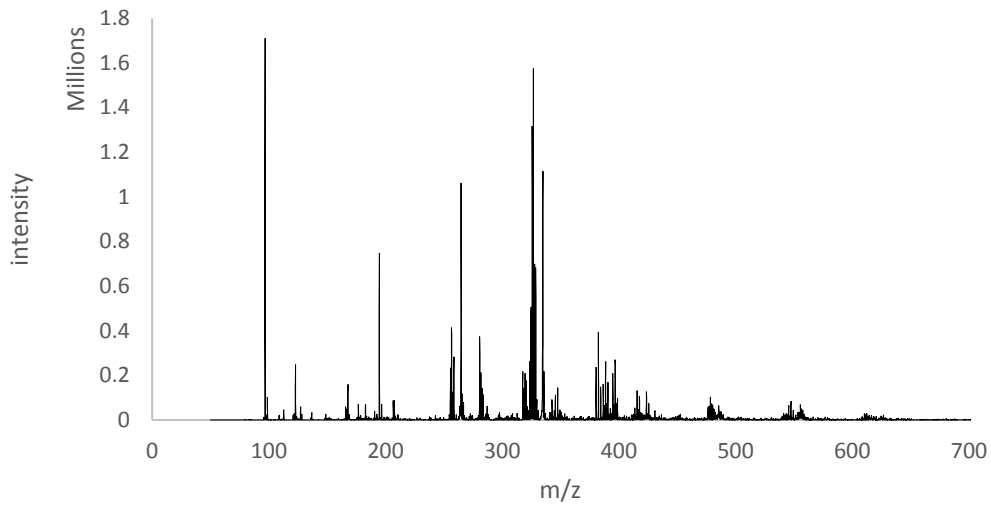


**Figure 38: Negative ion spectra of A. HGA and CuSO<sub>4</sub> left for 24hrs, B. SOD in the tube before the addition of HGA and CuSO<sub>4</sub> then left for 24hrs.**

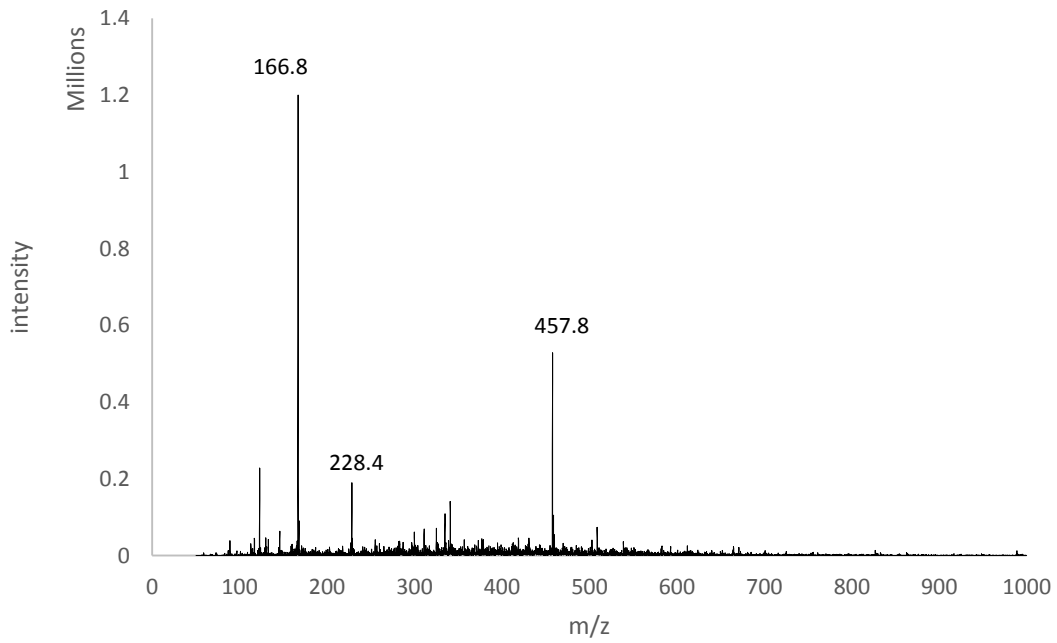
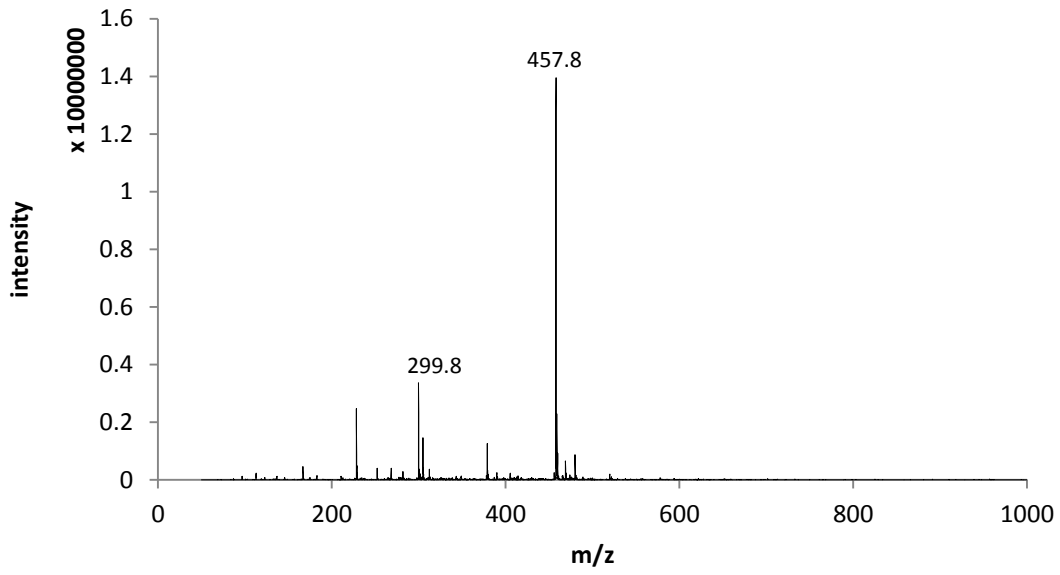


**Figure 39: Negative ion spectra of A. enzyme depolymerised porcine CS which was then added to HGA and CuSO<sub>4</sub>. B. Enzyme depolymerised porcine CS which was then added to SOD and then to HGA and CuSO<sub>4</sub>.**

## 7 Discussion

### 7.1 HPLC analysis of enzymatically digested CS

HPLC analysis of enzyme digested CS shows a distinct difference to the intact profile (figures 4 and 5), we found that fractions obtained between 17-19ml elution volume consisted of the disaccharide units that were confirmed via ESI-MS. The observed spectra showed the presence of  $m/z$  457.9 that corresponds to a 4/6S disaccharide. The refractive index detector was chosen due to the lack of UV active moieties within intact CS. As the enzyme degradation of CS yields an unsaturated disaccharide, this would be detectable using UV detector however the intact CS chains would remain undetected. Strong ion exchange chromatography could be used for disaccharide analysis and would also separate the 4/6S disaccharides. Further to this gas chromatography separation would require previous derivatization.

### 7.2 HPLC of free radical depolymerised CS

Size exclusion chromatograms of intact CS depolymerised by hydroxyl and superoxide radicals via Fenton type reactions yields almost identical profiles across species. Aliquots analysed 2hrs after intact CS was subject to Fenton type reaction yielded a profile similar to that of intact CS with a defined peak around 12.4ml eluent volume corresponding to intact CS chains (Figure 12). The additional peak at 17.4ml elution volume corresponds to the  $\text{CuSO}_4$  present in the reaction mixture.

Profiles obtained 24hrs after CS was subjected to Fenton like reaction shows a noticeable difference to intact CS. There is still a sharp peak at 12.4ml indicating that there is still intact CS present but there is a gradual decrease of the refractive index back down to the baseline V (figure 12). We attribute the signal highlighted in red indicates the presence of depolymerised CS chains. As mentioned in the introduction, the hw40s column used in this study is not able to differentiate the variety of depolymerised CS chains. However, as illustrated here it can differentiate between intact and depolymerised CS which is sufficient for this study.

Size exclusion chromatograms of CS subjected to Fenton reaction for 3 days shows a distinctly different profile to the 24 and 2hr samples (figure 12). The peak at 12.4ml eluent volume has been replaced by a broader region with multiple peaks, indicating that there is considerably less of the larger CS fragments present (figure 12) which indicates a more complete depolymerisation (i.e. yielding monosaccharides) of the CS chain. Samples taken at an eluent volume between 12 and 16ml would be expected to contain depolymerised CS (i.e. unsaturated 4/6S-monosaccharides).

The effect of changing the volume of  $\text{H}_2\text{O}_2$  was then investigated. It was found that using 175ul (10x that used in the previous experiment) of  $\text{H}_2\text{O}_2$  produced a profile almost identical to the sample left

for 3 days. It has been found that initial concentration of H<sub>2</sub>O<sub>2</sub> is independent of the reaction and does not influence the rate determining step when depolymerising carbohydrates and is in correspondence to the literature (Arturo Alberto Vitale, Eduardo A. Bernatene, Martín Gustavo Vitale 2016).

The addition of CuSO<sub>4</sub> to intact CS had little outcome on the obtained profile when comparing to just intact CS. For intact CS to be depolymerised to its constituent monosaccharides, it requires the addition of both CuSO<sub>4</sub>/Fecitrate and H<sub>2</sub>O<sub>2</sub>. This is supported by the theory of Fenton reactions that require the addition of fentons copper or iron to generate ROS from H<sub>2</sub>O<sub>2</sub>

The importance of the reaction components are highlighted in the HPLC data and re-enforced by the ESI-MS spectra obtained. Tables 2, 3 and 4 and statistical analysis shows that the reaction requires the addition of both CuSO<sub>4</sub> and H<sub>2</sub>O<sub>2</sub> to go ahead. Mass spectra analysis also showed that the reaction did not noticeably proceed without the presence of both CuSO<sub>4</sub> and H<sub>2</sub>O<sub>2</sub>. This again agrees with the literature that Fenton mediated ROS require the presence of both H<sub>2</sub>O<sub>2</sub> and a ferrous catalyst (Arturo Alberto Vitale, Eduardo A. Bernatene, Martín Gustavo Vitale 2016) The presence of m/z 299.9 and 315.9 at a great intensity (Unsaturated and hydroxyl coupled GalNAc) are used to indicate if depolymerisation has occurred.

### **7.3 MS of Enzyme depolymerisation**

Infusion ESI-MS analysis of intact CS digest yields 2 major peaks at m/z 457.9 and 479.9 (unsaturated and saturated disaccharide). There is no significant difference in the relative intensities of these two m/z across porcine, bovine and shark CS subjected to enzyme depolymerisation. This is surprising considering the varied sulfation patterns that occur across species (Martel-Pelletier et al 2015) The principle ion and base peak at m/z 457.9 corresponds to a 4/6S disaccharide that is generated as a result of the chondroitinase B-elimination mechanism. This is the cleavage of the glycosidic bond between the GlcAB(1,3)GalNAc. The peak at m/z 479.9 corresponds to its sodiated adduct (represented below) which has a relative abundance around 25% of the base peak (m/z 457.9) which is similar to that of previous studies (Desaire et al 2001). The adduction of single-charged potassium and sodium ions are the most commonly observed in electrospray analyses (Mortier et al 2004). However in electrospray form ions can form with more complex adducting species such as ammonium ions (McAnoy et al 2005) however these adducts were not observed in the above spectra. A common source of these adducts is contamination from glassware because many of these simple metal ion salts are used in the manufacturing process (Coates 2006).

MS2 analysis of the  $m/z$  457.9 ion allows us to identify the various isomers present, i.e. 4/6S-disaccharides via their fragmentation as reported (Poh et al 2015). Fragmentation of  $m/z$  457.9 yielded several ions illustrated by figure 17 with 4 major  $m/z$ : 341.8, 299.8, 281.8 and 198.9. The structures of these ions and their subsequent fragmentation pathways are illustrated in figure 41.  $m/z$  281.8 and 299.8 were found to have high abundances in both 4 and 6S disaccharides. It was therefore concluded that porcine tracheal CS had a greater composition of CS-A compared to bovine trachea or shark cartilage.



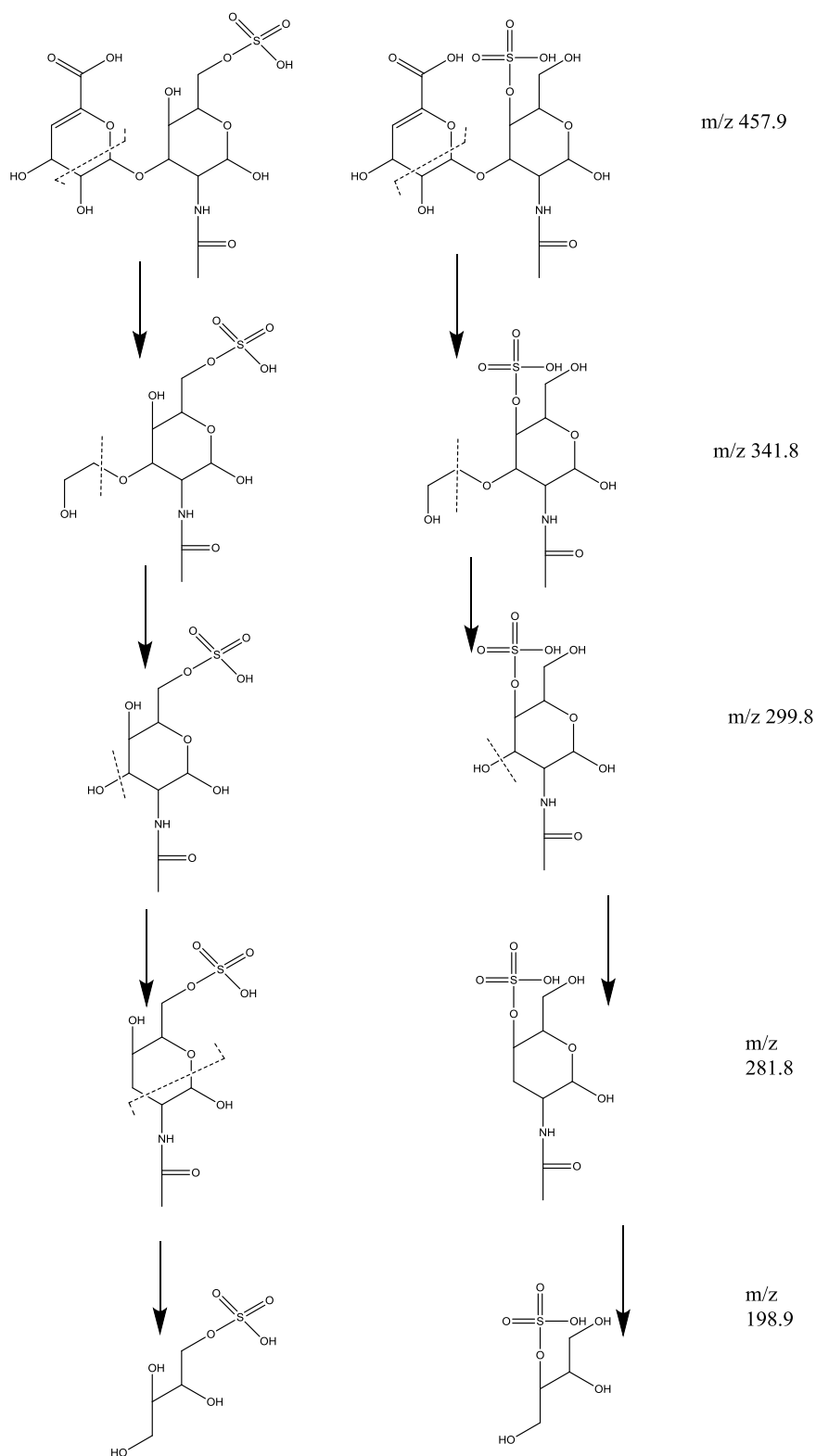


**Figure 40: proposed fragmentation pathway of unsaturated monosulfated disaccharide analysed in negative ion mode with a fragmentation energy of 0.7. Left is 6S-disaccharide fragmentation, right is 4S- disaccharide fragmentation. It must be noted that the represented fragmentation can occur as a sequence or simultaneously.**

The unsaturated monosulfated disaccharide and its sodiated adduct are the most abundant ions in the studied CS species. The  $m/z$  457.9 ion in each species yields the greatest abundance in MS1. Statistical analyses (T-Test) shows that there is no significant difference in the relative intensity of  $m/z$  457.8 and 479.9 across species. It was found that the 457.9 ion corresponded to around 6.8% of the total number of ions and this was also statistically insignificant across species.

The experiments investigating the enzyme depolymerisation of intact CS shows that an unsaturated 4/6S disaccharide unit is generated which can then be further investigated using MS2 fragmentation. Enzymatic depolymerisation occurs via the cleavage of the glycosidic bond between individual GlcA/GalNAc disaccharides.

## 7.4 MS of free radical depolymerisation

### 7.4.1 Shark

Infusion ESI-MS analysis of intact shark CS subjected to free radical depolymerisation via  $\text{CuSO}_4$  catalysis shows 6 ions of interest with  $m/z$ : 154.8, 184.8, 214.8, 240.8, 297.9 and 315.9 (Figure MS shark). The 2 major ions from the free radical depolymerisation were 297.9 and 315.9 which are proposed to correspond to the unsaturated monosulfated GalNAc and a hydroxy-coupled saturated monosulfated GalNAc (Figure 42).

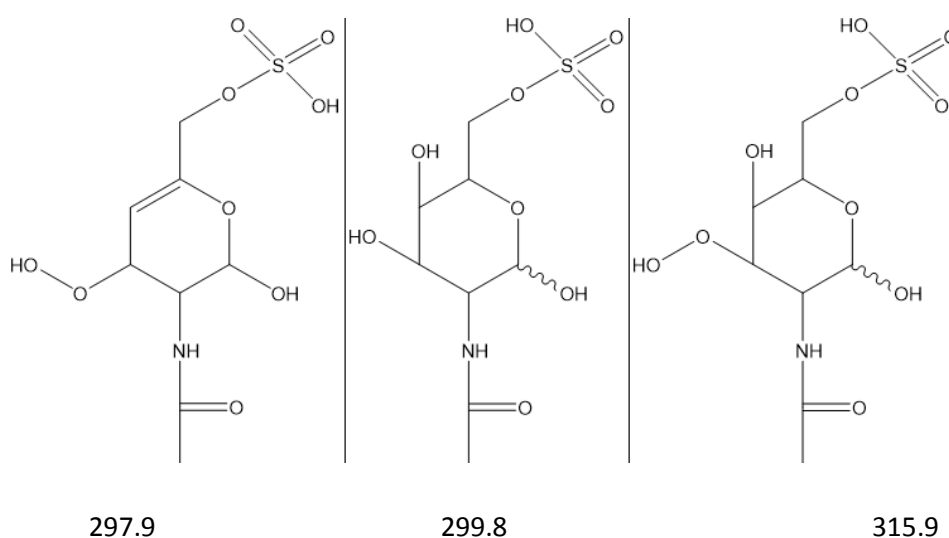


**Figure 41: Proposed monosaccharide structures as a result of intact CS being subjected to free radical depolymerisation via Fenton type reaction. 297.9- Unsaturated monosulfated monosaccharide, 299.8 saturated monosulfated monosaccharide and 315.9- hydroxy-coupled unsaturated monosulfated monosaccharide.**

#### 7.4.2 m/z 240.8

Of the 3 CS sources used in this study, it is shark CS disaccharides that contain the least 4S-GalNAc (figure 17) which agrees with the literature. MS data obtained in this study supports this theory with shark CS spectra showing a relative abundance of 0.275. This is statistically different to bovine and porcine which had relative intensities around 0.055 at an m/z of 240.8. The relative intensity of 240.8 in bovine and porcine are not statistically different.

CS source	Porcine	Bovine	Shark
Rel. intensity	0.065	0.0721	0.234
	0.034	0.0432	0.285
	0.074	0.0461	0.306
Ave	0.0576	0.0538	0.275
St Dev	0.020	0.0159	0.037
T test P:B	0.81		
T test P:S	0.0009		
T test B:S	0.0007		

**: Relative intensities of m/z 240.8 corresponding to a 5-GlcA in porcine, shark and bovine CS that has been subjected to free radical depolymerisation via Fenton type reaction. 2 sample T tests were carried out to evaluate statistical significance between each CS source.**

MS2 fragmentation of m/z 240.8 ion yields the following m/z: 196.8, 160.8, 154.8, 138.8 and 96.8.

The structures of these MS2 fragments can be seen in figure 20 and enables us to propose the structure of the parent 240.8. The large peak at m/z 96.8 corresponds to a SO<sub>4</sub> and shows that the parent ion and its constituent ions are also sulfated. It is unusual that the base peak is at m/z 154.8. It would be assumed that m/z 297.8 and 315.9 would yield the highest intensity as these are thought to be the major parent ions that are generated by free radical depolymerisation of intact CS.

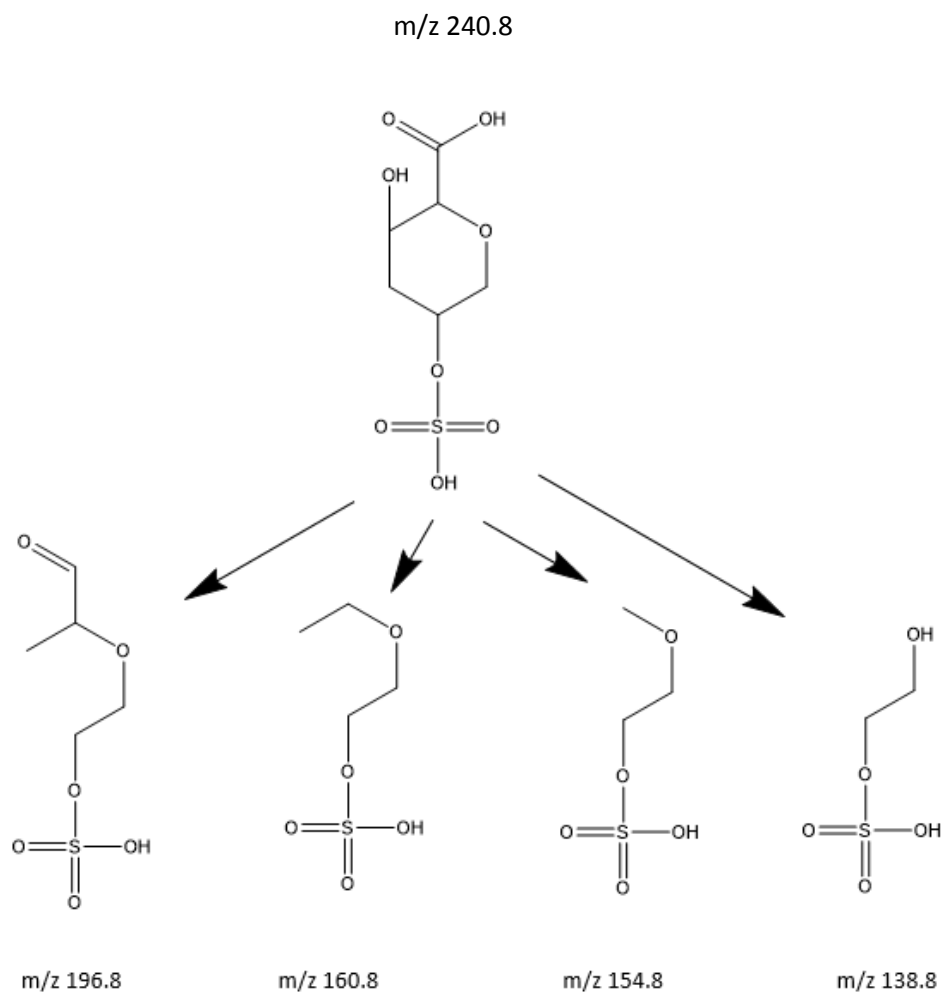


**Figure 42: Possible fragmentation pathway of  $m/z$  240.8 of intact shark CS (with 2S-GlcA) that has been subjected to free radical depolymerisation via Fenton type reaction and analysed by ESI-MS in the negative ion mode with a fragmentation energy of 0.7V.**

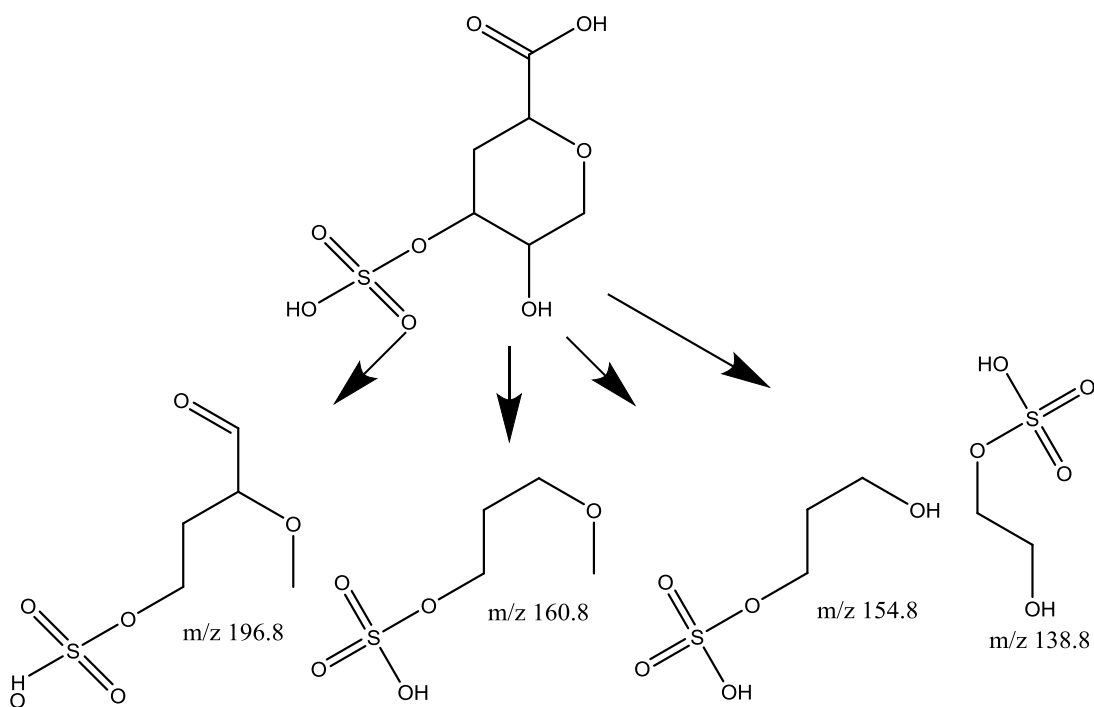


**Figure 43: Main proposed fragmentation pathway of m/z 240.8 of intact shark CS (with 3S-GlcA) that has been subjected to free radical depolymerisation via Fenton type reaction and analysed by ESI-MS in the negative ion mode with a fragmentation energy of 0.7V.**

#### **7.4.3 m/z 214.8**

Following on from m/z 240.8, the next ion of interest was m/z 214.8. MS2 fragmentation of this ion yielded m/z fragments 214.8, 184.8, 160.8 and 96.8, the structures of which can be seen in figure 23. Unlike m/z 240.8, 214.8 has the possibility of being 4/6S depending on the sulfation of the parent GAINAc. This particular CS source was shark cartilaginous skeleton which has a mostly 6S-GAINAc.

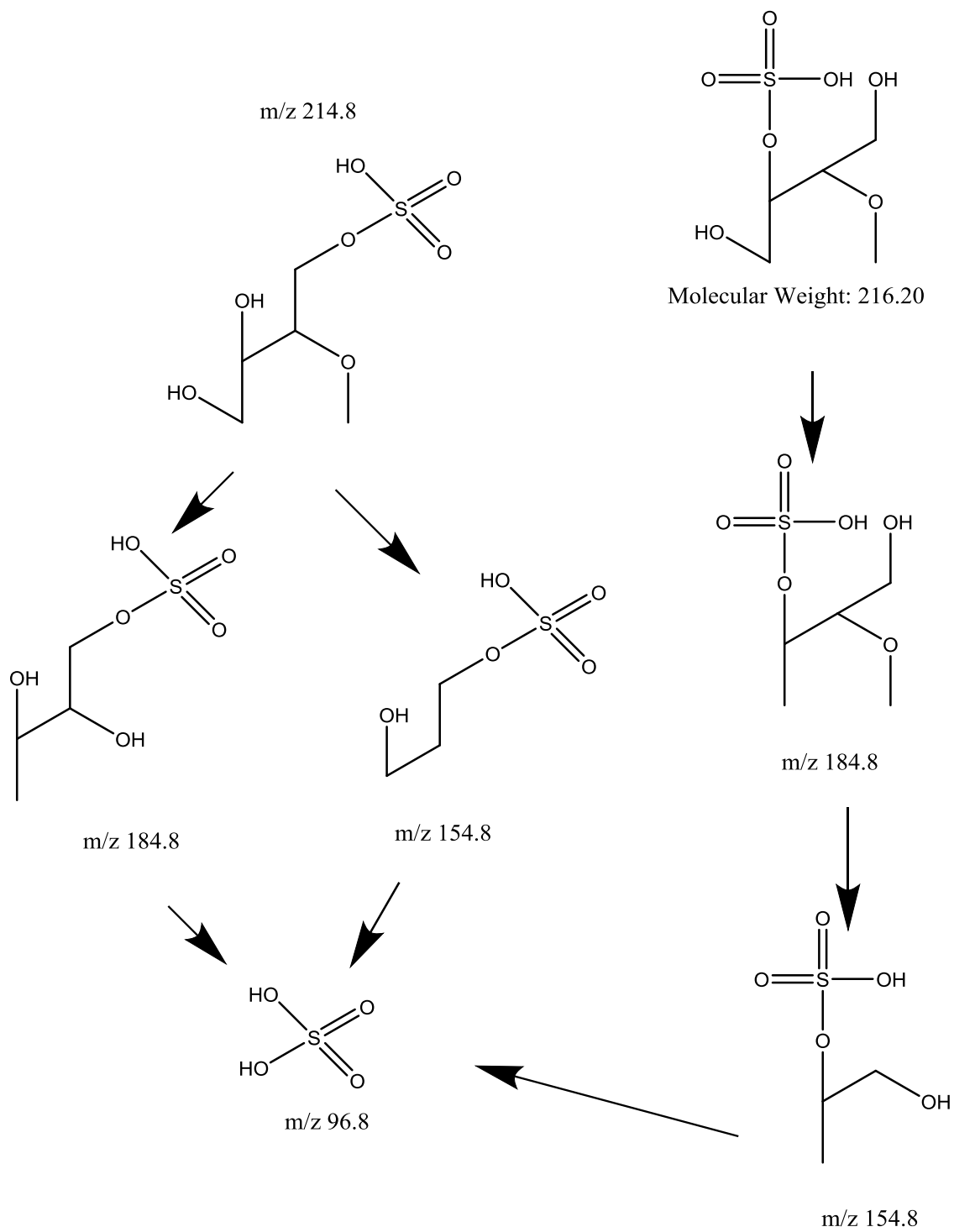


**Figure 44: 2 possible MS2 fragmentation pathways of m/z 214.8 in a sample of intact shark CS subjected to free radical depolymerisation via Fenton type reaction. Left is ion in 6 sulfated form whilst left is the ion in 4 sulfated form.**

#### **7.4.4 m/z 184.8 and 154.8**

These 2 ions are constituents of the parent m/z 214.8 which is itself most likely an ion generated from the fragmentation of m/z 297.9 (4/6S-GalNAc). Subsequent MS2 analysis of 184.8 yields 3 major peaks of m/z 184.8, 154.8 and 96.8. Fragmentation of 154.8 yields m/z 154.8 and 96.8. 184.8 and 154.8 arise due to ring cleavage of the 4/6S-GAINAc. These 2 ions are known to be sulfated due to the presence of the 96.8 ion which corresponds to SO<sub>4</sub> (figure 19).

#### **7.4.5 Bovine**

Infusion ESI-MS analysis of intact bovine CS that was subjected to free radical depolymerisation via Fenton type reaction yielded an MS spectra similar to that of shark. The major peaks mentioned earlier were all present and have statistically insignificant relative intensities. This was not true for m/z 154.8 or m/z 240.8 which has relative intensities statistically different to shark. This supports the theory that m/z 240.8 corresponds to a 3-sulfated GlcA which mostly occurs in shark CS. This was the proposed structure over 4 sulfated GlcA as this is the position of the glycosidic and therefore may not be sulfated unless functional group transfer occurred in the mass spec.

MS2 of the major ion peaks yielded the same fragmentation ions as shark. MS2 fragmentation of 315.9 and 297.9 both yielded the same m/z as in shark which suggests the structures in figure 41 being generated..

#### **7.4.6 m/z154.8**

It is proposed that the m/z 154.8 ion arises due to fragmentation of the parent fragments of m/z 214.8 and 240.8. m/z 240.8 corresponds to a 2S-GlcA whilst m/z 214.8 arises from in source fragmentation of 3S-GlcA generated from the free radical depolymerisation. The relative intensity of m/z 154.8 is significantly less in bovine compared to shark. This could be due to the fact that sulfation in shark CS can occur on carbon 4/6 on GAINAc as well as carbon 2 on GlcA. All yield plausible structures that fit the MS2 data, the possible outcomes of these fragmentations are shown in figures 43-45.

#### **7.4.7 m/z Porcine**

Infusion ESI-MS analysis of intact porcine CS that was subjected to free radical depolymerisation via Fenton type reaction yielded an MS spectra similar to shark and bovine CS. However it must be noted of the subtle differences in the spectra (figures 20-22): instead of a base peak at m/z 154.8 (shark) or 297.9 (bovine) it is instead at m/z 299.8 which corresponds to a saturated 4/6S GAINAc. The other noticeable difference is the presence of a peak at m/z 475.9 which corresponds to an saturated monosulfated disaccharide chain cap which compromises of a GlcA and GalNAc, the

structure of which is shown below. An  $m/z$  of 327.8 is also seen at a great intensity in porcine which is not seen in porcine or shark.

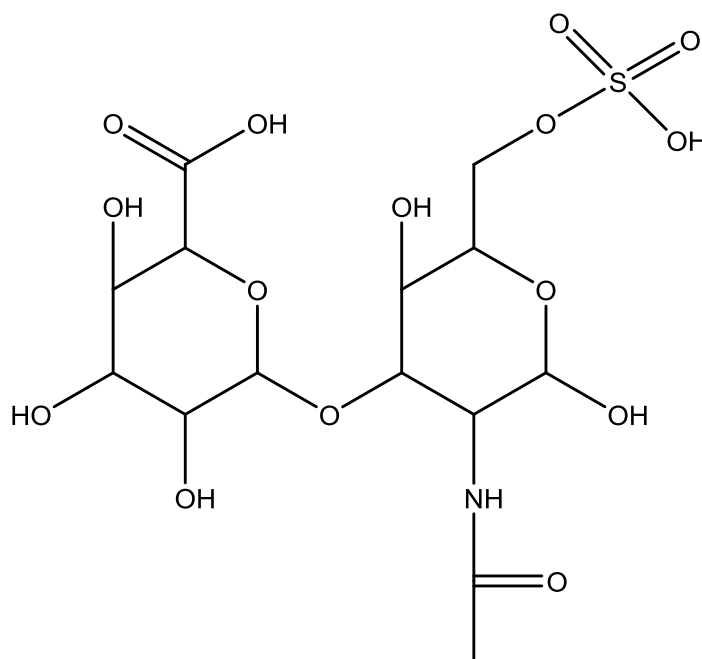


**Figure 45: Proposed structure of  $m/z$  475.9 which corresponds to a saturated monosulfated disaccharide cap.**

The spectra obtained from the porcine sample is slightly different to that of shark and bovine. There seems to be more undefined peaks in porcine (figure 37) that has similarities to the spectra of intact CS (figure 16). The presence of the 475.9 as well as the number of undefined peaks may suggest a partial depolymerisation of the intact CS chains. This is unusual considering the same conditions were used for all of these comparative experiments. The same concentration of ROS will be generated in all three experiments (As we use the same concentrations of H<sub>2</sub>O<sub>2</sub> of CuSO<sub>4</sub>) so it seems to be that the structure of porcine of CS makes it less susceptible to free radical depolymerisation, this may be due to the sulfation pattern of porcine CS.

### **7.5 Proposed mechanism of free radical depolymerisation of CS**

The previous data suggests that the free radical degradation of CS occurs at the (alpha)1-4 glycosidic bond between GlcA and GalNAc (at each glycosidic bond, as it is a polymer) which results in an increased abundance of the GalNAc residue. This proposed mechanism is an extension of those proposed by (Wu et al 2010). The hydroxyl radical generated by Fenton absorbs a hydrogen atom from C3 of the hexosamine (figure 47). This leads to the cleavage of the glycosidic bond and the formation of a GalNAc radical which then reacts with oxygen to create of fully formed GalNAc. Our findings suggest something slightly different to a previous study which suggests glycosidic bond



cleavage on carbohydrate radiolysis occurs due to radical hydrolysis with an unpaired electron at C-1 instead of C3. Both studies however suggest a Beta-scission mechanism (Dizdaroglu 2014).

This mechanism is open for discussion, it is presumed that the Beta glycosidic bond is more stable than the alpha bond. Beta is thought to be more stable due to the 'straight' configuration of the bond meaning that more hydrogen bonds can form between each monomer (Das et al 2012)(Figure 47).

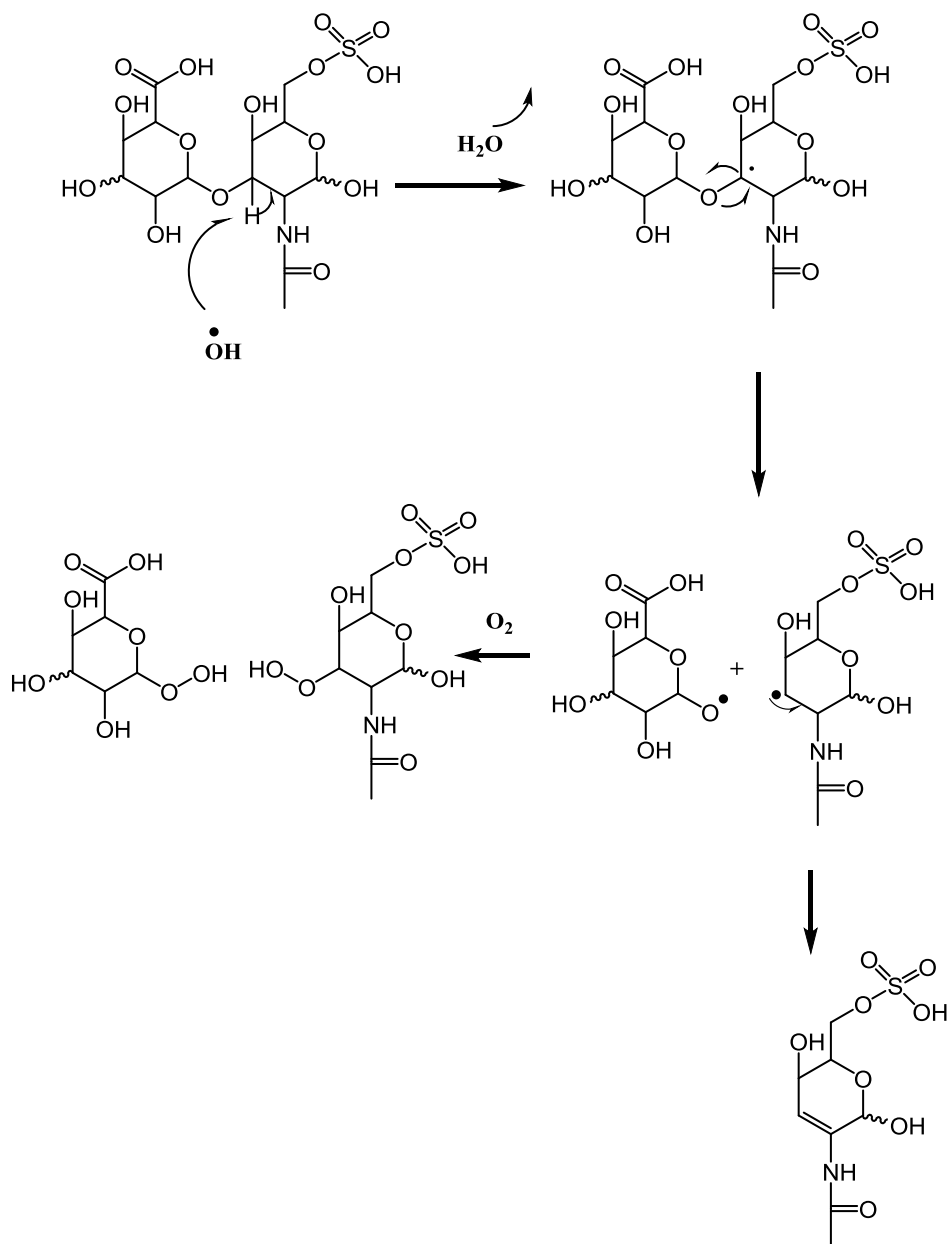
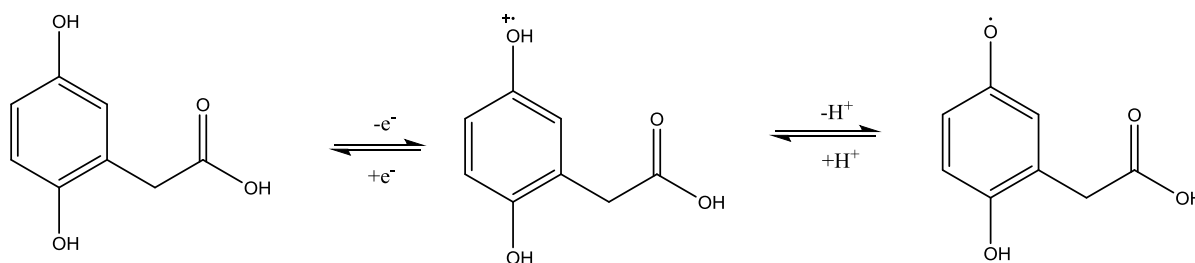


Figure 46: Proposed mechanism of the free radical degradation of chondroitin sulfate initiated by Fenton like reactions.

## 7.6 Conversion of homogentisic acid into homogentisate

The generation of the homogentisate ion from HGA is an important step in its polymerisation. This process is an excellent example of the unique redox characteristics of (hydro/semi) quinones which have the ability to serve as a one or two electron donor/acceptor (Song and Buettner 2010). Another important chemical feature is the ability to undergo reversible redox reactions without changing structure; this allows for redox recycling and is important in polymerisation. Patients with AKU display a deficiency in homogentisate 1,2-dioxygenase which normally breaks down HGA into maloleylacetic acid. A lack of this enzyme results in the accumulation of HGA which can then be oxidised to homogentisate.



**Figure 47: Mechanism of HGA oxidation to HGA benzoquinone (homogentisate) via a cation intermediate.**

The conversion of the HGA benzoquinone is a one electron process that involves the generation of an unstable cation intermediate which is not detected by mass spectrometry. The generation of the homogentisate ion is a vital component of HGA polymerisation as this is the point at which a phenoxyl radical is generated. This phenoxyl radical is then able to couple to other HGA molecules and polymerise.

## 7.7 Semiquinones and generation of ROS

To elucidate the potential reactions HGA can undergo we must first analyse the different reactions undertaken by its parent molecules. A major step in HGAs biochemistry is the generation of a benzoquinone radical (Figure 48)- These along with quinones and hydroquinones are some of the oldest organic molecules in the universe and important in many redox systems (Song and Buettner, 2010). Semiquinone generation of ROS has been addressed by Valgimigli et al., 2008. They propose that semiquinones undergo an unusual reaction with molecular oxygen that generates ROS (figure 3). In particular the 1,4-semiquinone radical reacts with oxygen in water and is thought to proceed via a sequential proton-loss electron-transfer (SPLET) mechanism at neutral/ alkaline pH.

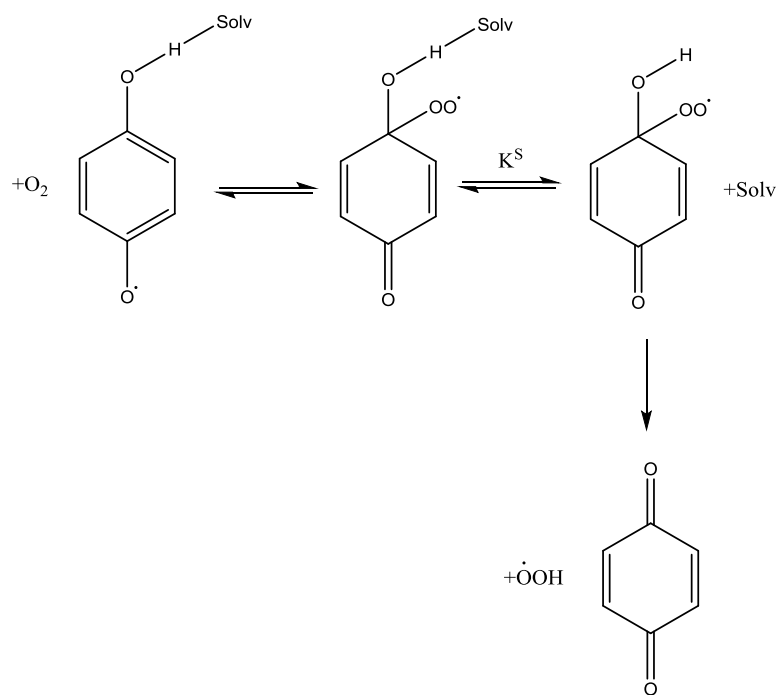
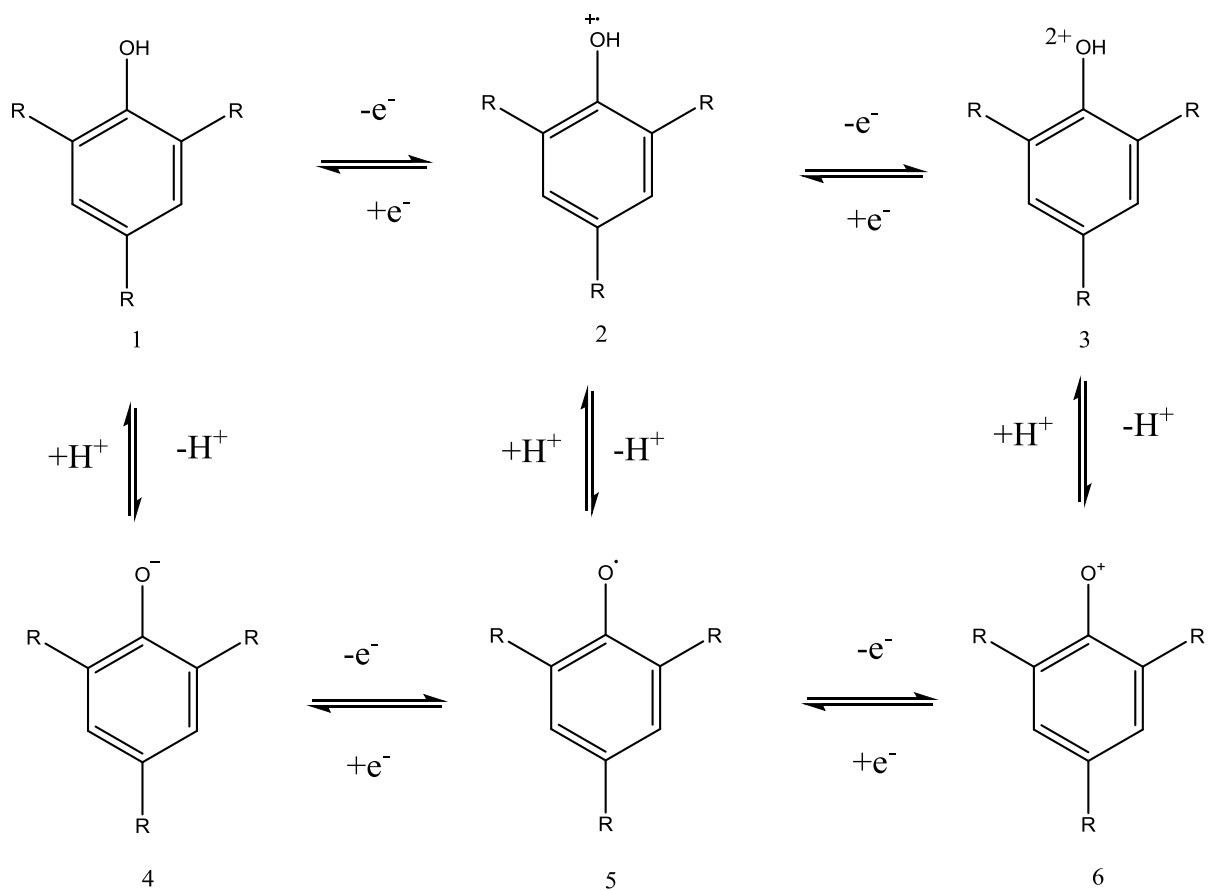


Figure 48: Reaction proposed Valgimigli et al., 2008 that postulates semiquinones unusual reaction with molecular oxygen and the generation of reactive oxygen species.

## 7.8 Oxidation and coupling of phenol

To understand the possible mechanism of HGAs polymerisation we must also look at the possible mechanisms of its dimerization which is most likely to occur at one of the phenol groups. This is a complex process which can be described as a scheme of squares where species are generated by electron and proton transfers. Although the system can be represented by figure 50, the real system is more complicated because every species of the system may react to produce 2 other species of the system. Other side reactions can take place such as dimerization of the radicals or electrophilic attack of the cations (Eickhoff et al 2001). The 2 phenol groups of HGA will undergo a similar mechanism. The generation of the phenoxyl radical then enables HGA to undergo further coupling to other phenoxyl radicals.



**Figure 49: Proposed square mechanism of the oxidation of phenol.**

Looking forward to dimerization, it is proposed that dimerization of 2 and 5 (figure 50) cannot occur due to steric hindrance and the absence of strong nucleophiles (Whitson et al 1973). One important point is that in the absence of a base, phenol 1 is oxidized to 2 which then deprotonates to 5 which is then oxidised to its desired state of 6. It is also possible for 2 and 5 to react to produce 1 and 6. From this scheme we can see that the phenoxyl radical (5) is most similar to the homogentisate ion proposed earlier.

## 7.9 Phenoxyl reactions

The final oxidation products will be determined by the reactivity of the phenoxyl which is stabilised by resonance. This has previously been proven using ESR measurements (Jørgensen et al 1999) in addition to these oxidation products, the phenoxyl can react with other radical (X.) which are added due to dehydrogenation of an excess of the phenoxyl. There are numerous possibilities of the identity of X: such as nitrogen or carbon radicals. In the case of HGA dimerization this may well very be another homogentisate (phenoxyl).

It is possible for 2 phenoxyls to combine and produce multiple dimers, the products can arise via homocoupling (identical phenoxyls) or heterocoupling (Different phenoxyls). It is possible for this process to start from the initial phenol or the phenoxyl due to the various electron and proton exchanges highlighted in figure 40. The type of coupling that arises is determined by the steric and electronic effects of the R groups. It can be assumed that homocoupling occurs when there is a large  $R_{ortho}$  and a small  $R_{para}$  will lead to the coupling highlighted in figure 42. Heterocoupling can occur with a large  $R_{ortho}$  and an any sized  $R_{para}$  with both of them donating electrons; this gives rise to the product highlighted in figure 41.

## 7.10 Oxidation of hydroquinone by copper

The importance of Cu as a catalyst of hydroquinone oxidation is highlighted in a number of studies (Osako et al 2003, Yuan et al 2013). It has previously been noted that the presence of  $Cu^{2+}$  had a large impact on the generation of dityrosine. It was highlighted earlier that the formation of dityrosine involved several oxidative steps so it may be assumed that Cu(II) also plays a role in these reactions. It was also found that the production of dityrosine was dependant on it being a free ion which in our Fenton system it was. The advantage of the Fenton system over the horseradish peroxidase system was also highlighted. There was no reported decrease in the yield of dityrosine when the pH was changed, this was not the case when using the horseradish peroxidase system (Ali et al 2004, Jacob et al 1996).

## 7.11 Benzoquinone dimerization

Once the benzoquinone of HGA (Figure..) is generated via Cu catalysis it then has the possibility to undergo polymerisation. It is the strong electron-acceptor characteristics that is important in this process and is important in a number of biological systems. The radical anion is stabilised by delocalization of the negative charge in quinone oligomers (Hayashi et al 2007). Like the HGA quinone dimer, there are very few quinone oligomers that have been characterised. This may be because they are so unstable that decompose when crystalized from ethanol.

## 7.12 HGA dimerization

Although there has been some work on the dimerization of benzoquinones, there has been very little applied to homogentisic acid when in its benzoquinone form. Hashimoto, Saikawa, & Nakata, (2007) provided some insight into the possible structure of this dimer. They do this through characterizing the structure of hippoduric acid which is a pigment found in sweat. They propose that HGA is the biogenital precursor to his acid.

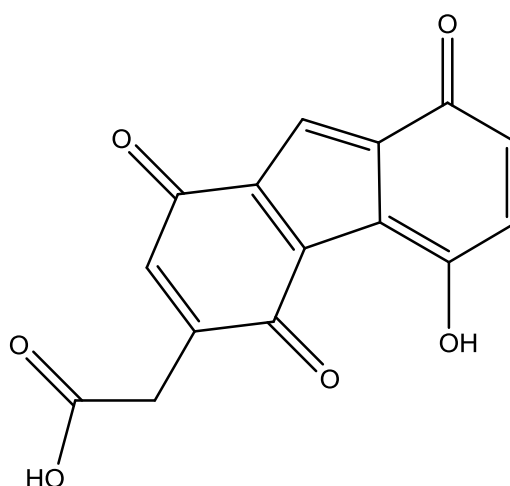
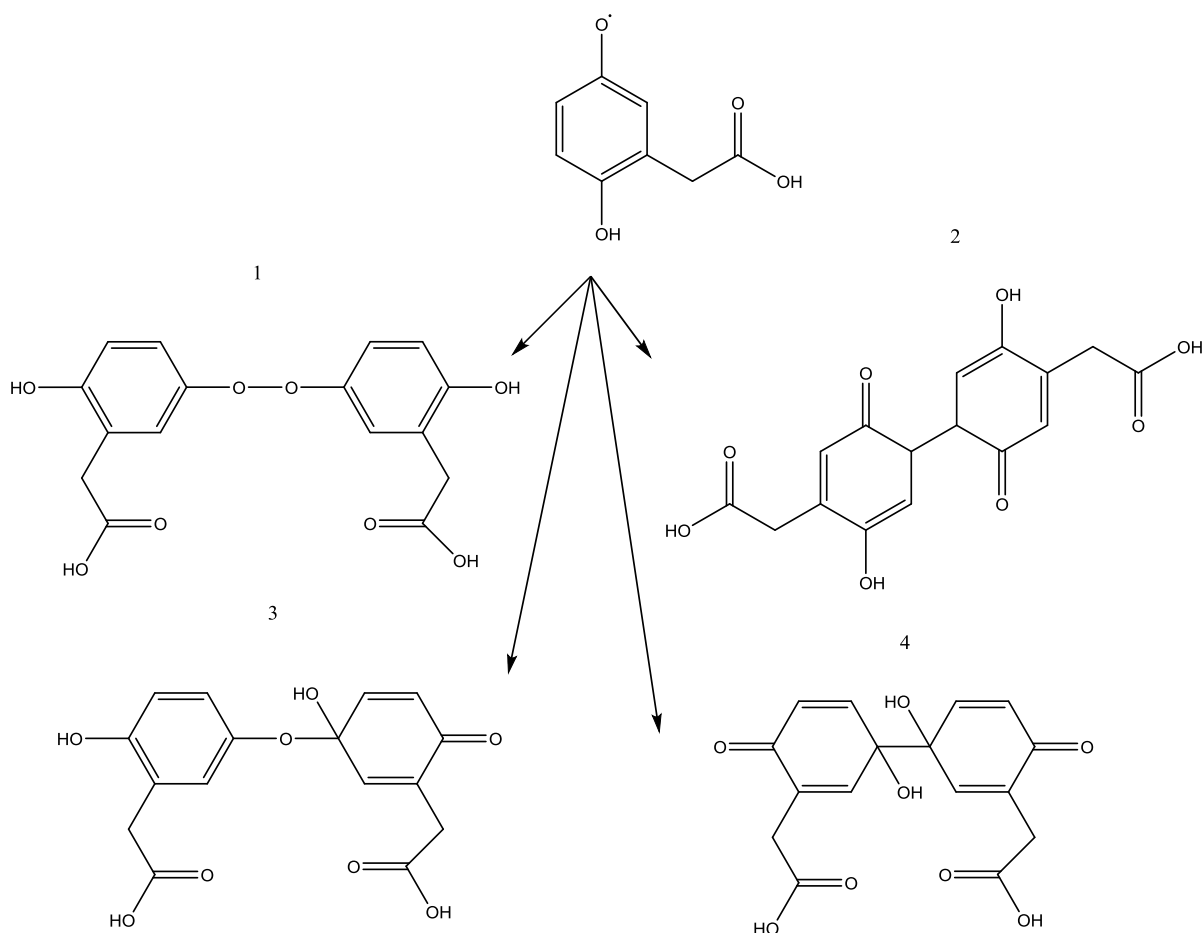


Figure 50: structure of hippoduric acid (orange pigment)

Hashimoto devoted 7 years to understanding the structure of hippoduric acid, yet they have still not resolved how HGA is converted to this pigment. It can be seen that the left-side ring is composed of the HGA benzoquinone whilst the right is the semiquinone with a lacking carboxyl arm. The corresponding  $m/z$  of this molecule would be around 282.8, when looking at figure 38 we can see there is no major peak in this area. This does not rule out this molecule being present but it does show that it is unlikely to be involved in the main mechanism of HGA polymerisation.

Based on the dimerization/ polymerisation of its parent molecules, we can propose some mechanisms of HGAs (dimer/polymer)isation. If HGA is in its phenoxyl radical form ( $\text{HGA}^\cdot$ ) it can undergo a number of feasible dimerizations highlighted by figure 52. The type of dimerization that occurs it dependent upon the constituent monomers. This dictates whether homo or heterocoupling occurs as previously discussed.



**Figure 51: Proposed structures of HGA dimers based on the coupling of phenoxyl radicals.**

The molecular weight of all these dimers is approximately 334.3 which corresponds to an  $m/z$  of around 333.6. This is around 1 dalton lighter than the recorded  $m/z$  that we thought was the HGA dimer. Further  $ms^2$  analysis of  $m/z$  334.9 highlighted that it was solely composed of a non-oxidized HGA ( $m/z$  166.8). However this should not be surprising as we are suggesting that for HGA dimerization to occur it must first be in its oxidised (phenoxyl) form. We believe that the presence of a ferrous ion ( $Fe^{2+}$ ) or copper ( $Cu^{2+}$ ) will catalyse this process and possibly allow us to observe the proposed dimers. However this does not shy away from the possible complexity of this reaction as previously discussed. Any one of these dimers can be formed stably and further NMR analysis of HGA in the presence of copper would be helpful, however this would require extensive work up that was not feasible for the time frame of this project. It must be noted that a structure very similar to structure 2 has been reported when investigating the effects of acetonitrile on HGA dimerization (Eslami et al 2014).

It must be noted that HGA does not contain one phenol group, it is a diphenol as well as a phenolic acid. Oxidation of diphenols can lead to intramolecular coupling of the diradical. The scheme of dimerization still follows that of figure 38 where the coupling pattern is determined by the molecular frame. It has been reported that a number of natural products can be generated through the dimerization of bi and diphenols- hippoduric acid being one of them (Kita et al 1998, Rama Krishna et al 1990)

### 7.13 HGA and the generation of ROS

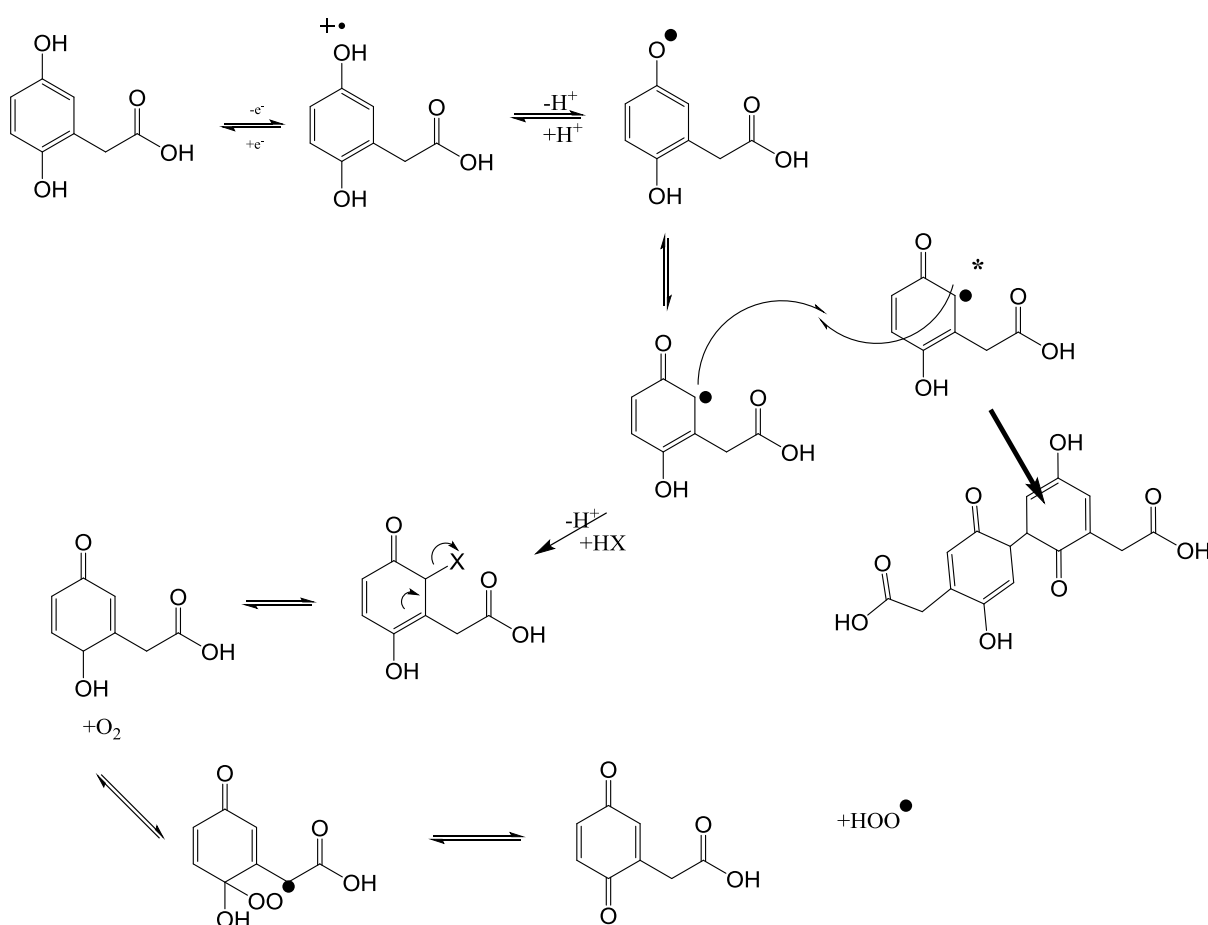


**Figure 52: Proposed mechanism of HGAs oxidation to a semiquinone and its unusual reaction with molecular oxygen to produce ROS. \* Part of the pathway where HGA dimerization may occur based on previous analysis of benzoquinone dimerization.**

Several lines of enquiry have proposed the potential polymerisation of HGA, below is a possible structure of the HGA polymer from a previous study (Braconi et al 2015). When looking at the (dimer/polymer)isation it seems that the most likely point of coupling would be the two oxidised



phenol groups. The MS2 data from our spectra suggests that the COOH is the easiest group to break off from HGA. It is more unlikely that polymerisation would occur at this point as it would require a carbon radical attack. Considering there are 2 free OH groups it seems that these are the most likely sites to generate radicals and join with other HGA molecules.

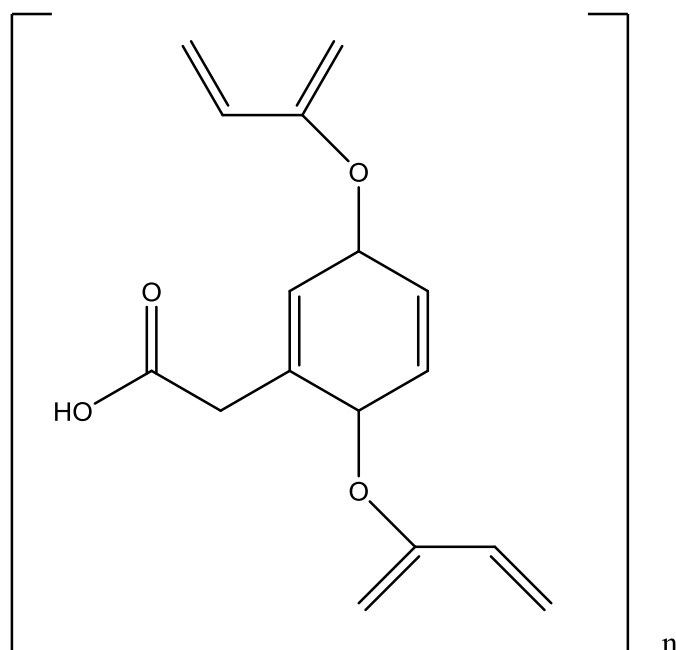


**Figure 53: Proposed structure of HGA polymer after the generation of the HGA benzoquinone leading to the ochronotic pigmentation observed in Alkaptonuria (Braconi et al 2015).**

This pathway has been created after reviewing the oxidation and polymerisation of tyrosine as well as the oxidation of the general classes of molecule that HGA belongs (e.g. benzoquinones, hydroquinone etc.). Future research is needed to agree or disagree with this theory. What is known is the ochronotic pigment found in AKU bone does contain polymerised HGA. This inevitably leads to the degradation of bone/cartilage and the development of arthritis in AKU patients.

The proposed generation of ROS in the final step of its oxidation generates many more avenues for future research. In the previous chapter, we discussed the free radical degradation of CS, a vital component of cartilage and bone ECM. In the next chapter, we discuss the possibility of HGA degrading CS through its own metal catalysed oxidation and polymerisation.

## 7.14 HGA interaction with CS

We propose the metal catalysed polymerisation of HGA will lead to the degradation of CS due to generation of ROS as a result of HGA polymerisation. The above figure provides some evidence that this is in fact possible.  $m/z$  457.9 corresponds to the unsaturated CS disaccharide which is composed of a 4/6S-GALNAc bound to GlcA via glycosidic bonds.  $m/z$  299.8 corresponds to 4/6S-GalNAc.

When compared to the spectra generated by the mixture of HGA and CS it becomes apparent that the intensity of  $m/z$  299.8 is significantly reduced to background intensity (figure 46). This again provides some evidence that the addition of  $\text{CuSO}_4$  (or Iron citrate) is required to catalyse the generation of ROS from HGA. It may be that HGA on its own would be able to degrade CS, however it would require years of study to conclude this.

Previous studies have hypothesised that free radicals generated by the oxidation of HGA to its benzoquinone were responsible for the change in connective tissue observed in AKU. A similar change in the connective tissue was observed in non-AKU arthritis and disorders or tyrosine metabolism (Hegedus and Nayak 1994, Rocha and Martins 2012). Specifically it was proposed that ROS generated from HGA was able to damage the GAG hyaluronic acid in the synovial fluid of joints (Hegedus and Nayak 1994). This is the only current evidence for HGA damaging a GAG. It was also proposed that the morphological changes in AKU arose due to the HGA benzoquinone linking to collagen ionic groups via its carboxyl arm. Furthermore, the linkage between HGA hydroxyl groups or activated CH groups and the keto-imide bonds in collagen (Braconi et al 2015).

Based on the mechanism in figure 53 we propose that HGA polymerisation will generate oxygen free radicals similar to those generated from the Fenton like reaction ( $\text{CuSO}_4 + \text{H}_2\text{O}_2$ ). These ROS can then go on to breakdown the disaccharide of chondroitin sulfate with the same mechanism as figure 47.

### **7.15 Addition of SOD preventing free radical depolymerisation of CS**

We propose that the metal catalysed oxidation/polymerisation of HGA generates ROS as well as radical forms of HGA (e.g. Phenoxyl radicals). The full mechanism of HGA polymerisation is still a mystery however it is believed to involve several electron/ proton transfers as well as complex interactions with various cofactors. From these figure 55 we can see the addition of SOD does have some effect on the ions generated from HGA-CuSO<sub>4</sub> reaction. What can be deduced is the reduced relative intensity of m/z 166.8 in A compared to B. This may suggest that SOD is playing a role in preventing the oxidation/polymerisation of HGA which would therefore yield more of the initial acid.

In this reaction 10ul of SOD (5000AU) was enough to halt the free radical depolymerisation of CS. Oxyradicals were generated from 10ul 20mg/mlCuSO<sub>4</sub> and 10ul 35%H<sub>2</sub>O<sub>2</sub>. It would be useful in future experiments to determine at what volume/activity the SOD would become insufficient to halt the reaction. From these experiments, it would be possible to determine the stoichiometry of the reaction. For our studies, it was sufficient to show that the SOD was able to stop free the free radical depolymerisation of CS.

It was previously discussed that it became apparent that HGA was possibly able to breakdown CS disaccharides when in the presence of a metal catalyst. It was postulated that HGA-Cu<sup>2+</sup> was not able to fully degrade the full length CS chain. The presence of m/z 299.8 was a marker for this degradation in porcine CS which corresponds to an unsaturated monosulfated GalNAc. From figure 5 we can see that the addition of SOD to the digest prior to HGA and CuSO<sub>4</sub> halted the generation of m/z 299.8. it is also clear that that m/z 166.8 (corresponding to HGA) is at present in the SOD spectra but not in the other. This suggests that SOD prevented that oxidation and depolymerisation of HGA which is supported by previous experiments. Through the actions of SOD preventing HGA oxidation/polymerisation, it was also able to prevent the HGA(Cu<sup>2+</sup>)-mediated degradation of the CS disaccharide.

This hypothesis has major implications in Alkaptonuria which is a disease that manifests as a result of HGAs oxidation/ polymerisation which results in the degradation of cartilage. Could SOD be used as a possible therapeutic in the treatment of the bone-associated symptoms of alkaptonuria? From these findings it may be possible to suggest that SOD may also act as preventative agent in non-AKU arthritis through the action of preventing CS degradation.

The possible beneficial effects of SOD in joint diseases has previously been discussed, it was found that SOD had protective effects in inflammation in animal models (Fujimura et al 2000). In mouse models it was found that SOD deficiency in mice lead to an increase in the production of proinflammatory cytokines and the severity of arthritis (Ross et al 2004). In the same model it was

discovered that SOD gene transfer resulted in a decrease in arthritis severity (Dai et al 2003). However in human models, SOD levels had an adverse effect on arthritis severity (Ugur et al 2004). These findings were met with conflicting results and available data does suggest SOD has a protective role in inflammatory joint disease (Afonso et al 2007).

## 8. Conclusions

The mass spectra suggests that free radical degradation of CS does not stop at the cleavage of the glycosidic bond but in fact carry on with the cleavage of the ring.; due to the high intensity of  $m/z$  154.8 (which corresponds to further breakdown of 4/6S-GlcA). If this  $m/z$  only arose as a result of MS2 fragmentation of  $m/z$  240.8 then it would surely be present at similar intensities to the other MS2 fragments and would not be present at a greater intensity than the 240.8 peak in the original spectra. We instead see a significantly increased presence of 154.8 which may be down to a number of factors in addition to the point above. One may be that artefacts with similar  $m/z$  are contributing to the large intensity or it may be that further fragmentation of the parent fragments that are contributing to the increased intensity.

What we do know is that there is evidence in literature of ROS cleaving benzene rings and forming aldehyde metabolites which then increased the hematoxicity of benzene (Witz et al 1996). In fact oxidative cleavage of 6 membered rings by transition metals is also of great interest in the petrol and biomass industries (Hu et al 2014). What this shows is there is evidence that free radical damage of stable C-C bonds is possible. Further work is needed to provide an insight for or against the proposed mechanism for the further breakdown of the GalNAc ring.

We have proposed a mechanism for the free radical degradation of CS, an important structural component of articular cartilage. The degradation of this molecule has been associated with the development of arthritis. As age increases so does the quantity of ROS generated. The proposed mechanism of free radical depolymerisation of CS may provide some insight into the development of arthritis. Chondroitin sulfate can elicit anti-inflammatory effects and regulate the anabolic/catabolic balance in chondrocytes (Du Souich 2014). Therefore, bodily free radical depolymerisation (i.e. free radicals generated via biological routes such as inflammation) of CS will not only degrade structural components of cartilage but will also be detrimental to the defence against further free radical (oxidant) damage of nearby structures.

Further work is needed to identify the potential implications of this proposed mechanism in vivo. However the data provided here does present evidence that the free radical degradation of CS occurs by the cleavage of the glycosidic bond between GlcA and GalNAc. The mass spectra also suggests either fragmentation of the generated monosaccharides or further free radical degradation of the hexose ring. This has massive implications when considering arthritis progression and severity with age.

This study aimed to characterize the structures generated from the free radical and enzyme depolymerisation of CS using ESI-MS. We concluded that ROS generated via Fenton reaction was able to breakdown both intact CS and its disaccharide unit. Structures were characterised using tandem MS data and theoretical modelling, alongside this we were also able to construct fragmentation pathways of the components of the CS disaccharide e.g. GlcA and GalNAc. This method can easily detect the presence of the free radical damaged CS by generating high intensity fragments of  $m/z$  299.9/297.8 and 315.9.

The use of HPLC and ESI-MS was then used to characterize structures from the analysis of HGA. Tandem MS analysis and theoretical modelling was also used to characterize structures from the fragmentation of HGA. This same method was used to investigate the potential Cu catalysed oxidation and polymerisation of HGA. Whilst these structures still remain elusive, we were able to show that the presence of copper was needed to catalyse the transition from the acid form of HGA through to its oxidised form (Hydroquinones, benzoquinones etc).

We were able to predict the possible mechanism of HGA polymerisation by using its parent molecules such as tyrosine and phenol. Using these as templates we concluded that the most likely point of polymerisation would be one of the OH groups. From this we proposed a mechanism of HGA dimerization with the generation of oxygen free radicals via its unusual reaction with molecular oxygen. The proposed mechanism involved the generation of ROS via its polymerisation and this would fit well with the prediction that HGA can in fact breakdown CS disaccharides in the presence of copper.

The use of SOD highlighted the ability to halt the free radical degradation of CS via its oxygen radical scavenging mechanism. SOD was also used to halt the HGA induced degradation of the CS disaccharide which again suggests that HGA induced degradation arises due to the generation of ROS via its own oxidation and polymerisation.

## 9. References

Abreu IA and Cabelli DE (2010) Superoxide dismutases—a review of the metal-associated mechanistic variations. *Biochimica et Biophysica Acta - Proteins and Proteomics*, 263–274.

Afonso V, Champy R, Mitrovic D, Collin P and Lomri A (2007) Reactive oxygen species and superoxide dismutases: Role in joint diseases. *Joint Bone Spine*, 324–329.

Alfadda AA and Sallam RM (2012) Reactive oxygen species in health and disease. *Journal of biomedicine & biotechnology* 2012.

Ali FE, Barnham KJ, Barrow CJ and Separovic F (2004) Metal catalyzed oxidation of tyrosine residues by different oxidation systems of copper/hydrogen peroxide. *Journal of Inorganic Biochemistry* 98(1): 173–184.

Arturo Alberto Vitale, Eduardo A. Bernatene, Martín Gustavo Vitale and ABP (2016) New Insights of the Fenton Reaction Using Glycerol as the Experimental Model. Effect of O<sub>2</sub>, Inhibition by Mg<sup>2+</sup>, and Oxidation State of Fe. *The Journal of Physical Chemistry A* 120(28): 5435–5445.

Batinić-Haberle I, Rebouças JS and Spasojević I (2010) Superoxide Dismutase Mimics: Chemistry, Pharmacology, and Therapeutic Potential. *Antioxidants & Redox Signaling* 13(6): 877–918.

Bayliss MT, Davidson C, Woodhouse SM and Osborne DJ (1995) Chondroitin sulphation in human joint tissues varies with age, zone and topography. *Acta Orthopaedica* 266, 22-25.

Bayliss MT, Osborne D, Woodhouse S and Davidson C (1999) Sulfation of chondroitin sulfate in human articular cartilage: The effect of age, topographical position, and zone of cartilage on tissue composition. *Journal of Biological Chemistry* 274(22), 15892–15900.

Bergès J, Trouillas P and Houée-Levin C (2011) Oxidation of protein tyrosine or methionine residues: From the amino acid to the peptide. *Journal of Physics: Conference Series* 261: 012003.

Bhattacharyya A, Chattopadhyay R, Mitra S and Crowe SE (2014) Oxidative Stress: An Essential Factor in the Pathogenesis of Gastrointestinal Mucosal Diseases. *Physiological Reviews* 94(2): 329–354..

Birben E, Sahiner UM, Sackesen C, Erzurum S and Kalayci O (2012) Oxidative stress and antioxidant defense. *The World Allergy Organization journal* 5(1): 9–19.

Braconi D, Millucci L, Bernardini G and Santucci A (2015) Oxidative stress and mechanisms of ochronosis in alkaptonuria. *Free Radical Biology and Medicine* 88: 70–80.

Brown MP, Trumble TN, Plaas AHK, Sandy JD, Romano M, Hernandez J and Merritt KA (2007) Exercise and injury increase chondroitin sulfate chain length and decrease hyaluronan chain length in synovial fluid. *Osteoarthritis and Cartilage* 15(11): 1318–1325.

Calamia V, Fernández-Puente P, Mateos J, Lourido L, Rocha B, Montell E, Vergés J, Ruiz-Romero C and Blanco FJ (2012) Pharmacoproteomic study of three different chondroitin sulfate compounds on intracellular and extracellular human chondrocyte proteomes. *Molecular & cellular proteomics : MCP* 11(6): M111.01341

Cantley MD, Rainsford KD and Haynes DR (2013) Comparison of the ability of chondroitin sulfate derived from bovine, fish and pigs to suppress human osteoclast activity in vitro. *Inflammopharmacology* 21(6): 407–412.

Ceroni A, Maass K, Geyer H, Geyer R, Dell A and Haslam SM (2008) GlycoWorkbench: A tool for the computer-assisted annotation of mass spectra of glycans. *Journal of Proteome Research* 7(4): 1650–1659.

Chen Z, Li Y and Yuan Q (2015) Expression, purification and thermostability of MBP-chondroitinase ABC I from *Proteus vulgaris*. *International Journal of Biological Macromolecules* 72: 6–10.

Clegg DO, Reda DJ, Harris CL, Klein MA, O'Dell JR, Hooper MM, Bradley JD, Bingham CO, Weisman MH, Jackson CG, Lane NE, Cush JJ, Moreland LW, Schumacher HR, Oddis C V., Wolfe F, Molitor JA, Yocum DE, Schnitzer TJ, Furst DE, Sawitzke AD, Shi H, Brandt KD, Moskowitz RW and Williams HJ (2006) Glucosamine, Chondroitin Sulfate, and the Two in Combination for Painful Knee Osteoarthritis. *New England Journal of Medicine* 354(8): 795–808.

Coates J (2006) Encyclopedia of Analytical Chemistry. *Encyclopedia of analytical chemistry*, 10815–10837. Available at:

Conrad HE (2001) Beta-elimination for release of O-linked glycosaminoglycans from proteoglycans. *Current protocols in molecular biology / edited by Frederick M. Ausubel ... [et al.]* Chapter 17(1995): Unit17.15A.

Dai L, Claxson a, Marklund SL, Feakins R, Yousaf N, Chernajovsky Y and Winyard PG (2003) Amelioration of antigen-induced arthritis in rats by transfer of extracellular superoxide dismutase and catalase genes. *Gene therapy* 10(7): 550–8.

Das RS, Samaraweera M, Morton M, Gascón JA and Basu AK (2012) Stability of N-glycosidic bond of (5' S)-8,5'-Cyclo-2'- deoxyguanosine. *Chemical Research in Toxicology* 25(11): 2451–2461.



David-Raoudi M, Deschrevel B, Leclercq S, Gaïera P, Boumediene K and Pujol JP (2009) Chondroitin sulfate increases hyaluronan production by human synoviocytes through differential regulation of hyaluronan synthases: Role of p38 and Akt. *Arthritis and Rheumatism* 60(3): 760–770.

Desaire H, Sirich TL and Leary JA (2001) Evidence of block and randomly sequenced chondroitin polysaccharides: Sequential enzymatic digestion and quantification using ion trap tandem mass spectrometry. *Analytical Chemistry* 73(15): 3513–3520.

Dizdaroglu M (2014) Clemens von Sonntag and the early history of radiation-induced sugar damage in DNA. *International journal of radiation biology* 90(6): 446–58.

Eickhoff H, Jung G and Rieker A (2001) Oxidative phenol coupling - Tyrosine dimers and libraries containing tyrosyl peptide dimers. *Tetrahedron* 57(2): 353–364.

Eslami M, Zare HR and Namazian M (2014) The effect of solvents on the electrochemical behavior of homogentisic acid. *Journal of Electroanalytical Chemistry* 720–721: 76–83.

Fang L and Miller YI (2012) *Free Radic Biol Med. Growth (Lakeland)* 53(7): 1411–1420.

Fujimura M, Morita-Fujimura Y, Noshita N, Sugawara T, Kawase M and Chan PH (2000) The cytosolic antioxidant copper/zinc-superoxide dismutase prevents the early release of mitochondrial cytochrome c in ischemic brain after transient focal cerebral ischemia in mice. *The Journal of neuroscience : the official journal of the Society for Neuroscience* 20(8): 2817–2824.

Hardingham TE and Fosang AJ (1992) Proteoglycans: many forms and many functions. *The FASEB journal : official publication of the Federation of American Societies for Experimental Biology*.

Hashimoto K, Saikawa Y and Nakata M (2007) Studies on the red sweat of the Hippopotamus amphibius. *Pure and Applied Chemistry* 79(4): 507–517.

Hayami T, Pickarski M, Wesolowski GA, McLane J, Bone A, Destefano J, Rodan GA and Duong LT (2004) The Role of Subchondral Bone Remodeling in Osteoarthritis: Reduction of Cartilage Degeneration and Prevention of Osteophyte Formation by Alendronate in the Rat Anterior Cruciate Ligament Transection Model. *Arthritis and Rheumatism* 50(4): 1193–1206.

Hayashi N, Yoshikawa T, Ohnuma T, Higuchi H, Sako K and Uekusa H (2007) Synthesis, structure, and properties of benzoquinone dimer and trimers bearing t-Bu substituents. *Organic Letters* 9(26): 5417–5420.

Hegedus ZL and Nayak U (1994) Homogentisic Acid and Structurally Related-Compounds As

Intermediates in Plasma Soluble Melanin Formation and in Tissue Toxicities. *Archives Internationales de Physiologie de Biochimie et de Biophysique* 102(3): 175–181.

Henrotin Y, Marty M and Mobasheri A (2014) What is the current status of chondroitin sulfate and glucosamine for the treatment of knee osteoarthritis? *Maturitas*, 184–187.

Hidalgo C and Donoso P (2008) Crosstalk Between Calcium and Redox Signaling: From Molecular Mechanisms to Health Implications. *Antioxidants & Redox Signaling* 10(7): 1275–1312.

Hitchcock AM, Bowman MJ, Staples GO and Zaia J (2008) Improved workup for glycosaminoglycan disaccharide analysis using CE with LIF detection. *Electrophoresis* 29(22): 4538–4548.

Hitchcock AM, Costello CE and Zaia J (2006) Glycoform quantification of chondroitin/dermatan sulfate using a liquid chromatography-tandem mass spectrometry platform. *Biochemistry* 45(7): 2350–2361.

Ho CS, Lam CWK, Chan MHM, Cheung RCK, Law LK, Lit LCW, Ng KF, Suen MWM and Tai HL (2003) Electrospray ionisation mass spectrometry: principles and clinical applications. *The Clinical biochemist*.

Hochberg MC, Zhan M and Langenberg P (2008) The rate of decline of joint space width in patients with osteoarthritis of the knee: a systematic review and meta-analysis of randomized placebo-controlled trials of chondroitin sulfate. *Curr Med Res Opin* 24(11): 3029–3035.

Hu S, Shima T and Hou Z (2014) Carbon–carbon bond cleavage and rearrangement of benzene by a trinuclear titanium hydride. *Nature* 512(7515): 413–415.

Jacob JS, Cistola DP, Hsu FF, Muzaffar S, Mueller DM, Hazen SL and Heinecke JW (1996) Human phagocytes employ the myeloperoxidase-hydrogen peroxide system to synthesize dityrosine, trityrosine, pulcherosine, and isodityrosine by a tyrosyl radical-dependent pathway. *Journal of Biological Chemistry* 271(33): 19950–19956.

Jørgensen L V, Madsen HL, Thomsen MK, Dragsted LO and Skibsted LH (1999) Regeneration of phenolic antioxidants from phenoxyl radicals: an ESR and electrochemical study of antioxidant hierarchy. *Free Radical Research* 30(3): 207–20.

Karsdal MA, Leeming DJ, Dam EB, Henriksen K, Alexandersen P, Pastoureau P, Altman RD and Christiansen C (2008) Should subchondral bone turnover be targeted when treating osteoarthritis? *Osteoarthritis and Cartilage*, 638–646.

Kiselova N, Dierker T, Spillmann D and Ramström M (2014) An automated mass spectrometry-based screening method for analysis of sulfated glycosaminoglycans. *Biochemical and Biophysical Research Communications*.

Kita Y, Arisawa M, Gyoten M, Nakajima M, Hamada R, Tohma H and Takada T (1998) Oxidative Intramolecular Phenolic Coupling Reaction Induced by a Hypervalent Iodine(III) Reagent: Leading to Galanthamine-Type Amaryllidaceae Alkaloids. *The Journal of Organic Chemistry* 63(19): 6625–6633.

Kosman VM, Karlina MN, Pozharitskaya ON, Shikov AN and Makarov VG (2017) HPLC determination of glucosamine hydrochloride and chondroitin sulfate, weakly absorbing in the near UV region, in various buffer media. *Journal of Analytical Chemistry*.

Lauder RM (2009) Chondroitin sulphate: A complex molecule with potential impacts on a wide range of biological systems. *Complementary Therapies in Medicine* 17(1): 56–62.

Lawrence R, Olson SK, Steele RE, Wang L, Warrior R, Cummings RD and Esko JD (2008) Evolutionary differences in glycosaminoglycan fine structure detected by quantitative glycan reductive isotope labeling. *Journal of Biological Chemistry* 283(48): 33674–33684.

Ledin J, Staatz W, Li JP, G?tte M, Selleck S, Kjell?n L and Spillmann D (2004) Heparan sulfate structure in mice with genetically modified heparan sulfate production. *Journal of Biological Chemistry* 279(41): 42732–42741.

Mahajan A and Tandon V (2004) Antioxidants and rheumatoid arthritis. *J Indian Rheumatol Assoc* 139–142.

Martel-Pelletier J, Farran A, Montell E, Vergés J and Pelletier JP (2015) Discrepancies in composition and biological effects of different formulations of chondroitin sulfate. *Molecules*, 4277–4289.

McAnoy AM, Wu CC and Murphy RC (2005) Direct qualitative analysis of triacylglycerols by electrospray mass spectrometry using a linear ion trap. *Journal of the American Society for Mass Spectrometry*.

Miller MJ, Costello CE, Malmstrom A and Zaia J (2006) A tandem mass spectrometric approach to determination of chondroitin/dermatan sulfate oligosaccharide glycoforms. *Glycobiology* 16(6): 502–513.

Millucci L, Giorgetti G, Viti C, Ghezzi L, Gambassi S, Braconi D, Marzocchi B, Paffetti A, Lupetti P, Bernardini G, Orlandini M and Santucci A (2015) Chondroptosis in alkaptonuric cartilage. *Journal of Cellular Physiology* 230(5): 1148–1157.

Miyazaki T, Miyauchi S, Tawada A, Anada T and Suzuki O (2010) Effect of chondroitin sulfate-E on the osteoclastic differentiation of RAW264 cells. *Dental materials journal* 29(4): 403–10.

Mortier KA, Zhang GF, Van Peteghem CH and Lambert WE (2004) Adduct formation in quantitative bioanalysis: Effect of ionization conditions on paclitaxel. *Journal of the American Society for Mass Spectrometry*.

Osako T, Ohkubo K, Taki M, Tachi Y, Fukuzumi S and Itoh S (2003) Oxidation mechanism of phenols by dicopper-dioxygen (Cu<sub>2</sub>/O<sub>2</sub>) complexes. *Journal of the American Chemical Society*.

Pavão MSG, Aiello KRM, Werneck CC, Silva LCF, Valente AP, Mulloy B, Colwell NS, Tollefsen DM and Mourão PAS (1998) Highly sulfated dermatan sulfates from ascidians. Structure versus anticoagulant activity of these glycosaminoglycans. *Journal of Biological Chemistry*.

Pham-Huy LA, He H and Pham-Huy C (2008) Free radicals, antioxidants in disease and health. *International journal of biomedical science : IJBS* 4(2): 89–96.

Poh ZW e., Gan CH en., Lee EJ, Guo S, Yip GW and Lam Y (2015) Divergent Synthesis of Chondroitin Sulfate Disaccharides and Identification of Sulfate Motifs that Inhibit Triple Negative Breast Cancer. *Scientific reports*.

Rainsford KD (2009) Importance of pharmaceutical composition and evidence from clinical trials and pharmacological studies in determining effectiveness of chondroitin sulfate and other glycosaminoglycans: a critique. *J Pharm Pharmacol* 61(10): 1263–1270.

Rama Krishna K V., Sujatha K and Kapil RS (1990) Phenolic oxidative coupling with hypervalent organo iodine compound (diacetoxyiodo) benzene. *Tetrahedron Letters* 31(9): 1351–1352.

Ray PD, Huang B-W and Tsuji Y (2012) Reactive oxygen species (ROS) homeostasis and redox regulation in cellular signaling. *Cellular Signalling*.

Reddi AR, Jensen LT, Naranuntarat A, Rosenfeld L, Leung E, Shah R and Culotta VC (2009) The overlapping roles of manganese and Cu/Zn SOD in oxidative stress protection. *Free Radical Biology and Medicine* 46(2): 154–162.

Richy F, Bruyere O, Ethgen O, Cucherat M, Henrotin Y, Reginster JY, Meta-analysis AC, Richy F, Bruyere O, Ethgen O, Cucherat M, Henrotin Y and Reginster JY (2003) Structural and symptomatic efficacy of glucosamine and chondroitin in knee osteoarthritis: A comprehensive meta-analysis. *Archives of Internal Medicine* 163(13): 1514–

- Rocha JC and Martins MJ (2012) Oxidative stress in Phenylketonuria: Future directions. *Journal of Inherited Metabolic Disease*, 381–398.
- Ross AD, Banda NK, Muggli M and Arend WP (2004) Enhancement of collagen-induced arthritis in mice genetically deficient in extracellular superoxide dismutase. *Arthritis and Rheumatism* 50(11): 3702–3711.
- Saad OM, Ebel H, Uchimura K, Rosen SD, Bertozzi CR and Leary JA (2005) Compositional profiling of heparin/heparan sulfate using mass spectrometry: Assay for specificity of a novel extracellular human endosulfatase. *Glycobiology* 15(8): 818–826.
- Seidler DG and Dreier R (2008) Decorin and its galactosaminoglycan chain: Extracellular regulator of cellular function? *IUBMB Life*, 729–733.
- Silbert JE and Sugumaran G (2002) Biosynthesis of Chondroitin / Dermatan Sulfate. *IUBMB life* 54: 177–186.
- Singh JA, Noorbaloochi S, Macdonald R and Maxwell LJ (2015) Chondroitin for osteoarthritis. *Cochrane Database of Systematic Reviews*.
- Sisu E, Flangea C, Serb A and Zamfir AD (2011) Modern developments in mass spectrometry of chondroitin and dermatan sulfate glycosaminoglycans. *Amino Acids*.
- Song Y and Buettner GR (2010) Thermodynamic and kinetic considerations for the reaction of semiquinone radicals to form superoxide and hydrogen peroxide. *Free Radical Biology and Medicine*, 919–962.
- Du Souich P (2014) Absorption, distribution and mechanism of action of SYSADOAS. *Pharmacology and Therapeutics*, 362–374.
- Staples, Gregory O.; Zaia J (2011) Analysis of Glycosaminoglycans Using Mass Spectrometry. *Curr Proteomics* 8(4): 325–336.
- Suhr OB, Ando Y, Ohlsson PI, Olofsson A, Andersson K, Lundgren E, Ando M and Holmgren G (1998) Investigation into thiol conjugation of transthyretin in hereditary transthyretin amyloidosis. *European Journal of Clinical Investigation* 28(8): 687–692.
- Tat SK, Pelletier J-P, Vergés J, Lajeunesse D, Montell E, Fahmi H, Lavigne M and Martel-Pelletier J (2007) Chondroitin and glucosamine sulfate in combination decrease the pro-resorptive properties of human osteoarthritis subchondral bone osteoblasts: a basic science study. *Arthritis research &*

*therapy* 9(6): R117.

Tat SK, Pelletier JP, Mineau F, Duval N and Martel-Pelletier J (2010) Variable effects of 3 different chondroitin sulfate compounds on human osteoarthritic cartilage/chondrocytes: Relevance of purity and production process. *Journal of Rheumatology* 37(3): 656–664.

Taylor AM, Boyde A, Wilson PJM, Jarvis JC, Davidson JS, Hunt JA, Ranganath LR and Gallagher JA (2011) The role of calcified cartilage and subchondral bone in the initiation and progression of ochronotic arthropathy in alkaptonuria. *Arthritis and Rheumatism* 63(12): 3887–3896.

Thelin MA, Bartolini B, Axelsson J, Gustafsson R, Tykesson E, Pera E, Oldberg Å, MacCarana M and Malmstrom A (2013) Biological functions of iduronic acid in chondroitin/dermatan sulfate. *FEBS Journal*, 2431–2446.

Tovmasyan A, Carballal S, Ghazaryan R, Melikyan L, Weitner T, Maia CGC, Reboucas JS, Radi R, Spasojevic I, Benov L and Batinic-Haberle I (2014) Rational design of superoxide dismutase (sod) mimics: The evaluation of the therapeutic potential of new cationic Mn porphyrins with linear and cyclic substituents. *Inorganic Chemistry* 53(21): 11467–11483.

Uebelhart D (2008) Clinical review of chondroitin sulfate in osteoarthritis. *Osteoarthritis and Cartilage*.

Ugur M, Yildirim K, Kiziltunc A, Erdal A, Karatay S and Senel K (2004) Correlation between soluble intercellular adhesion molecule 1 level and extracellular superoxide dismutase activity in rheumatoid arthritis: a possible association with disease activity. *Scandinavian journal of rheumatology* 33(4): 239–243.

Volpi N (2009) Quality of different chondroitin sulfate preparations in relation to their therapeutic activity. *The Journal of pharmacy and pharmacology* 61(10): 1271–80.

Walston J, Xue Q, Semba RD, Ferrucci L, Cappola AR, Ricks M, Guralnik J and Fried LP (2006) Serum antioxidants, inflammation, and total mortality in older women. *American Journal of Epidemiology* 163(1): 18–26.

Whitson PE, VandenBorn HW and Evans DH (1973) Acquisition and analysis of cyclic voltammetric data. *Analytical Chemistry* 45(8): 1298–1306.

Witz G, Zhang Z and Goldstein BD (1996) Reactive ring-opened aldehyde metabolites in benzene hematotoxicity. *Environmental Health Perspectives*, 1195–1199.

Wu M, Xu S, Zhao J, Kang H and Ding H (2010) Free-radical depolymerization of glycosaminoglycan from sea cucumber *Thelenata ananas* by hydrogen peroxide and copper ions. *Carbohydrate Polymers* 80(4): 1116–1124.

Yuan X, Pham AN, Miller CJ and Waite TD (2013) Copper-catalyzed hydroquinone oxidation and associated redox cycling of copper under conditions typical of natural saline waters. *Environmental Science and Technology*.